2003-12

Fin stabilizers as maneuver control surfaces

Sarch, Martin G.

Monterey, California. Naval Postgraduate School

NAVAL POSTGRADUATE SCHOOL

MONTEREY, CALIFORNIA

THESIS

FIN STABILIZERS AS MANEUVER CONTROL SURFACES

by

Martin G. Sarch

December 2003

Thesis Advisor:	Fotis A. Papoulias
Co-Advisor:	Charles N. Calvano

Approved for public release; distribution is unlimited

THIS PAGE INTENTIONALLY LEFT BLANK

REPORT DOCUMENTATION PAGE			Form Approved OMB No. 0704-0188
Public reporting burden for this collection of information is estimated to average 1 hour per response, including the time for reviewing instruction, searching existing data sources, gathering and maintaining the data needed, and completing and reviewing the collection of information. Send comments regarding this burden estimate or any other aspect of this collection of information, including suggestions for reducing this burden, to Washington headquarters Services, Directorate for Information Operations and Reports, 1215 Jefferson Davis Highway, Suite 1204, Arlington, VA 22202-4302, and to the Office of Management and Budget, Paperwork Reduction Project (0704-0188) Washington DC 20503.			
1. AGENCY USE ONLY ***(Leave blank)***	**2. REPORT DATE** December 2003	**3. REPORT TYPE AND DATES COVERED** Master's Thesis	
4. TITLE AND SUBTITLE: Fin Stabilizers As Maneuver Control Surfaces			**5. FUNDING NUMBERS**
6. AUTHOR(S) Martin G. Sarch			
7. PERFORMING ORGANIZATION NAME(S) AND ADDRESS(ES) Naval Postgraduate School Monterey, CA 93943-5000			**8. PERFORMING ORGANIZATION REPORT NUMBER**
9. SPONSORING /MONITORING AGENCY NAME(S) AND ADDRESS(ES) N/A			**10. SPONSORING/MONITORING AGENCY REPORT NUMBER**
11. SUPPLEMENTARY NOTES The views expressed in this thesis are those of the author and do not reflect the official policy or position of the Department of Defense or the U.S. Government.			
12a. DISTRIBUTION / AVAILABILITY STATEMENT Approved for public release; distribution is unlimited			**12b. DISTRIBUTION CODE**

13. ABSTRACT (maximum 200 words)

Roll angle is often a limiting factor during high-speed turns and repetitive turning maneuvers. Navy and Coast Guard surface ships are designed for high-speed operation. Sharper turns at higher speeds, and repetitive high-speed turns can increase ship survivability by helping these vessels avoid incoming threats. This is particularly true if the amount and direction of roll during the turn is controlled, since the ship's susceptibility to radar and other sensors may be diminished at certain angles. Sharper turns at higher speeds can also reduce the time it takes to reach a person in the water, improving the chances for successful rescue. Controlled roll during repetitive sharp turns can make high-speed pursuit safer and more likely to succeed. The objective of this thesis is to study the effects of fin stabilizers on a ship's turning performance. Fin stabilizers, commonly added to a ship design for the sole purpose of minimizing unwanted roll during ordinary operations, are shown to also favorably influence both the magnitude and direction of heel experienced during high speed and repetitive maneuvers. The effects of fin stabilizers on other turn performance characteristics are also examined. A strategy for actively employing fins during maneuvers is proposed.

14. SUBJECT TERMS Surface Ship; Fin Stabilizers; Maneuver; Roll; Turning			**15. NUMBER OF PAGES** 131
			16. PRICE CODE
17. SECURITY CLASSIFICATION OF REPORT Unclassified	**18. SECURITY CLASSIFICATION OF THIS PAGE** Unclassified	**19. SECURITY CLASSIFICATION OF ABSTRACT** Unclassified	**20. LIMITATION OF ABSTRACT** UL

NSN 7540-01-280-5500 Standard Form 298 (Rev. 2-89)
Prescribed by ANSI Std. 239-18

THIS PAGE INTENTIONALLY LEFT BLANK

Approved for public release; distribution is unlimited.

FIN STABILIZERS AS MANEUVER CONTROL SURFACES

Martin G. Sarch
Lieutenant Commander, United States Coast Guard
B.A., University of Chicago, 1980
J.D., Rutgers University School of Law – Camden, 1993

Submitted in partial fulfillment of the
requirements for the degree of

MASTER OF SCIENCE IN MECHANICAL ENGINEERING

from the

NAVAL POSTGRADUATE SCHOOL
December 2003

Author: Martin G. Sarch

Approved by: Fotis A. Papoulias
Thesis Advisor

Charles N. Calvano
Co-Advisor

Anthony J. Healey
Chairman, Department of Mechanical Engineering

THIS PAGE INTENTIONALLY LEFT BLANK

ABSTRACT

Roll angle is often a limiting factor during high-speed turns and repetitive turning maneuvers. Navy and Coast Guard surface ships are designed for high-speed operation. Sharper turns at higher speeds, and repetitive high-speed turns can increase ship survivability by helping these vessels avoid incoming threats. This is particularly true if the amount and direction of roll during the turn is controlled, since the ship's susceptibility to radar and other sensors may be diminished at certain angles. Sharper turns at higher speeds can also reduce the time it takes to reach a person in the water, improving the chances for successful rescue. Controlled roll during repetitive sharp turns can make high-speed pursuit safer and more likely to succeed. The objective of this thesis is to study the effects of fin stabilizers on a ship's turning performance. Fin stabilizers, commonly added to a ship design for the sole purpose of minimizing unwanted roll during ordinary operations, are shown to also favorably influence both the magnitude and direction of heel experienced during high speed and repetitive maneuvers. The effects of fin stabilizers on other turn performance characteristics are also examined. A strategy for actively employing fins during maneuvers is proposed.

THIS PAGE INTENTIONALLY LEFT BLANK

TABLE OF CONTENTS

LIST OF FIGURES

DEDICATION

To my wife, Toni, without whose continuous support and encouragement this work would never even have been attempted.

THIS PAGE INTENTIONALLY LEFT BLANK

ACKNOWLEDGMENTS

The author wishes to thank Professors Papoulias and Calvano for their tireless efforts making this research pipe-dream into reality. Special thanks to Tristan M. Perez for making a pre-publication version of the DCMV Toolbox available. The work of Mr. Perez and his colleague, Morgens Blanke, forms the foundation upon which the model used in this study is built. Special thanks also go to Lieutenant Jerrold Sgobbo, USCG, for providing the computer code and other working papers he used to model the rudders and fins for roll stabilization of USCG WMEC 901 Class vessels. These documents provided critical insight into the present studies' coordination of rudder and fin controls. Finally, Вбольшое спасибо to Oleg Yakimenko, for advice concerning optimization strategy.

THIS PAGE INTENTIONALLY LEFT BLANK

I. INTRODUCTION

A. CURRENT SCHEMA FOR MANEUVERING AND ROLL REDUCTION

The vast majority of ships rely upon one or more vertically oriented rudders to accomplish all maneuvers. To turn a ship, a rudder need only produce forces and moments large enough to generate rotation about the ship's vertical axis in the intended direction. However, water flowing across an angled rudder also generates roll, or rotation about the ship's longitudinal axis. [Blanke and Christensen (1993)] Various schemes for taking advantage of the roll generated by an angled rudder have been proposed and implemented; it is now well documented that coordinated rudder movements can be used to reduce the amount of roll a ship steering a straight course experiences when subjected to wind and waves. [Son and Nomoto (1981); Sgobbo and Parsons (1999)] Roll reduction during straight course steaming is beneficial because it produces a more stable platform for weapons and flight operations, decreases crew fatigue and reduces the likelihood of injury or damage to crew or ship contents.

Many other roll reduction devices exist. Some ships, including several classes of United States Navy and United States Coast Guard vessels, are equipped with fin stabilizers. Until very recently, the size, location, composition, and controls of fin stabilizers on naval vessels were all determined with one primary purpose in mind: production of maximum roll-canceling moments. [Gatzoulis and Keane (1977)]. For this reason, fin stabilizers are mounted in pairs on opposite sides of the hull at fixed angles with respect to the transverse plane of the ship. The pairs are typically rotated through angles of equal magnitude and opposite directions about their spanwise axis. This causes the pair of fins to develop complementary moments of roughly equal magnitude in the direction opposed to the rolling motion. Various methods for sensing roll angle, roll velocity, and roll accelerations exist. Most rely on some combination of pendula, gyroscopes, or accelerometers. [Bettcher, C. W. U.S. Patent No. 4,777,899]. During development of concepts for the United States Navy's Small Waterplane Area Twin Hull (SWATH) vessels, fins were designed that would stabilize vertical plane motions of the ship as well. [Lee (1975)]. Later, it was noted that, in addition to the desired roll and pitch-canceling moments, fin stabilizers also produce forces and moments that tend to

turn the ship; researchers commented that, in some specialized applications, vertical rudders might not be necessary if fin stabilizers generated sufficient rotation about the ship's vertical axis. [David W. Taylor NSRDC (1986)]. *See also* Kallstrom (1981) (improved autopilot through a rudder/fin combination minimizing both roll and yaw)]. To date, the author has found no published quantitative analysis of this proposal.

B. BASIC MANEUVERING WITH A RUDDER

The definitions for the turning path of a ship steered by rudder(s) located at the stern are shown in Figure 1. Before the turn is commenced, the depicted vessel is traveling in a straight line with rudder amidships. At the outset of the turn, the rudder is commanded to deflect. In the depicted case, to cause the ship to turn to starboard, the trailing edge of the rudders will deflect to starboard. The rudder machinery takes a certain amount of time to effect the commanded deflection. During this period, called the Approach Phase, the ship has not yet begun to turn, so it continues to advance at the same rate as before. Once the rudder begins its deflection, the ship enters the First Phase of the turn. During this phase, the aft end of the ship pivots to port, but, as the ship's mass and inertia are resisting the turn, the ship will heel inward, *i.e.*, starboard side down. Because the ship is a rigid body, the motion of the stern section forces its center of gravity to sideslip to port. The First Phase lasts a very short time, ending when the velocity vector at the center of gravity begins to include components in the direction of the intended turn. During the Second Phase, the vessel's rudder continues to force the aft end of the ship to port. However, as the ship's bow is now turning to starboard, the ship begins to roll, passing through upright and adopting a port side down (outward heel) attitude. Finally, an equilibrium between the rudder's forces and moments and the ship's velocity is achieved. At this point, the vessel reaches the Third Phase of the turn. The center of gravity approximates a circular orbit about a central point; the ship maintains an approximately steady outward heel that can be greater or less than the angle adopted during the Second Phase of the turn. [Lewis (1989)]

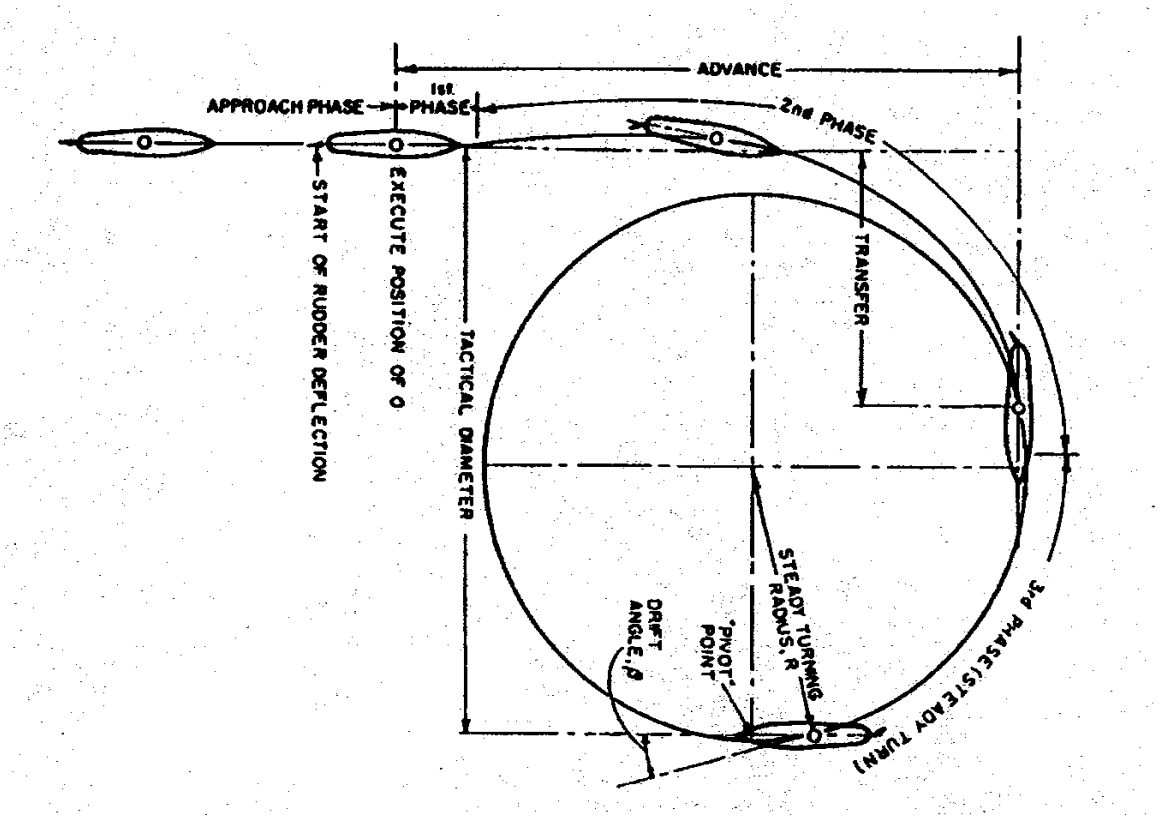

Figure 1. Turning Path of a Ship [Lewis (1989)].

C. LIMITATIONS OF MANEUVERING WITH RUDDERS ALONE

Rudders produce turning forces and moments in much the same way airplane wings generate lift. Just as in the case of an airplane wing, the amount of turning force a rudder can produce from a given fluid flow velocity is limited – at some angles of attack relative to the fluid's free stream velocity, the rudder will "stall." See [Perez and Goodwin (2003)]. In effect, this rudder limitation places a lower bound on the tactical diameter for rudder induced turns at various ship speeds.

The ship's roll angle is another important limitation of maneuvering with rudders. Increasing either rudder deflection angle or ship's surge velocity tends to increase the magnitude of roll produced. [Lewis (1989); Son and Nomoto (1981)]. Although "[t]he [International Maritime Organization] does not provide recommendations regarding roll angles . . . [during turns, but] maximum roll angles while manoeuvring above 13 degrees and constant roll angles while turning above 8 degrees are thought to be very large." [Toxeopeus and Loeff (2002)] (computer simulation of high speed cruise ship indicated podded propulsors generated peak roll angles up to 28 degrees and constant roll angles up

to 17 degrees with pod trained at 35 degrees). Metacentric height has been shown to have a significant impact on the magnitude of roll and heel a ship experiences during a turn. [Oltmann (1993)] Figure 2 demonstrates, however, that very large vessels designed to have the greatest transverse stability can experience large roll angles during high speed rudder-induced turns – even in the absence of significant waves, wind, or other environmental disturbances.

Figure 2. USS NIMITZ (CVN 68) (From http://www.1000pictures.com with permission).

D. MANEUVERING WITH RUDDERS AIDED BY FIN STABILIZERS

As noted above, fin stabilizer systems are currently added to ship designs for the primary purpose of producing roll-canceling moments. However, just as rudders induce roll in addition to turning forces and moments, fin stabilizers induce turning forces and moments in addition to roll. The present study explores whether, and to what extent, fin

stabilizers can be used to enhance a ship's performance during various maneuvers. The study has several different motivations. Navy and Coast Guard surface ships are designed for high speed operation. Sharper turns at higher speeds, and repetitive high speed turns, can increase ship survivability by helping these vessels avoid incoming threats. This is particularly true if the use of fin stabilizers affords greater control over the roll angle during the turn, since the ship's susceptibility to radar and other sensors may be diminished at certain angles. Sharper turns at higher speeds can also reduce the time it takes to reach a person in the water, improving the chances for successful rescue. Controlled roll during repetitive high speed maneuvers can make high speed pursuit safer and more likely to succeed.

The study presented herein uses a computer simulation of a generic multi-mission naval vessel first developed by Blanke and Perez [Blanke and Christensen (1993)' Perez and Blanke (2002); Perez]. The ship's length between perpendiculars is 51.5 meters, its beam is 8.6 meters, and its volumetric displacement is 357 cubic meters. The ship's differential equations of motion, described in Chapter II, are derived from information provided in Perez [Perez]. These equations are solved, as described in Chapter III, and the results of simulations involving the use of various combinations of rudder and fin deflections are presented in Chapters IV and V. It is important to note that the model does not take into account any modifications that may be required to either the fins or the fin operating machinery to make them capable of moving independently or to make them strong enough to endure the forces and moments associated with any simulated maneuver. The model simply assumes that the fins can be made to rotate in two planes, act independently, and survive all simulated maneuvers intact.

The analysis performed is expected to help determine the feasibility of using fin stabilizers as control surfaces during maneuvers. An analysis of basic turn maneuvers is found in Chapter IV. A strategy for deploying fin stabilizers to improve specific characteristics of basic turns is proposed. Analysis of, and a proposed strategy for improving specific characteristics of various repeated turn maneuvers is found in Chapter V. The parameters used for these analyses are: the ship's position in the xy-plane, the roll angle ϕ, the surge speed, u, and either the total distance traveled during the

simulation (for basic turns) or the time history of rudder deflection angles (for repeated turns). These parameters are plotted for each set of maneuvers and are then used to study the ship's performance characteristics. The conclusions drawn from the analysis performed are presented in Chapter VI. Areas of further research are also recommended.

II. THEORY AND PROBLEM FORMULATION

A. GENERAL EQUATIONS OF MOTION IN SIX DEGREES OF FREEDOM

Beginning with the fundamental expressions of Newtonian Mechanics, the equations of motion for a rigid body of constant mass can be expressed in many ways. Equation Section 2

$$\sum \mathbf{F} = \frac{d(mv)}{dt} \qquad \sum \mathbf{M} = \frac{d(I\boldsymbol{\omega})}{dt} \tag{2.1}$$

This study, concerned with the motion of ocean-going vessels, follows the Society of Naval Architects and Marine Engineers notation convention. [SNAME (1950)]. This notation employs a combination of two separate right-handed orthogonal coordinate systems: one attached to the earth and a second attached to the body of the ship. See Figure 3 and Table 1.

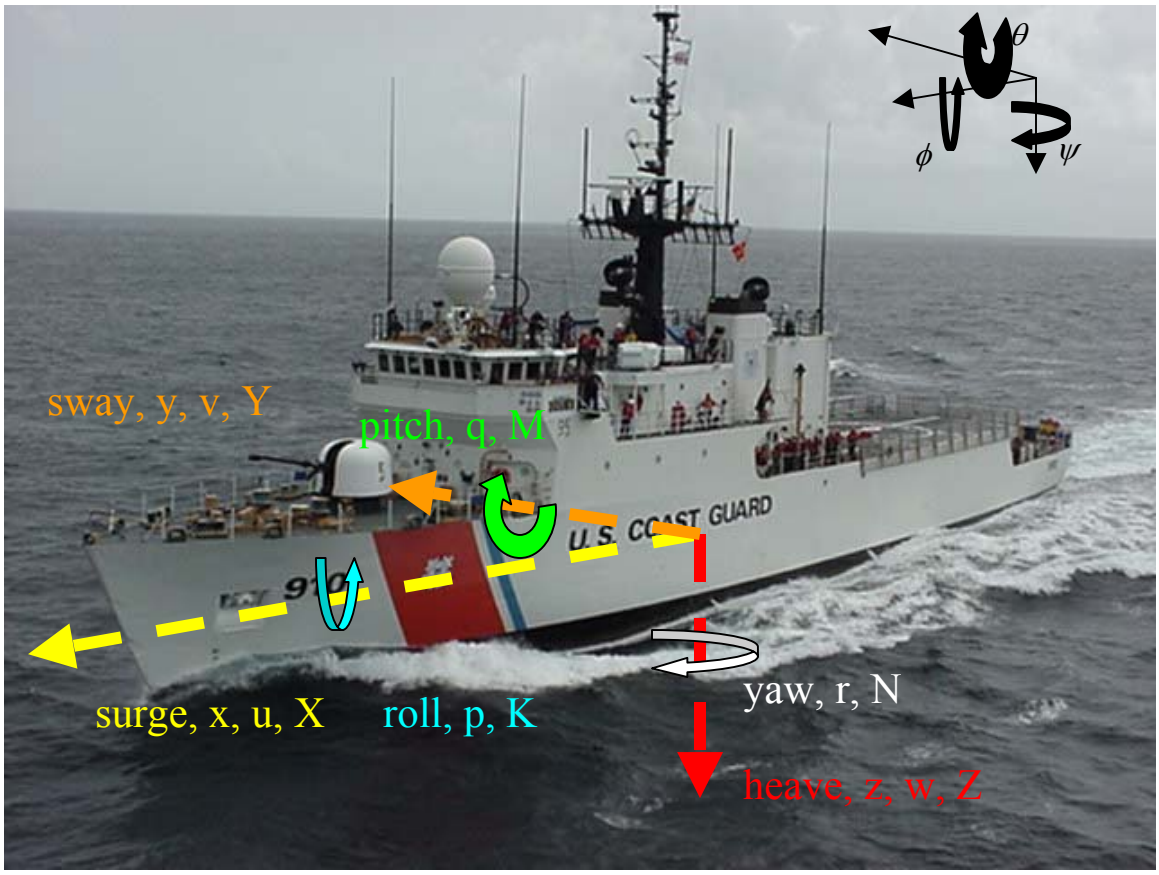

Figure 3. Coordinate Frames Drawn on USCGC THETIS (WMEC 910).

Parameter	Value	Description
x,y,z		Distance along body-fixed system axes
u,v,w		Translational velocity components in body-fixed frame
p,q,r		Rotational velocity components of ship in body-fixed frame
X,Y,Z		Force components along body axes
K,M,N		Moment components along body axes
ψ		Yaw angle: Pos. bow to stbd in inertial reference system
θ		Pitch angle: bow up positive in inertial reference system
ϕ		Roll angle: port up positive in inertial reference system
m	$3.66\times10^5\ kg$	Mass of ship
x_G, y_G, z_G	(-3.38, 0, -1.75)	Coordinates of the center of gravity in the body axis system
I_{xx}	$3.4\times10^6\ kg\cdot m^2$	Moment of inertia about the body longitudinal axis
I_{yy}	Assumed 0	Moment of inertia about the body transverse axis
I_{zz}	$6.0\times10^7\ kg\cdot m^2$	Moment of inertia about the body vertical axis
I_{xy}, I_{yz}, I_{xy}	Assumed small	Products of inertia about the body axis system

Table 1. Coordinate Frame and Vessel Parameters.

The relationship between the inertial and body-fixed coordinate frames is defined by the transformation: [Mathworks (2003); Kwon (2003)]

$$\begin{bmatrix}\dot{x}\\ \dot{y}\\ \dot{z}\\ \dot{\phi}\\ \dot{\theta}\\ \dot{\psi}\end{bmatrix}=\begin{bmatrix}\cos\theta\cos\psi & \sin\phi\sin\theta\cos\psi-\cos\phi\sin\psi & \cos\phi\sin\theta\cos\psi+\sin\phi\sin\psi & 0 & 0 & 0\\ \cos\theta\sin\psi & \sin\phi\sin\theta\sin\psi+\cos\phi\cos\psi & \cos\phi\sin\theta\sin\psi-\sin\phi\cos\psi & 0 & 0 & 0\\ -\sin\theta & \sin\phi\cos\theta & \cos\phi\cos\theta & 0 & 0 & 0\\ 0 & 0 & 0 & 1 & \sin\phi\tan\theta & \cos\phi\tan\theta\\ 0 & 0 & 0 & 0 & \cos\phi & -\sin\phi\\ 0 & 0 & 0 & 0 & \sin\phi\sec\theta & \cos\phi\sec\theta\end{bmatrix}\begin{bmatrix}u\\ v\\ w\\ p\\ q\\ r\end{bmatrix} \quad (2.2)$$

The equations of motion in six degrees of freedom can be expressed in the body-fixed coordinates as:

$$
\begin{aligned}
&\textit{Surge}: \quad m\left[\dot{u}-x_G\left(q^2+r^2\right)+y_G\left(pq-\dot{r}\right)+z_G\left(\dot{q}+pr\right)-rv+wq\right]=X\\
&\textit{Sway}: \quad m\left[\dot{v}+x_G\left(pq+\dot{r}\right)-y_G\left(p^2+r^2\right)+z_G\left(qr-\dot{p}\right)+ur-wp\right]=Y\\
&\textit{Heave}: \quad m\left[\dot{w}+x_G\left(rp-\dot{q}\right)+y_G\left(qr+\dot{p}\right)-z_G\left(p^2+q^2\right)+pv-qu\right]=Z\\
&\textit{Roll}: \quad I_{xx}\dot{p}+qr\left(I_{zz}-I_{yy}\right)+I_{xy}\left(rp+\dot{q}\right)+I_{xz}\left(\dot{r}-pq\right)+I_{yz}\left(r^2-q^2\right)+y_G\dot{w}-mz_G\left(\dot{v}+ur-wp\right)=K\\
&\textit{Pitch}: \quad I_{yy}\dot{q}+rp\left(I_{xx}-I_{zz}\right)+I_{xy}\left(\dot{p}-qr\right)+I_{xz}\left(p^2-r^2\right)+I_{yz}\left(\dot{r}+pq\right)+m\left[z_G\left(\dot{u}+qw-rv\right)-x_G\left(\dot{w}+ur-wp\right)\right]=M\\
&\textit{Yaw}: \quad I_{zz}\dot{r}+pq\left(I_{yy}-I_{zz}\right)+I_{xy}\left(q^2-p^2\right)+I_{xz}\left(qr+\dot{p}\right)+I_{yz}\left(\dot{q}-rp\right)+m\left[x_G\left(\dot{v}+ur-wp\right)+y_G\left(vr-wq-\dot{u}\right)\right]=N
\end{aligned}
\tag{2.3}
$$

These equations are derived from [6 D.O.F. (2003)]

B. SIMPLIFYING ASSUMPTIONS

Since the present work involves only the case of a ship maneuvering on a calm ocean surface, the following assumptions are made [Logsdon (1992)]:

- The rotational velocity and acceleration about the y-axis $\left(q \textit{ and } \dot{q}\right)$ are zero.
- The translational velocity and acceleration in the z direction $\left(w \textit{ and } \dot{w}\right)$ are zero.
- The vertical heave and pitch motions are decoupled from the horizontal plane motions; their impact on maneuvering can be neglected.
- The products of inertia $I_{xy}, I_{xz}, \textit{and } I_{yz}$ are small and can be neglected.
- The origin of the body-fixed coordinate system is at the ship's center of gravity, located amidships, on the centerline, and at the design waterplane.
- The ship is symmetrical about its longitudinal axis; thus $y_G = 0$.

C. SIMPLIFIED EQUATIONS IN FOUR DEGREES OF FREEDOM

Applying the above-stated assumptions to Equation 2.3, yields a set of simplified equations in four degrees of freedom:

$$
\begin{aligned}
&\textit{Surge}: \quad m\left[\dot{u}-x_G r^2+z_G pr-rv\right]=X\\
&\textit{Sway}: \quad m\left[\dot{v}+x_G\dot{r}-z_G\dot{p}+ur\right]=Y\\
&\textit{Roll}: \quad I_{xx}\dot{p}-mz_G\left(\dot{v}+ur\right)=K\\
&\textit{Yaw}: \quad I_{zz}\dot{r}+mx_G\left(\dot{v}+ur\right)=N
\end{aligned}
\tag{2.4}
$$

or, in matrix form:

$$\begin{bmatrix} m & 0 & 0 & 0 \\ 0 & m & -mz_G & mx_G \\ 0 & -mz_G & I_{xx} & 0 \\ 0 & mx_G & 0 & I_{zz} \end{bmatrix} \begin{bmatrix} \dot{u} \\ \dot{v} \\ \dot{p} \\ \dot{r} \end{bmatrix} = \begin{bmatrix} X \\ Y \\ K \\ N \end{bmatrix} + \begin{bmatrix} m\left(x_G r^2 - z_G pr + rv\right) \\ m\left(-ur\right) \\ mz_G\left(ur\right) \\ -mx_G\left(ur\right) \end{bmatrix} \tag{2.5}$$

Additionally, these assumptions can be used to simplify two important relations between inertial and body-fixed reference frames: $\dot{\phi} = p$ and $\dot{\psi} = r\cos\phi$.

D. FORCES AND MOMENTS

There are many different forces and moments acting on a vessel floating partially submerged in water. The forces that generate surge and sway, and the moments that generate roll and yaw can be grouped according to their sources:

$$\begin{aligned} \sum \mathbf{F} &= \mathbf{F}_{hydrodynamic} + \mathbf{F}_{propulsive} + \mathbf{F}_{environmental} + \mathbf{F}_{control\ surfaces} \\ \sum \mathbf{M} &= \mathbf{M}_{hydrodynamic} + \mathbf{M}_{propulsive} + \mathbf{M}_{environmental} + \mathbf{M}_{control\ surfaces} \end{aligned} \tag{2.6}$$

1. Hydrodynamic Forces and Moments

Using the method of Abkowitz [Abkowitz], the hydrodynamic forces and moments in four degrees of freedom can be expressed as unknown nonlinear functions of position, velocity, and acceleration using both body-fixed and inertial reference frames:

$$\begin{aligned} &\textit{Hydrodynamic Surge Force}: && X_{hyd} = f_1\left(u, v, r, \phi\right) \\ &\textit{Hydrodynamic Sway Force}: && Y_{hyd} = f_2\left(u, \dot{u}, v, \dot{v}, p, \dot{p}, r, \dot{r}, \phi, \dot{\phi}\right) \\ &\textit{Hydrodynamic Roll Moment}: && K_{hyd} = f_3\left(u, \dot{u}, v, \dot{v}, p, \dot{p}, r, \dot{r}, \phi, \dot{\phi}, \ddot{\phi}\right) \\ &\textit{Hydrodynamic Yaw Moment}: && N_{hyd} = f_4\left(u, \dot{u}, v, \dot{v}, r, \dot{r}, \phi, \dot{\phi}\right) \end{aligned} \tag{2.7}$$

Approximating each function with the first three non-zero terms of its Taylor Series yields:

$$X_{hyd} = X_{\dot{u}}\dot{u} + X_{u|u|}u\,|u| + X_{vr}vr \tag{2.8}$$

$$\begin{aligned} Y_{hyd} = {} & Y_{\dot{v}}\dot{v} + Y_{\dot{r}}\dot{r} + Y_{\dot{p}}\dot{p} + Y_{|u|v}\,|u|\,v + Y_{ur}ur + Y_{v|v|}v\,|v| + Y_{v|r|}v\,|r| \\ & + Y_{r|v|}r\,|v| + Y_{\phi|uv|}\phi\,|uv| + Y_{\phi|ur|}\phi\,|ur| + Y_{\phi uu}\phi uu \end{aligned} \tag{2.9}$$

$$\begin{aligned} K_{hyd} &= K_{\dot{v}}\dot{v} + K_{\dot{p}}\dot{p} + K_{|u|v}\,|u|\,v + K_{ur}ur + K_{v|v|}v\,|v| + K_{v|r|}v\,|r| \\ &\quad + K_{r|v|}r\,|v| + K_{\phi|uv|}\phi\,|uv| + K_{\phi|ur|}\phi\,|ur| + K_{\phi uu}\phi uu \\ &\quad + K_{|u|p}\,|u|\,p + K_{p|p|}p\,|p| + K_{p}p + K_{\phi\phi\phi}\phi\phi\phi - \Delta G_z(\phi) \end{aligned} \tag{2.10}$$

$$\begin{aligned} N_{hyd} &= N_{\dot{v}}\dot{v} + N_{\dot{r}}\dot{r} + N_{|u|v}\,|u|\,v + N_{|u|r}\,|u|\,r + N_{r|r|}r\,|r| \\ &\quad + N_{r|v|}r\,|v| + N_{\phi|uv|}\phi\,|uv| + N_{\phi|ur|}\phi\,|ur| + N_{\phi u|u|}\phi u\,|u| \end{aligned} \tag{2.11}$$

Each term of these equations is composed of a multiplier and a multiplicand. With one exception, the multiplier is a partial derivative of the force or moment with respect to some combination of the ship's position, velocity, and acceleration; the multiplicand is that same combination of position, velocity, and acceleration terms. The subscript notation scheme employed here reflects the order in which the partial derivatives are to be taken. For example, X_{vr} is the equivalent, in Leibniz' notation of $\frac{\partial^2 X}{\partial r \partial v} = \frac{\partial}{\partial r}\left(\frac{\partial X}{\partial v}\right)$. Each partial derivative is treated as a constant, time invariant quantity; collectively, they are known as the ship's "hydrodynamic coefficients." Traditionally, these coefficients were obtained from experiments with scale models in towing tanks, or during sea trials of a full-scale vessel. Due to recent advances in computer simulation techniques, hydrodynamic coefficients of a ship design can now be predicted numerically with reasonable accuracy. [See, *e.g.*, VMA-CFD]. At different times, different authors have presented sets of data relating to the multi-role naval vessel modeled here. The data in Table 2, Hydrodynamic Coefficients, were deemed the most recent, and were used to generate all results presented in the following chapters.

The hydrodynamic roll moment equation includes one non-derivative term $\Delta G_z(\phi)$. In this instance, $\Delta =$ ship's weight displacement $= \rho_{water} * g_{local} * \nabla$ with $\rho =$ mass density of salt water, $1025\,kg/m^3$, $g =$ gravitational constant, $9.81\,m/s^2$ and $\nabla =$ ship's volumetric displacement, $357\,m^3$. $G_Z(\phi)$ is an expression of the ship's resistance to capsizing (righting moment) as a function of roll angle. A reasonable approximation of this function is $\overline{GM_Z}\sin\phi$ with $\overline{GM_Z}$ representing the distance between the ship's instantaneous z_G and its metacenter, here 1.1 meter. In general,

$\overline{GM_Z}$ can be obtained from the relations $\overline{GM_z} = \overline{KM_z} - \overline{Kz_G}$ with $\overline{KM_z} = \overline{Kz_B} + \overline{BM_z}$, $\overline{BM_z} = distance\ from\ instantaneous\ Z_{Center\ of\ Buoyancy}\ to\ metacenter = \frac{I_z}{\nabla}$, and K = nearest point on ship's keel (baseline). [NavArchWeb; Zubaly (1996) pp. 62 – 74.]

Subscript	Units	X	Y	K	N
$\dot{u}$	m/s^2	-1.74×10^4	0	0	0
$\dot{v}$	m/s^2	0	-3.93×10^5	5.38×10^5	2.96×10^5
$\dot{p}$	$rads/s^2$	0	-2.96×10^5	-7.74×10^5	0
$\dot{r}$	$rads/s^2$	0	-1.40×10^6	0	-3.87×10^7
$u\|u\|$	m^2/s^2	-1.96×10^3	0	0	0
$\|u\|v$	m^2/s^2	0	-1.18×10^4	9.26×10^3	-9.20×10^4
$\|u\|r$	$rads\cdot m/s^2$	0	1.31×10^5	-1.02×10^5	-4.71×10^6
$v\|v\|$	m^2/s^2	0	-3.70×10^3	2.93×10^4	0
$r\|r\|$	$rads^2/s^2$	0	0	0	-2.02×10^8
$v\|r\|$	$rads\cdot m/s^2$	$.33*m$	-7.94×10^5	6.21×10^5	0
$r\|v\|$	$rads\cdot m/s^2$	0	-1.82×10^5	1.42×10^5	-1.56×10^7
$\phi\|uv\|$	$rads\cdot m^2/s^2$	0	1.08×10^4	-8.40×10^3	-2.14×10^5
$\phi\|ur\|$	$rads^2\cdot m/s^2$	0	2.51×10^5	-1.96×10^5	-4.98×10^6
ϕuu	$rads\cdot m^2/s^2$	0	-7.4×10^1	-1.18×10^3	-8.00×10^3
$\|u\|p$	$rads\cdot m/s^2$	0	0	-1.55×10^4	0
$p\|p\|$	$rads^2/s^2$	0	0	-4.16×10^5	0
p	$rads/s$	0	0	-5.00×10^5	0
$\phi\phi\phi$	$rads^3$	0	0	$-.325\Delta$	0

Table 2. Multi-Role Naval Vessel Hydrodynamic Coefficients (Dimensional).

2. Propulsive Forces and Moments

As explained in Perez [Perez], a ship's propulsion plant is not easily modeled accurately. A simple model can be constructed by applying three assumptions: (a) the ship is initially traveling on a calm ocean surface at constant forward velocity, U_0; (b) all other velocity and acceleration terms are initially equal to zero, and (c) all components of thrust and resistance other than in the direction of surge velocity can be neglected. With these assumptions in place, the force balance becomes:

$$X_{resistive} + T_{prop} = 0 \tag{2.12}$$

Perez [Perez], suggests that, as a first approximation, $X_{u|u|}U_0^2$ can be set equal to $X_{resistive}$, making the thrust equation:

$$T_{prop} = -X_{u|u|}U_0^2 \tag{2.13}$$

For purposes of the present study, $X_{resistive}$ is taken to include the added resistance of all underwater appendages, including rudders and fin stabilizers, when in their neutral positions.

3. Control Surface Forces and Moments

There are numerous methods for modeling the forces and moments induced by fluid flowing across rudders and fins. A simplified version of the method described in Perez [Perez] treats the total force as composed of two orthogonal components: Lift and Drag. These are related as follows:

$$F = \sqrt{L^2 + D^2} \tag{2.14}$$

$$L = \frac{1}{2}\rho_{fluid}\bar{V}_{fluid}^2 A_{surface} C_L \tag{2.15}$$

$$D = \frac{1}{2}\rho_{fluid}\bar{V}_{fluid}^2 A_{surface}\left(C_D + \frac{C_L^2}{.9\pi\Lambda}\right) \tag{2.16}$$

In these equations, A is the surface area of the control surface, $\bar{V}_{fluid}$ is the average relative velocity of the fluid across the control surface, Λ is the control surface aspect ratio, and C_D *and* C_L are the drag and lift coefficients for the control surface, respectively. While Perez notes that the lift coefficient is a complicated function that varies with the difference between the angle of attack of the control surface and the fluid free stream velocity, the present study treats this parameter as if it were a constant to be later multiplied by the angle of attack. All drag across the rudder or fin in the neutral position is incorporated in the Thrust equation. Only additional drag caused by rotation of the surface contributes to a reduction in surge velocity.

a. Rudder Forces and Moments

By neglecting contributions from sway velocity and sway velocity astern, the forces and moments passed to the hull from each rudder can be expressed as:

$$X_{rudder} = -D_{rudder} * \delta \tag{2.17}$$

$$Y_{rudder} = L_{rudder} * \delta \tag{2.18}$$

$$N_{rudder} = -\overline{LCG} * L_{rudder} * \delta \tag{2.19}$$

$$K_{rudder} = -\overline{R_{arm}} * L_{rudder} * \delta \tag{2.20}$$

$\overline{LCG}$ is the longitudinal distance between the ship's center of gravity and the rudder's center of pressure. $\overline{R_{arm}}$ is the distance between the rudder's center of pressure and the nearest point on the ship's midplane at the height of the center of gravity. Rudder deflection angles, δ, are taken positive when inducing a turn to port, see Figure 4, and the fluid flow velocity across each rudder is treated as if it were equivalent to the vessel's surge velocity. The ship has two rudders. As most vessels with multiple rudders employ a mechanical steering system that moves all rudders simultaneously through equal displacement angles, the model exercises control of both rudders in this fashion. The model also contemplates two rudder turn rates: a fast rate for making large turning motions and a slow one for making small course corrections. These two rates correspond to the use of a tandem hydraulic pump system frequently employed on vessels. When the difference between actual and ordered rudder deflection is large, the output of both pumps is used to operate the turning gear. When the difference is small, the output of one of the pumps operates the turning gear, while the other pump is placed in standby. The relevant characteristics for each rudder are provided in Table 3.

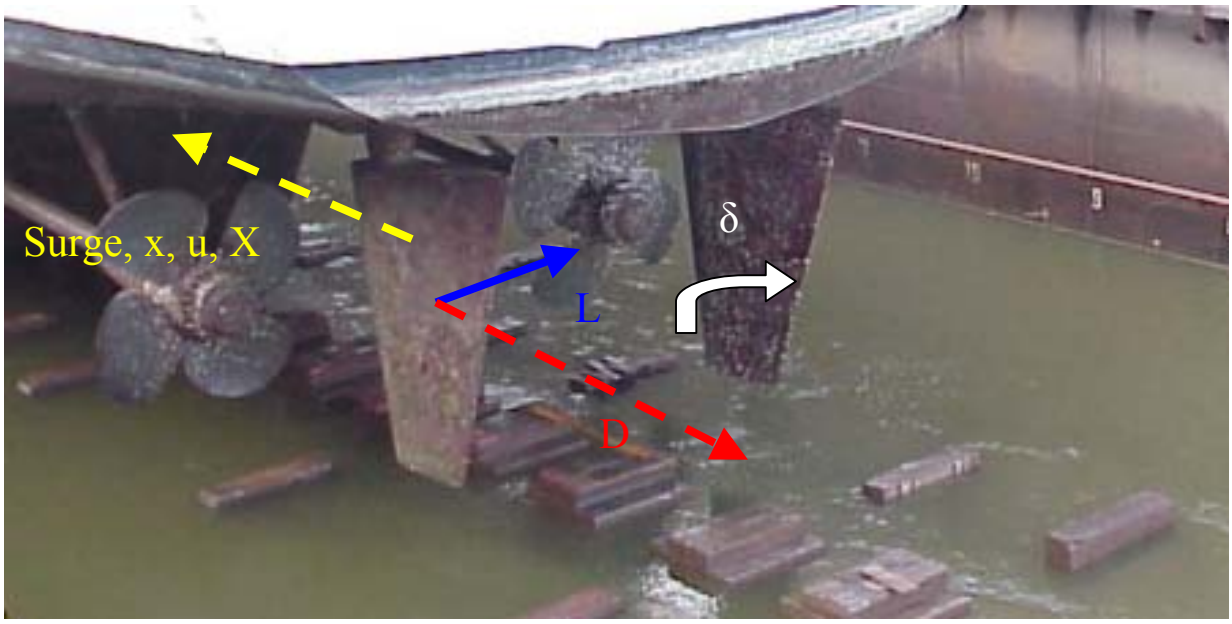

Figure 4. Rudder Forces, Moments, and Deflections.

Parameter	Value	Description
δ	-45° to +45°	Angle of deflection (Starboard & Port Rudder Equal)
Ar	$1.5m^2$	Surface Area
Λ_r	3	Aspect Ratio
$\overline{LCG}$	20.4 m	Distance from X_G to Rudder Center of Pressure
$\overline{R_{arm}}$	$\sqrt{2.61^2+(\pm 2)^2}$ ~3.3 m	Distance from (Y_G, Z_G) to Rudder Center of Pressure
C_D	0.0065	Drag Coefficient
C_L (max)	1.25	Lift Coefficient
$\dot{\delta}$ (max)	$15^\circ/s$ or $7.5^\circ/s$	Rudder Turn Rate: Two Pumps / One Pump

Table 3. Rudder Characteristics.

b. Fin Stabilizer Forces and Moments

For the sake of convenience in calculations, the total force on a vessel's submerged control surfaces can also be expressed as a function of components that are Normal and Tangential to the control surface:

$$F = \sqrt{L^2 + D^2} = \sqrt{N^2 + T^2} \tag{2.21}$$

$$N = L\cos\alpha + D\sin\alpha \tag{2.22}$$

$$T = D\cos\alpha - L\sin\alpha \tag{2.23}$$

with α = the angle of attack of the control surface to the fluid free stream velocity. See Figure 5. The angle of attack is deemed positive when the leading edge of the starboard fin is up and the leading edge of the port fin is down. On a calm, flat ocean surface, the vessel will roll to port when both fin angles are positive. Neglecting differences between the two fins caused by the differing flow fields in which they travel, the forces and moments passed to the hull from each fin can be expressed as

$$X_{fin} = -T_{fin} * \alpha$$

$$Y_{fin} = N_{fin}\sin\beta_{fin} * \alpha$$

$$N_{fin} = -\overline{FCG} * N_{fin}\sin\beta_{fin} * \alpha$$

$$K_{fin} = -2\overline{F_{arm}} * N_{fin} * \alpha$$

$\overline{FCG}$ is the longitudinal distance from the ship's center of gravity to the fin's center of pressure. $\overline{F_{arm}}$ is the distance from the fin's center of pressure to the nearest point on the ship's midplane at the same height as the center of gravity. The angle β is measured from the horizontal to a line extending from the hull spanwise through the fin's midline. See Figure 6. The fluid flow velocity across each fin is treated as if it were equivalent to the vessel's surge velocity and the angle of attack is taken as the mechanical angle between the fin and the free stream fluid velocity. The ship has one pair of fins. The model allows for independent control of both α and β for each fin. Just as it did for the rudders, the model also contemplates two fin turn rates. The relevant characteristics for each fin are provided in Table 4.

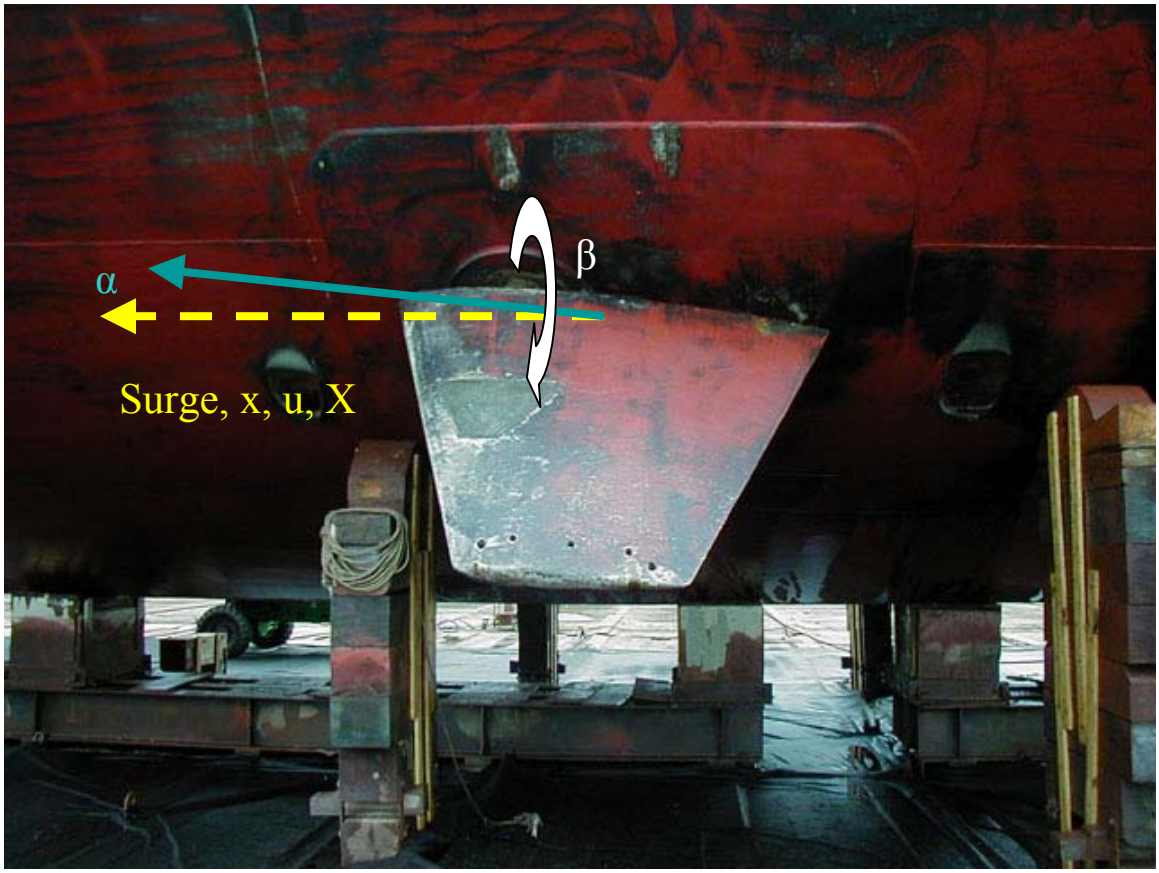

Figure 5. Fin Stabilizer Angular Displacements.

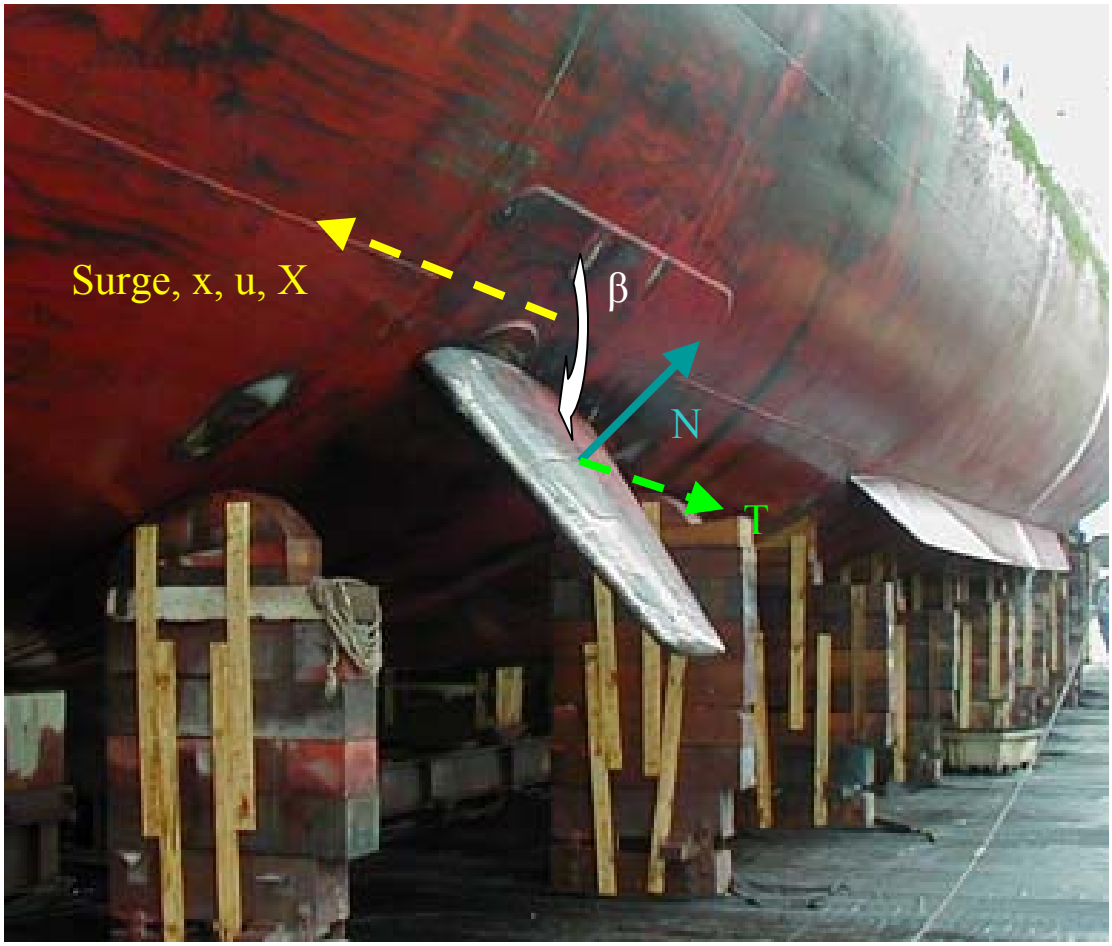

Figure 6. Fin Stabilizer Forces and Moments.

Parameter		Description
α_S, α_P	-40° to +40°	Angle of attack (Starboard Fin / Port Fin)
Af	$1.6m^2$	Surface Area
Λ_f	1	Aspect Ratio
$\overline{FCG}$	-2 m	Distance from X_G to Fin Center of Pressure
$\overline{F_{arm}}$	4.22 m	Distance from (Y_G, Z_G) to Fin Center of Pressure
C_D	0.0065	Drag Coefficient
C_L (max)	1.26	Lift Coefficient
β_S, β_P (max)	10°-80°	Angle between horizontal & Fin Midplane
$\dot{\alpha}_S, \dot{\alpha}_P$ (max)	$20^\circ/s$ or $10^\circ/s$	Fin Turning Rate (2 Pumps / 1 Pump)

Table 4. Fin Stabilizer Characteristics.

4. Environmental Forces and Moments

Numerous studies of the forces and moments induced upon a surface vessel by wind, waves, currents, and other environmental factors have been undertaken. These factors play a very large role in a ship's course keeping ability. However, quantifying these forces and moments while a vessel is maneuvering requires significant computational effort. The effects of environmental forces and moments are not treated in the present study, but this is an area needing further development.

E. MODEL EQUATIONS OF MOTION WITH FORCES AND MOMENTS

Putting the results of the prior sections together yields the following sets of equations used to construct the model:

1. Differential Form

$$\begin{aligned}
&Surge: && m\left[\dot{u} - x_G r^2 + z_G pr - rv\right] = X_{hydrodynamic} + X_{propulsive} + X_{rudder} + X_{fin} \\
&Sway: && m\left[\dot{v} + x_G \dot{r} - z_G \dot{p} + ur\right] = Y_{hydrodynamic} + Y_{rudder} + Y_{fin} \\
&Roll: && I_{xx}\dot{p} - mz_G\left(\dot{v} + ur\right) = K_{hydrodynamic} + K_{rudder} + K_{fin} \\
&Yaw: && I_{zz}\dot{r} + mx_G\left(\dot{v} + ur\right) = N_{hydrodynamic} + N_{rudder} + N_{fin}
\end{aligned} \tag{2.24}$$

2. Collected Differential Form

Collecting and re-arranging terms yields the following set of equations:

$$\begin{bmatrix} m-X_{\dot{u}} & 0 & 0 & 0 \\ 0 & m-Y_{\dot{v}} & -mz_G-Y_{\dot{p}} & mx_G-Y_{\dot{r}} \\ 0 & -mz_G-K_{\dot{v}} & I_{xx}-K_{\dot{p}} & 0 \\ 0 & mx_G-N_{\dot{v}} & 0 & I_{zz}-N_{\dot{r}} \end{bmatrix} \begin{bmatrix} \dot{u} \\ \dot{v} \\ \dot{p} \\ \dot{r} \end{bmatrix} =$$

$$\begin{bmatrix} X_{u|u|}u|u| + X_{vr}vr + m\left(x_G r^2 - z_G pr + rv\right) + T_{prop} \\ Y_{|u|v}|u|v + Y_{ur}ur + Y_{v|v|}v|v| + Y_{v|r|}v|r| + Y_{r|v|}r|v| + Y_{\phi|uu|}\phi|uv| + Y_{\phi|ur|}\phi|ur| + Y_{\phi uu}\phi uu - mur \\ K_{|u|v}|u|v + K_{ur}ur + K_{v|v|}v|v| + K_{v|r|}v|r| + K_{r|v|}r|v| + K_{\phi|uv|}\phi|uv| + K_{\phi|ur|}\phi|ur| + K_{\phi uu}\phi uu + K_{|u|p}|u|p + K_{p|p|}p|p| + K_p p + K_{\phi\phi\phi}\phi\phi\phi - \Delta G_z + mz_G ur \\ N_{|u|v}|u|v + N_{|u|r}|u|r + N_{r|r|}r|r| + N_{r|v|}r|v| + N_{\phi|uv|}\phi|uv| + N_{\phi|ur|}\phi|ur| + N_{\phi u|u|}\phi u|u| - mx_G ur \end{bmatrix} \tag{2.25}$$

$$+ \begin{bmatrix} -T_{Port\ Fin} & -T_{Starboard\ Fin} & -D_{rudders} \\ N_{Port\ fin}\sin\beta_{Port\ fin} & N_{Starboard\ fin}\sin\beta_{Starboard\ fin} & L_{rudders} \\ -\overline{FCG} * N_{Port\ fin}\sin\beta_{Port\ fin} & -\overline{FCG} * N_{Starboard\ fin}\sin\beta_{Starboard\ fin} & -\overline{LCG} * L_{rudders} \\ -2\overline{F_{arm}} * N_{Port\ fin} & -2\overline{F_{arm}} * N_{Starboard\ fin} & -\overline{R_{arm}} * L_{rudders} \end{bmatrix} \bullet \begin{bmatrix} \alpha_{Port} \\ \alpha_{Starboard} \\ \delta \end{bmatrix}$$

THIS PAGE INTENTIONALLY LEFT BLANK

III. MODEL BUILDING, INPUT AND OUTPUT

A. CHOOSING SOFTWARE

At the outset of model construction, Matlab® was selected as the modeling software. This choice was driven by three equally important factors: (1) a Matlab® file containing a working, validated, linearized model of an early prototype for the same ship was available to be used as a starting point [Lauvdal and Fossen (1994)]; (2) Matlab® affords a broad selection of non-linear differential equation solvers and optimization routines; and (3) Matlab® code can easily be integrated into a Simulink® model which, in turn, is readily converted into software capable of operating the actual machinery on a ship. Equation Section 3

B. NUMERICAL SOLUTION OF THE EQUATIONS OF MOTION

Equation 2.25 is a set of simultaneous non-linear, ordinary differential equations. Provided sufficient information about the ship's initial condition is known, the vector of time derivatives on the left-hand side of that equation can be found numerically for all subsequent times. After substantial testing of various differential equation solvers, Euler Integration was selected for all model simulations. This straightforward, iterative method is based on the assumption that an adequate guess about the value of any time-varying function over a sufficiently short, finite time interval, Δt, can be obtained from the combination of the function's value and its first time derivative at the outset of the time interval. Successive function value guesses are of the form:

$$\mathbf{X}_{t+1} = \mathbf{X}_t + \left(\Delta t * \dot{\mathbf{X}}_t\right) \tag{3.1}$$

The choice of Euler Integration was driven primarily by the desire to use an optimization routine to select fin angles. Optimization requires a great number of calculations to be performed quickly. Although the accuracy of Euler Integration is only first order, $O(h)$, this was deemed adequate for purposes of the optimization routines.

C. INPUT, CONTROL DYNAMICS, AND OUTPUT

1. Rudders

A typical flow chart for maneuvering a ship that employs rudders as the primary steering device, outfitted with steering machinery similar to that used in the model, is presented in Figure 7.

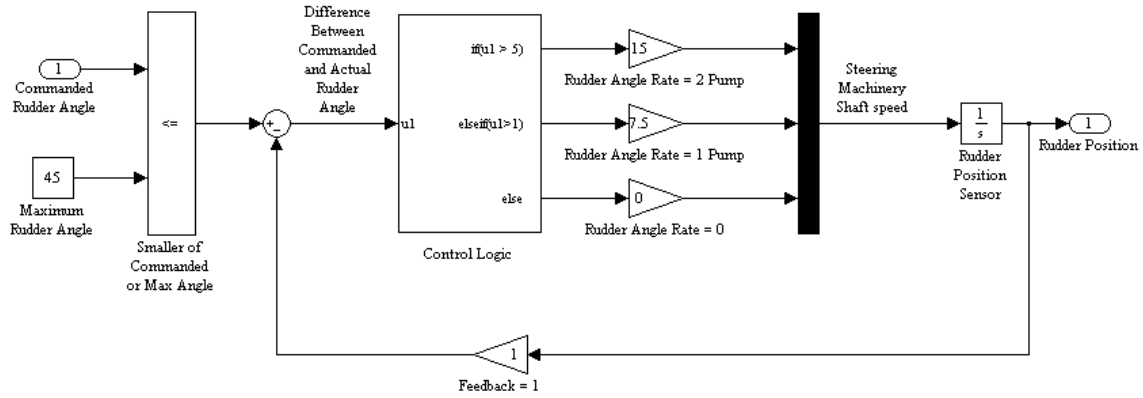

Figure 7. Rudder Dynamics and Control Schematic.

A helm command is converted to a commanded rudder angle signal, $\delta_{Commanded}$. This signal is compared to the signal value at the maximum rudder angle. The signal provided by the rudder position sensor is subtracted from the smaller of these input signals. If the difference between these signals is large, the steering machinery is operated at a higher rate than if the difference is small. If the difference is very small, the commanded angle is deemed equal to the actual angle and the steering machinery is idled. The model employs a control logic that differs slightly from that presented in the figure. A real controller operates with imperfect feedback. To keep a real system from continuously making minute adjustments, some misalignment between commanded and actual rudder angles is tolerated. Since the model is not constrained in this way, the model's control logic tolerance is set to an unrealistic .001 degrees. Real helm commands can be originated manually or from an autopilot. The model does not include an autopilot simulator; all helm commands were treated as if originated manually.

2. Fins

Fin stabilizers are normally added to a ship design to accomplish a single purpose: provide roll-canceling moments. Fin deployment therefore directly affects roll angle, ϕ. In addition to providing roll moment generating lift, fluid flowing across the fins dissipates energy through drag. Throughout the useful range of fin angles of attack, the amount of energy lost will increase as the magnitude of the fin angle increases. Accordingly, surge velocity and total distance traveled are adversely affected by deploying fins. Numerical assessment of the surge velocity at each time step, $u(t)$, is a direct output of the Euler Integration. Distance traveled is simply:

$$\sum_{t=0}^{t=t_f} u(t) * \Delta t \tag{3.2}$$

Distance traveled in each simulation is therefore easily obtained from the Euler Integration surge velocity output. Since the primary focus of this study is on maneuver, the vessel's position in the inertial reference frame was also of interest. The time derivatives of position in the inertial frame were obtained through transformation of the body-fixed velocity components as follows:

$$\dot{\phi} = p \tag{3.3}$$

$$\dot{\psi} = r\cos(\phi) \tag{3.4}$$

$$\dot{x} = u\cos(\psi) - v\sin(\psi)\cos(\phi) \tag{3.5}$$

$$\dot{y} = u\sin(\psi) + v\cos(\psi)\cos(\phi) \tag{3.6}$$

Position in the inertial frame was obtained through Euler Integration of these time derivatives. Since the study was limited to a surface ship maneuvering on a calm ocean, z = 0 was maintained throughout.

Ships equipped with fin stabilizers rarely use manual input to command the fins; nor are typical fin stabilizer systems designed for use during rapid maneuvering. Indeed, many fin operating manuals caution against both of these practices. [See, *e.g.*, USCG TP 3907 (1999)]. Current reality notwithstanding, to quantify the way fin stabilizer angles

affect ship maneuvers, the model accepts user input for the angle of attack of each fin, $\alpha_{P\,Commanded}$, $\alpha_{S\,Commanded}$, as well as the angle between horizontal and the spanwise direction of each fin, $\beta_{P\,Commanded}$, $\beta_{S\,Commanded}$. Figure 8 depicts the control logic used for these model tests.

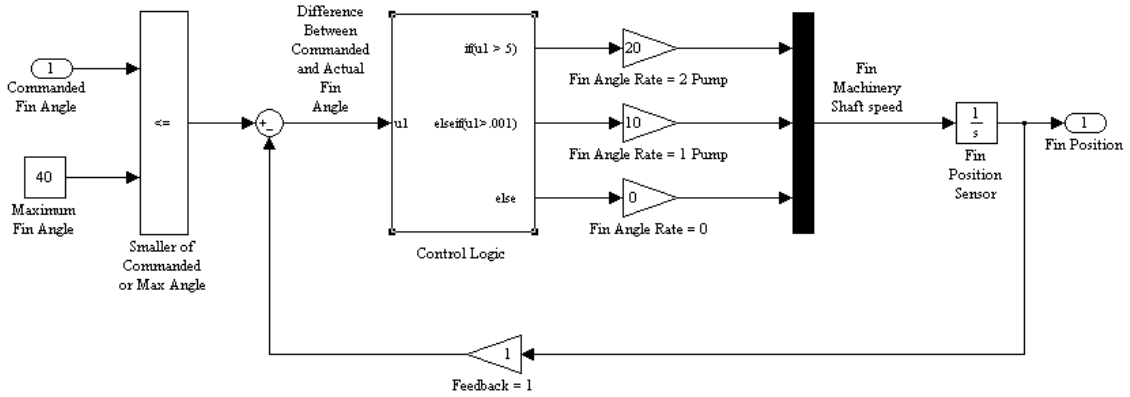

Figure 8. Fin Stabilizer Dynamics and Control Schematic.

3. Combined Equations

The model combines all input and output into a single equation:

$$\begin{bmatrix} u \\ v \\ p \\ r \\ \phi \\ \psi \\ x \\ y \\ \alpha_P \\ \alpha_S \\ \beta_P \\ \beta_S \\ \delta \end{bmatrix}_{t+\Delta t} = \begin{bmatrix} u \\ v \\ p \\ r \\ \phi \\ \psi \\ x \\ y \\ \alpha_P \\ \alpha_S \\ \beta_P \\ \beta_S \\ \delta \end{bmatrix}_t + \left(\Delta t * \begin{bmatrix} \dot{u} \\ \dot{v} \\ \dot{p} \\ \dot{r} \\ \dot{\phi} \\ \dot{\psi} \\ \dot{x} \\ \dot{y} \\ \dot{\alpha}_P \\ \dot{\alpha}_S \\ \dot{\beta}_P \\ \dot{\beta}_S \\ \dot{\delta} \end{bmatrix}_t \right) \tag{3.7}$$

D. CONTROLS FIXED DIRECTIONAL STABILITY

Directional stability is a measure of how well a vessel maintains a steady course with no changes in control input. For a self-propelled surface ship, horizontal plane directional stability is only possible if the vessel's original course is a straight line. [Papoulias (1995)]. Even then, a surface ship will only have controls-fixed directional stability if Inequality 3.8 is true:

$$C_{DS} = \left(N_{|u|r} - mx_G U_0 \right) Y_{|u|v} - \left(Y_{ur} - mU_0 \right) N_{|u|v} > 0 \tag{3.8}$$

For all non-negative values of initial surge velocity, U_0, the modeled vessel does not satisfy this inequality. As the initial surge velocity increases, C_{DS} becomes increasingly negative. Thus, as a first test of the model, plots were made with all input and all initial conditions except surge velocity set to zero. Figure 9 demonstrates that for all appreciable surge velocities, the model lacks directional stability: the vessel executes a turn to starboard even when the only disturbance is contributed by the cumulative error of numerical integration.

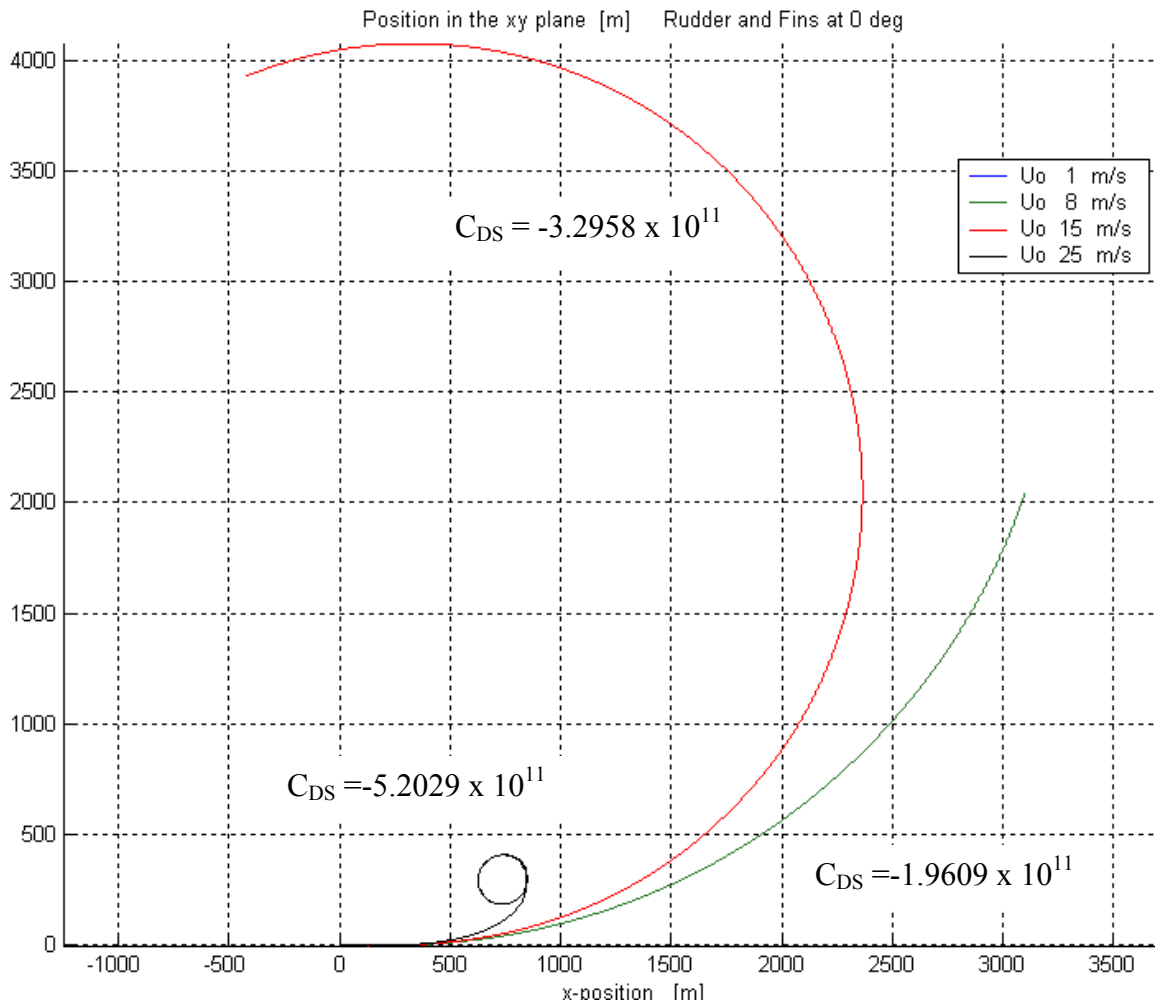

Figure 9. Controls Fixed Course History.

The ship's roll angle response with no control surface input in all simulations up to 35 knots is small. The inward roll angle remains less than 0.15° and the steady outward heel angle does not exceed 3.5°. While a simulated surge velocity of about 48 knots produced a roll capable of capsizing the ship, as the response is entirely devoid of oscillations and other dynamic effects, it is discounted. This response casts doubt on the model's ability to accurately simulate extremely high speed operation. In defense of the model, it is unlikely that this ship design is capable of achieving speeds approaching 48 knots.

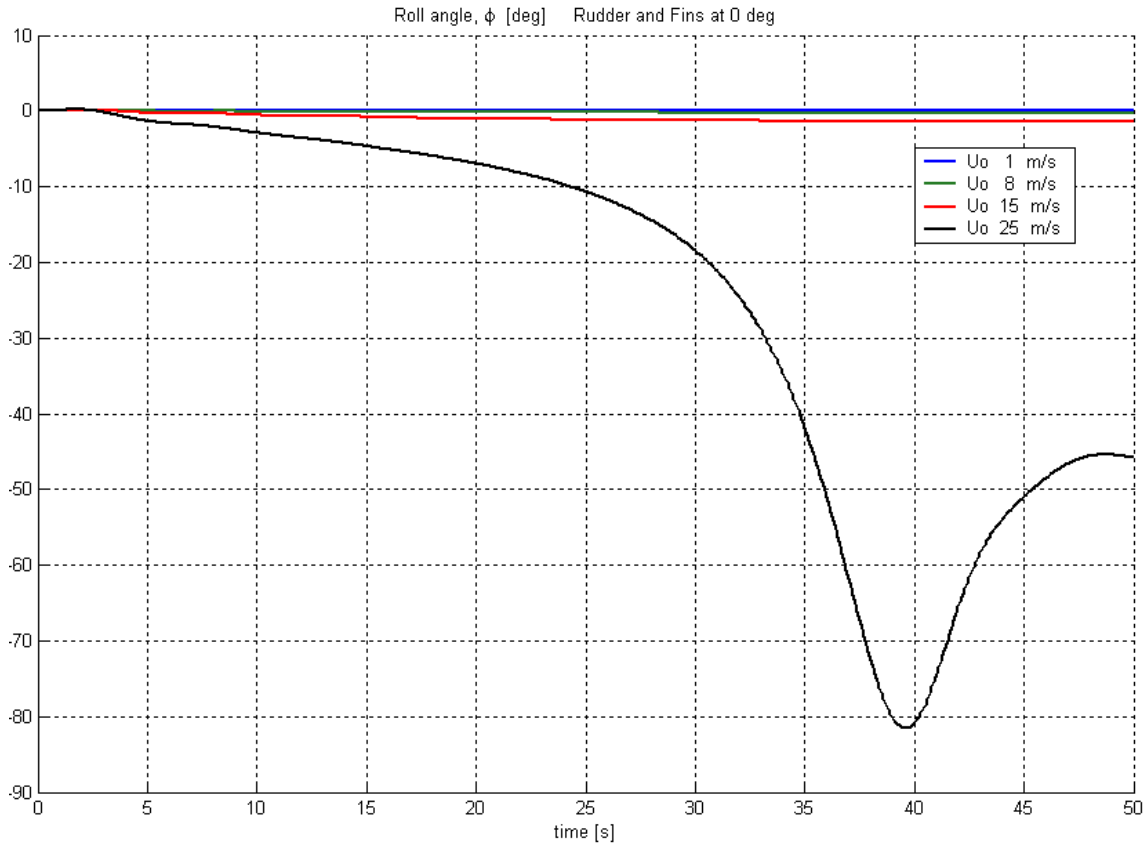

Figure 10. Controls Fixed Roll History.

THIS PAGE INTENTIONALLY LEFT BLANK

IV. BASIC TURNS WITH RUDDERS AND FINS

A. EFFECTS OF RUDDERS ALONE

To establish a baseline of vessel turning performance, a battery of tests over a simulated time period of 150 seconds was conducted using various combinations of rudder angle and initial surge velocity. For this series of tests, fin angles were $\alpha_P = \alpha_S = \beta_P = \beta_S = 0^\circ$.

1. Slow Speed Turns

At very low initial surge velocity, near bare steerageway, large rudder angles are necessary to effect a turn. Negative rudder angles produce a turn to starboard; positive rudder angles produce a turn to port. Both roll angle and the change in surge velocity are negligible. Neither of these parameters is in steady state at 50 seconds.

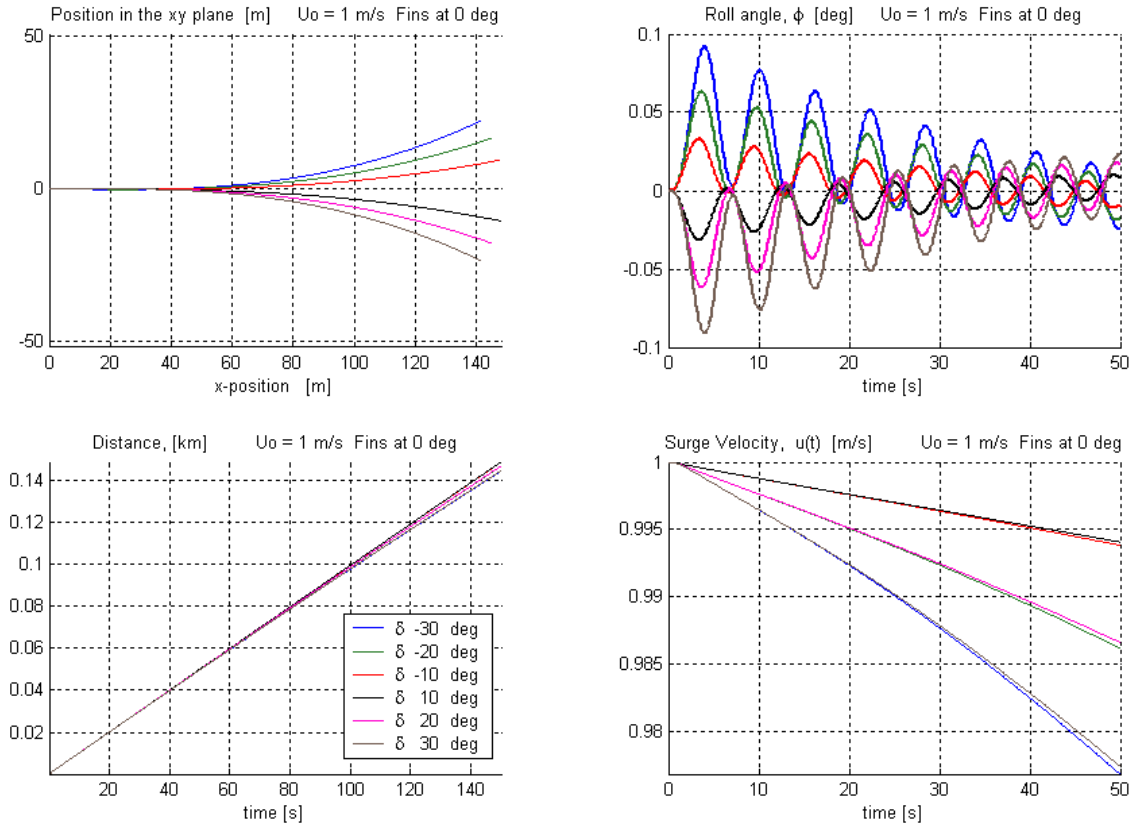

Figure 11. Slow Speed Rudder Only.

2. Moderate Speed Turns

At speeds between about 8 and 25 knots, large rudder angles can still be used safely, but the cost in surge velocity is dramatically increased. For negative rudder angles, an initial positive roll (port side up, or inward heel) is followed by a negative roll (outward heel). The roll angle oscillates, crossing the upright position several times, before approaching a steady outward heel before 50 seconds have elapsed. Positive rudder angles produce the mirror image of this effect. The decrease in surge velocity is no longer negligible, and, for higher speeds, it reaches steady state at about 50 seconds.

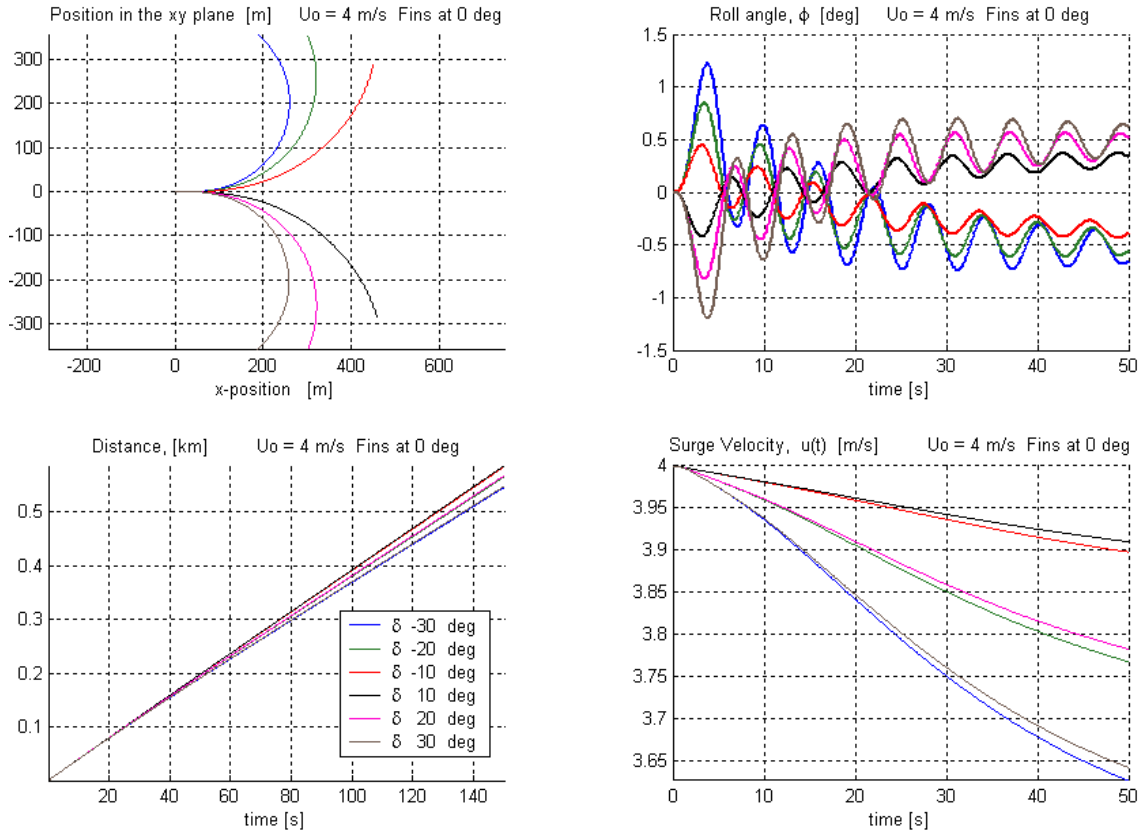

Figure 12. 8 Knots Rudder Only.

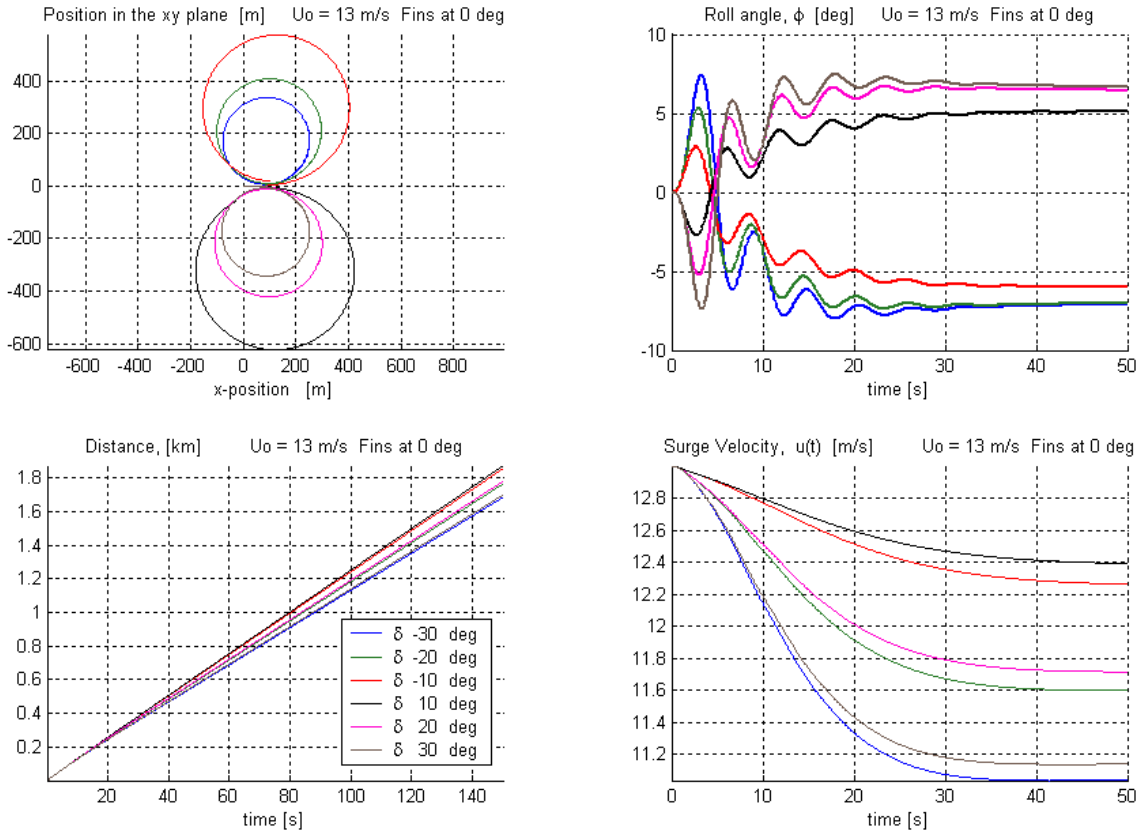

Figure 13. 25 Knots Rudder Only.

3. High Speed Turns

Above 25 knots, even moderate rudder commands can induce sustained roll angles exceeding 8 degrees. At 35 knots, sustained roll angles are about 20 degrees, and at 38 knots, sustained roll angles are nearly 30 degrees. In all of these cases, roll angles and surge velocity reach steady state at or before 50 seconds.

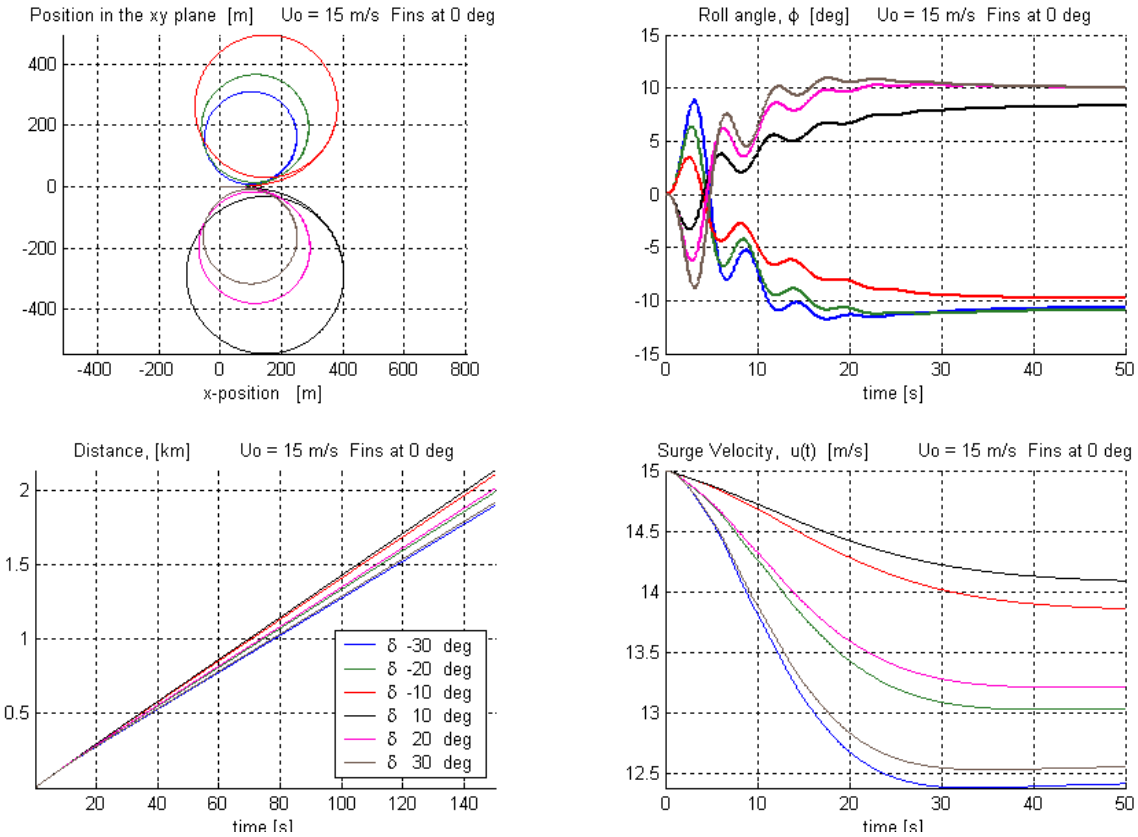

Figure 14. 29 Knots Rudder Only.

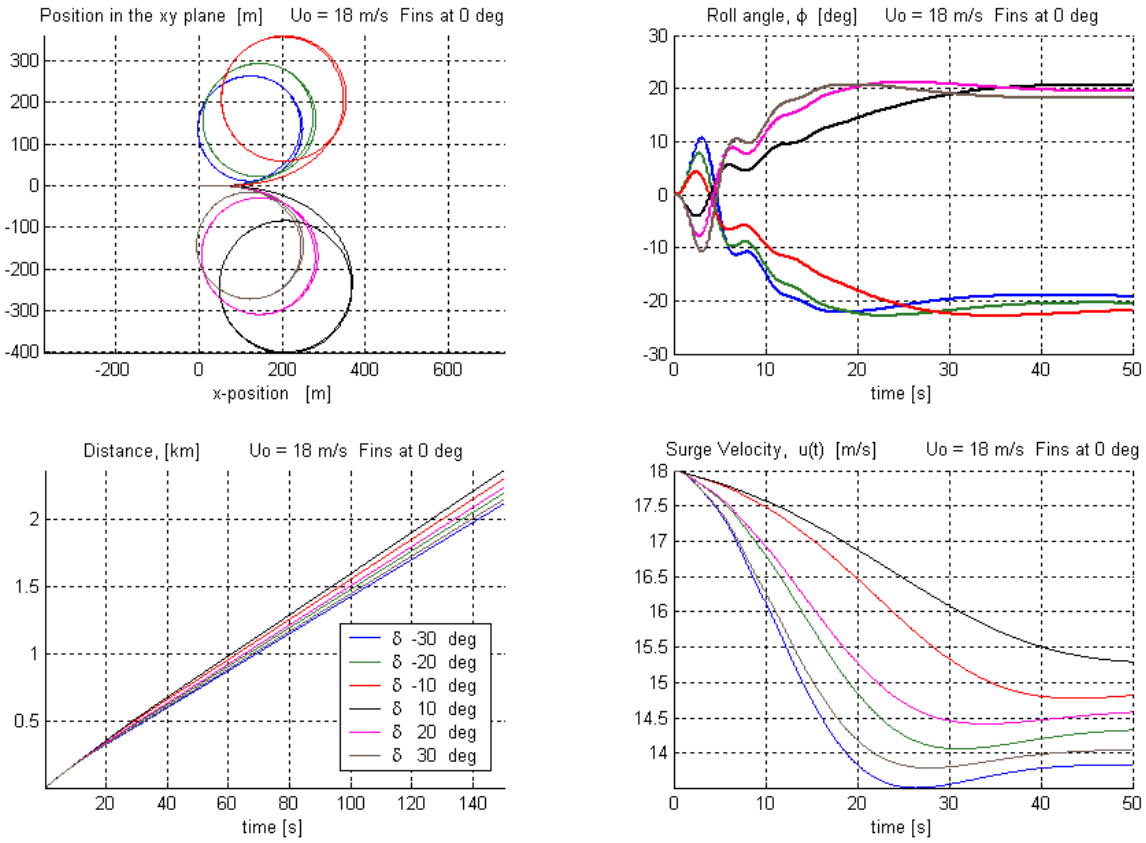

Figure 15. 35 Knots Rudder Only.

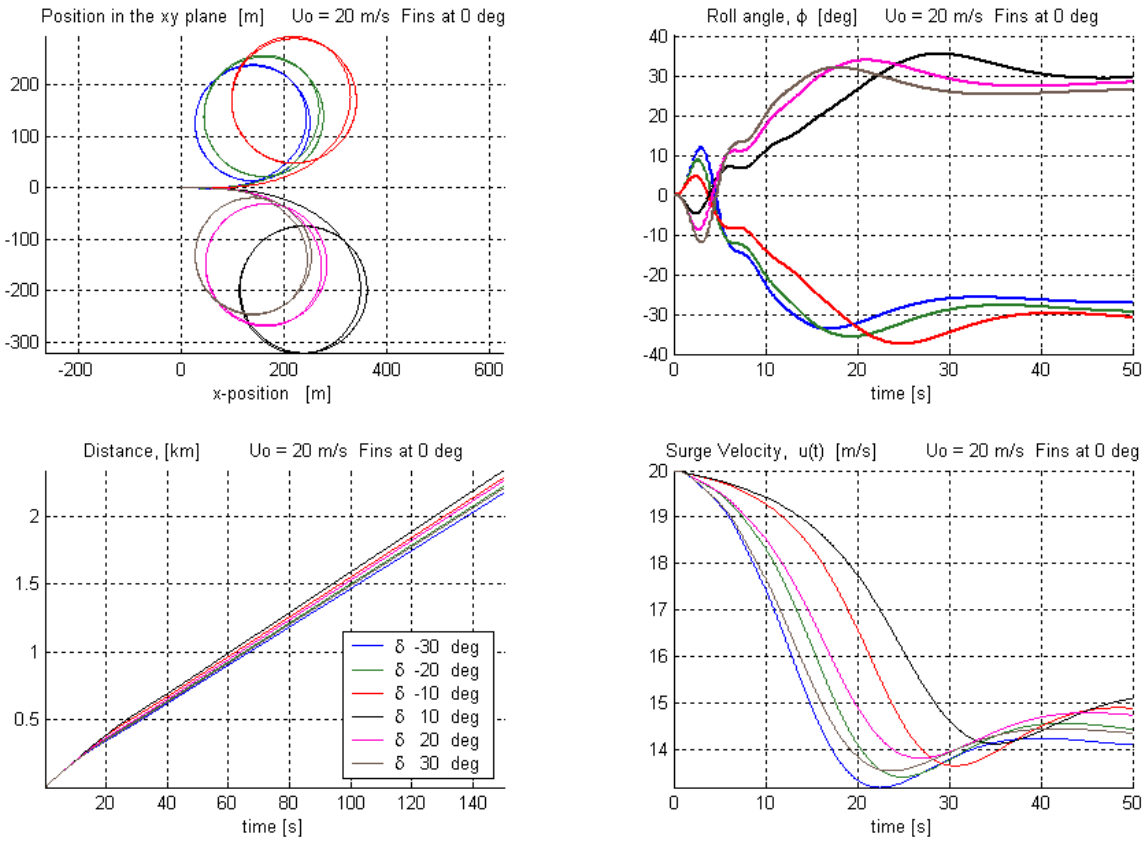

Figure 16. 39 Knots Rudder Only.

B. EFFECTS OF FIN ANGLE OF ATTACK ALONE

A battery of tests over a simulated time period of 500 seconds was conducted using various combinations of fin angle of attack input and initial surge velocity. For these tests, the rudder was held steady amidships and $\beta_p = \beta_s = 34^\circ$ (design setting).

1. Fin Angles Paired for Maximum Roll Moment

With $\alpha_P = \alpha_S$, both positive, at moderate speed the vessel experiences heading change to port along with roll to port (inward heel). Both effects increase as the fin angle of attack is increased. Significantly, no outward heel is developed. Neither surge velocity nor roll reach steady state within the first 50 seconds. Roll angles and surge velocity losses tend to increase as α increases, but the loss in surge velocity for mid-range α departs from this trend.

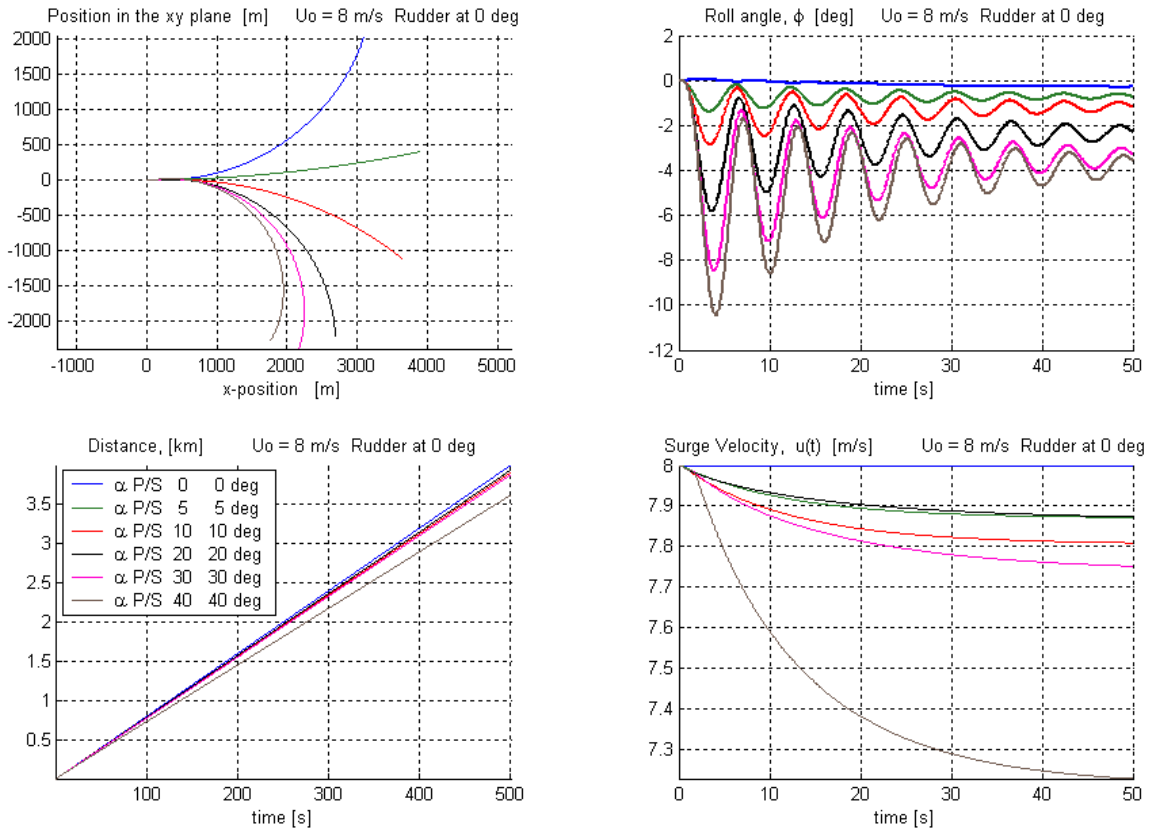

Figure 17. 15.5 Knots, No Rudder – Fins: Angles of Attack Paired >0 $\beta_p = \beta_s = 34^\circ$.

At higher speed, small values of α cause a heading change to port, but large α causes heading change to starboard. The remaining effects are similar to those observed for moderate speeds.

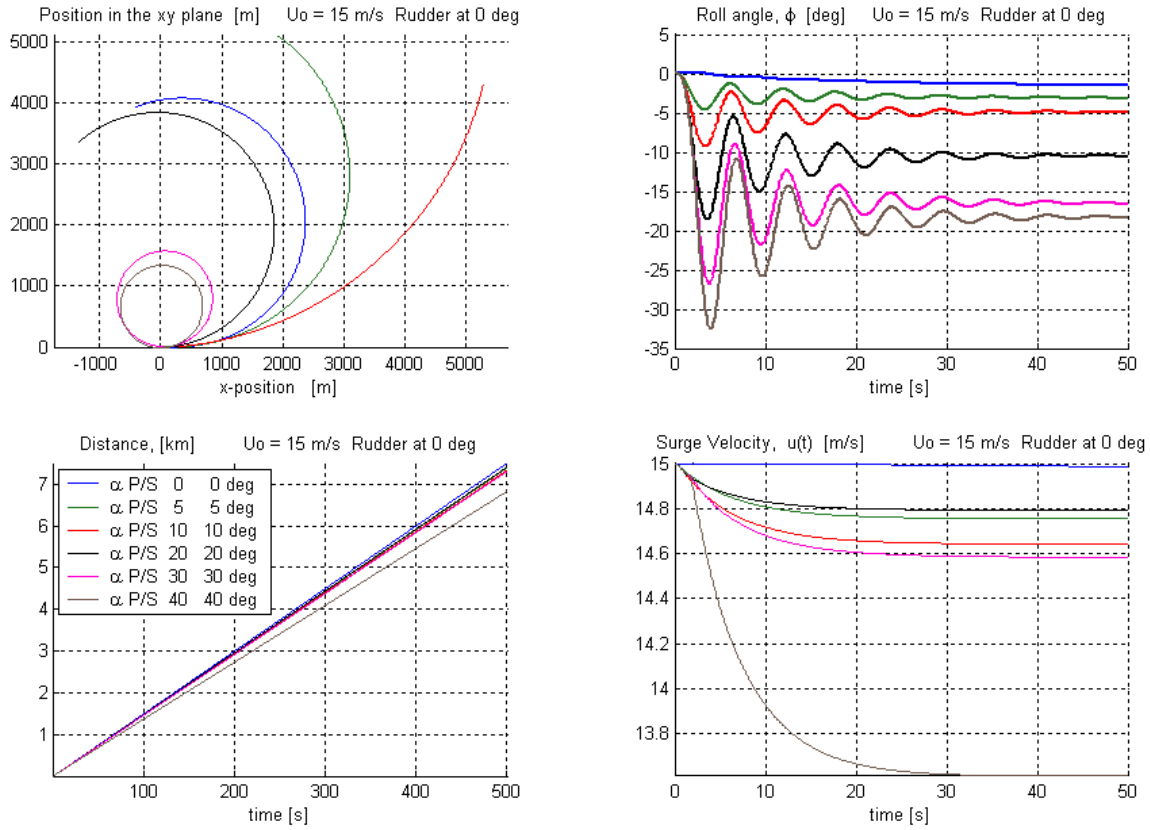

Figure 18. 29 Knots, No Rudder – Fins: Angles of Attack Paired >0 $\beta_p = \beta_s = 34^\circ$.

With $\alpha_P = \alpha_S$, both negative, at moderate speed the vessel's natural tendency to steer to starboard is enhanced, and a roll to starboard is induced. Both effects increase as the fin angle of attack is increased. For all cases, surge velocity approaches steady state within the first 50 seconds but roll angle does not.

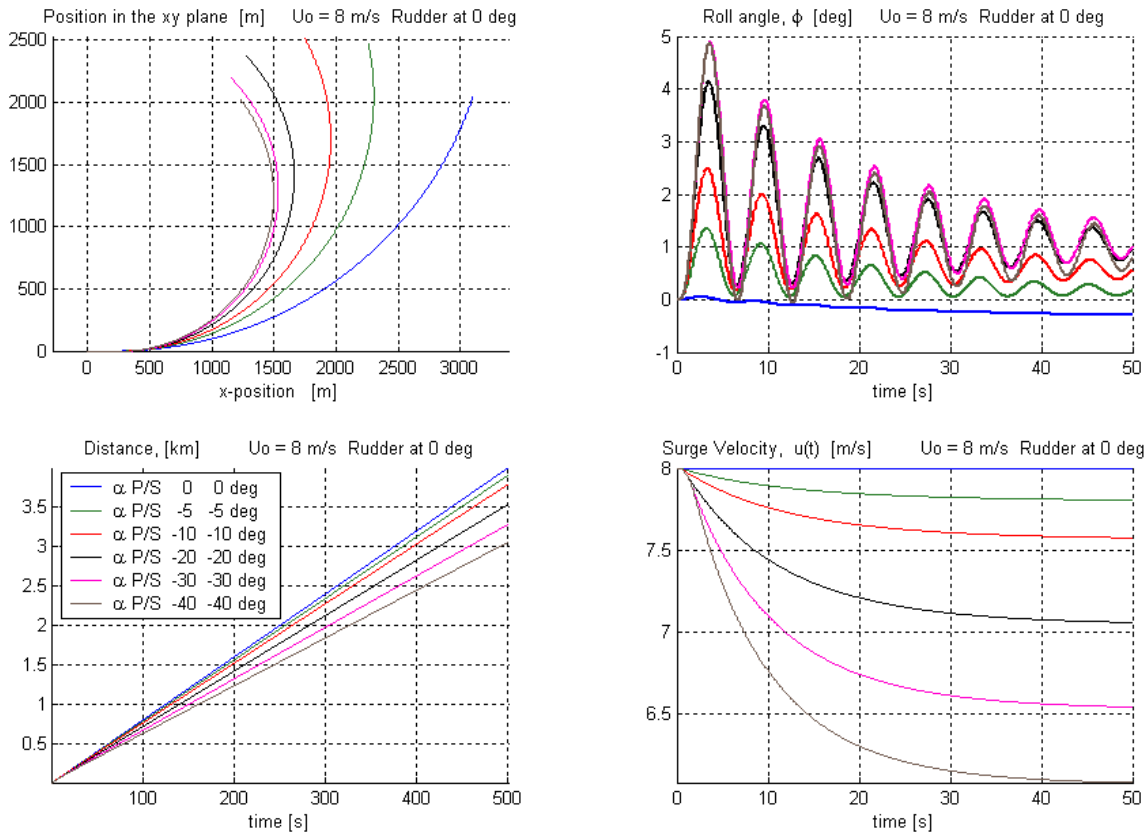

Figure 19. 15.5 Knots, No Rudder – Fins: Angles of Attack Paired <0 $\beta_p = \beta_s = 34^\circ$.

At higher speed, the ship's natural tendency to turn to starboard is diminished. For all but the largest fin angle, this effect increases as α increases. Nor does the largest fin angle produce the greatest steady state roll angle. This is probably because the surge velocity is reduced so much that the roll angle and turning radius become constrained.

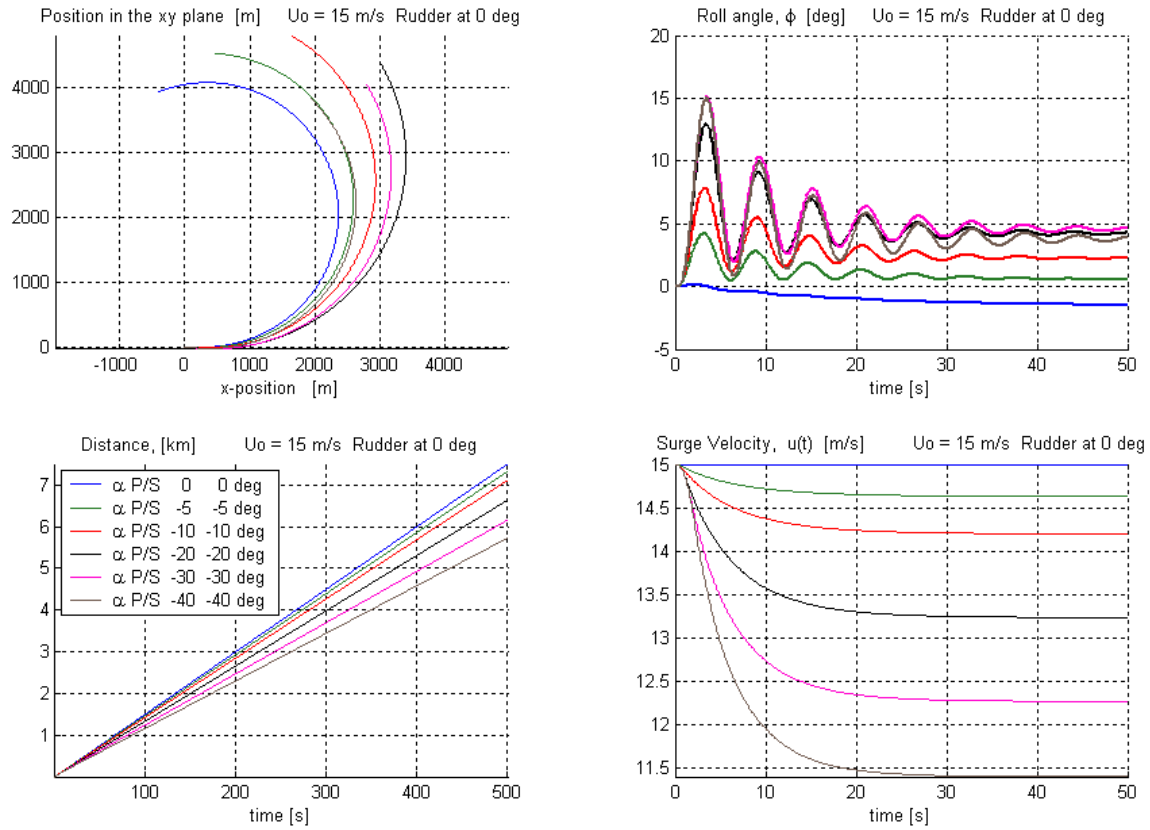

Figure 20. 29 Knots, No Rudder – Fins: Angles of Attack Paired <0 $\beta_p = \beta_s = 34^\circ$.

2. Net Fin Angle of Zero

As expected, with $\alpha_P = -\alpha_S$, either one positive, the vessel experiences significantly less roll with this configuration than with paired fin angles. There remains, however, a fairly strong link between the magnitude of fin angle of attack and the magnitude of heading change even when the net fin angle is zero. As the magnitude of α increases, the ship's natural tendency to turn to starboard is diminished, and finally, overcome. Both surge and roll angle approach steady state within 50 seconds.

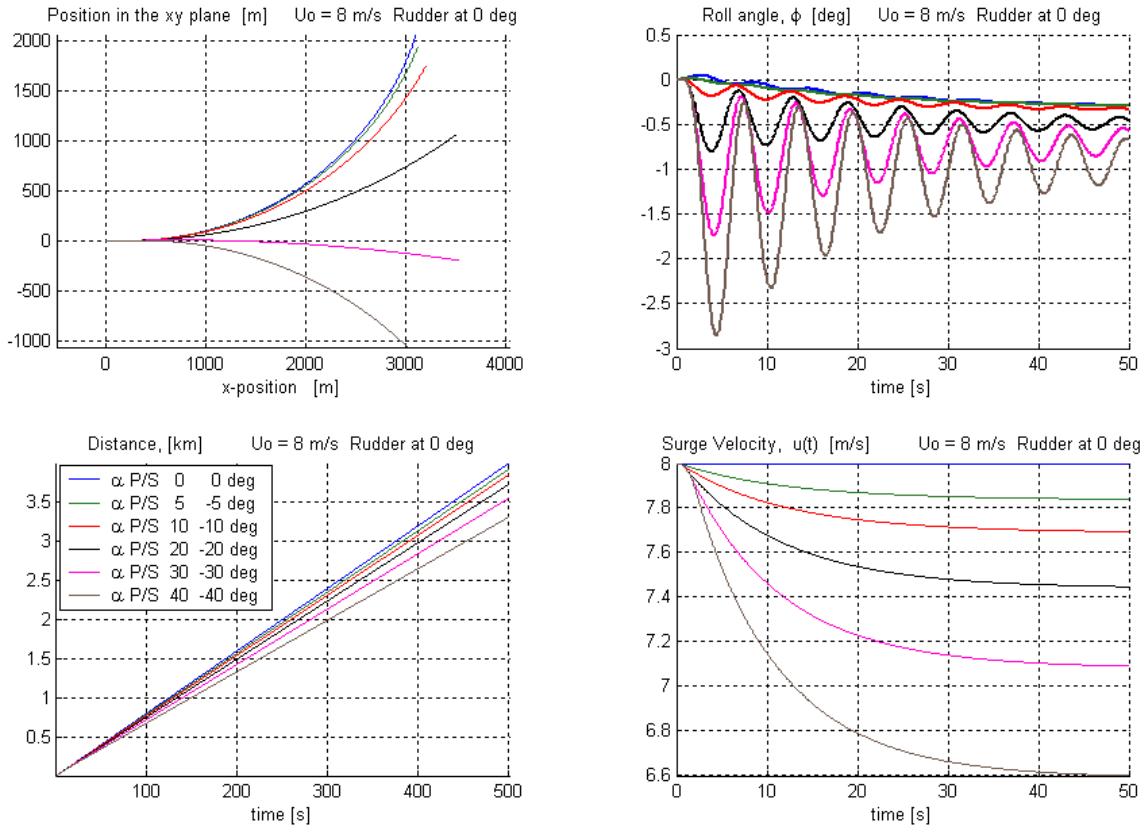

Figure 21. 15.5 Knots, No Rudder – Fins: Angles of Attack Sum to 0, Port >0 $\beta_p = \beta_s = 34^\circ$.

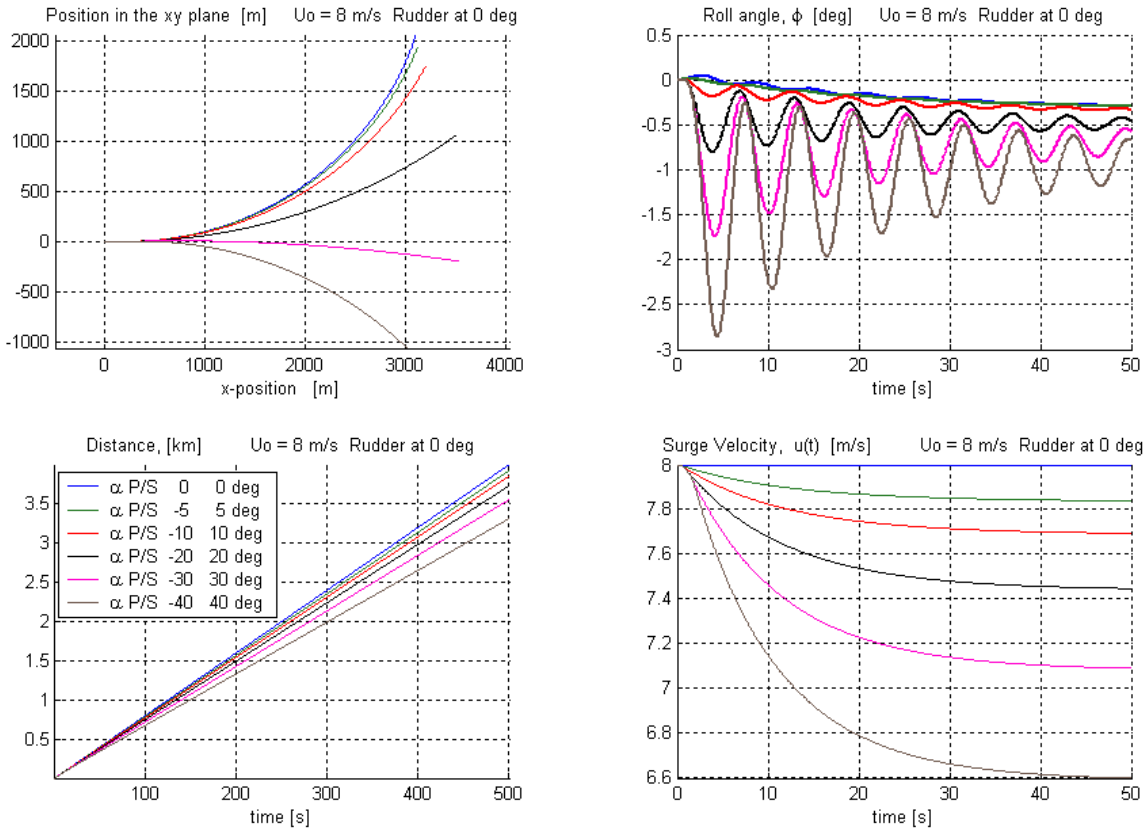

Figure 22. 15.5 Knots, No Rudder – Fins: Angles of Attack Sum to 0, Port <0 $\beta_p = \beta_s = 34^\circ$.

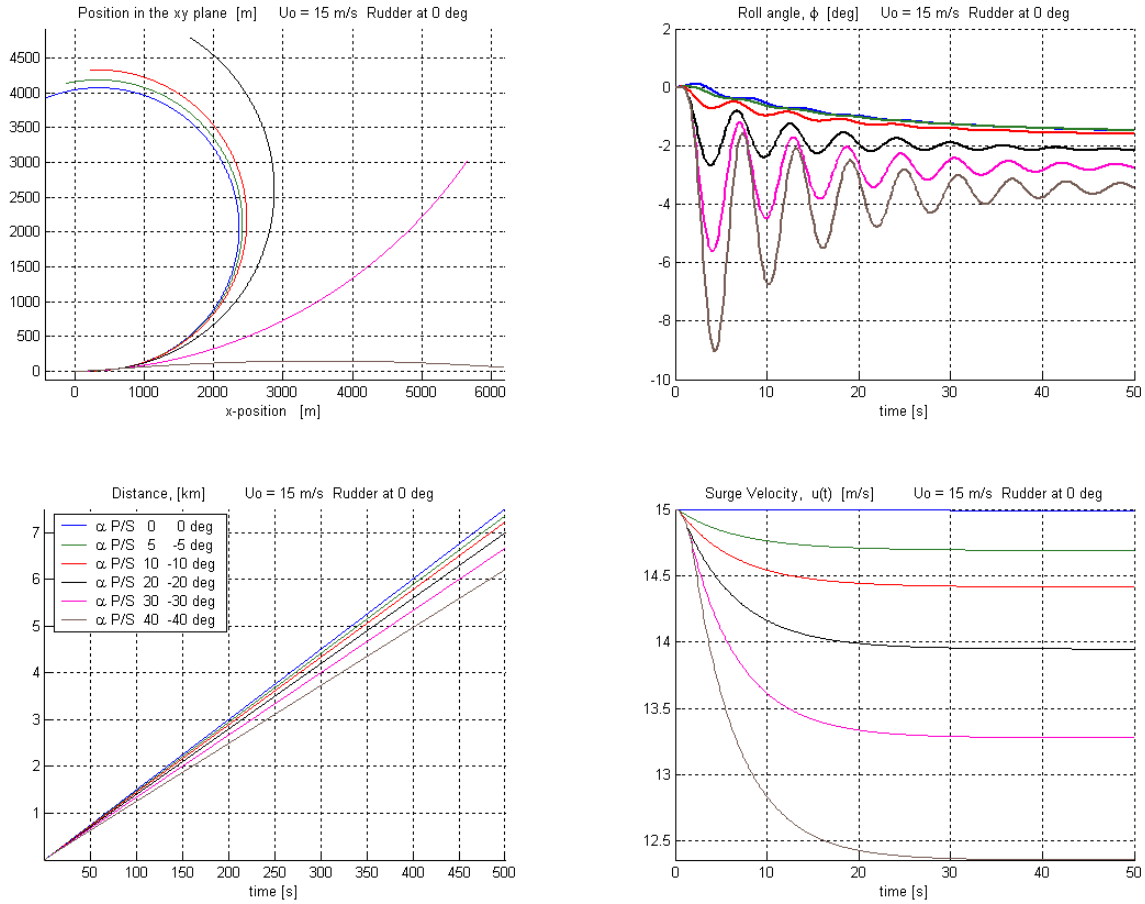

Figure 23. 29 Knots, No Rudder – Fins: Angles of Attack Sum to 0, Port > 0 $\beta_p = \beta_s = 34^\circ$.

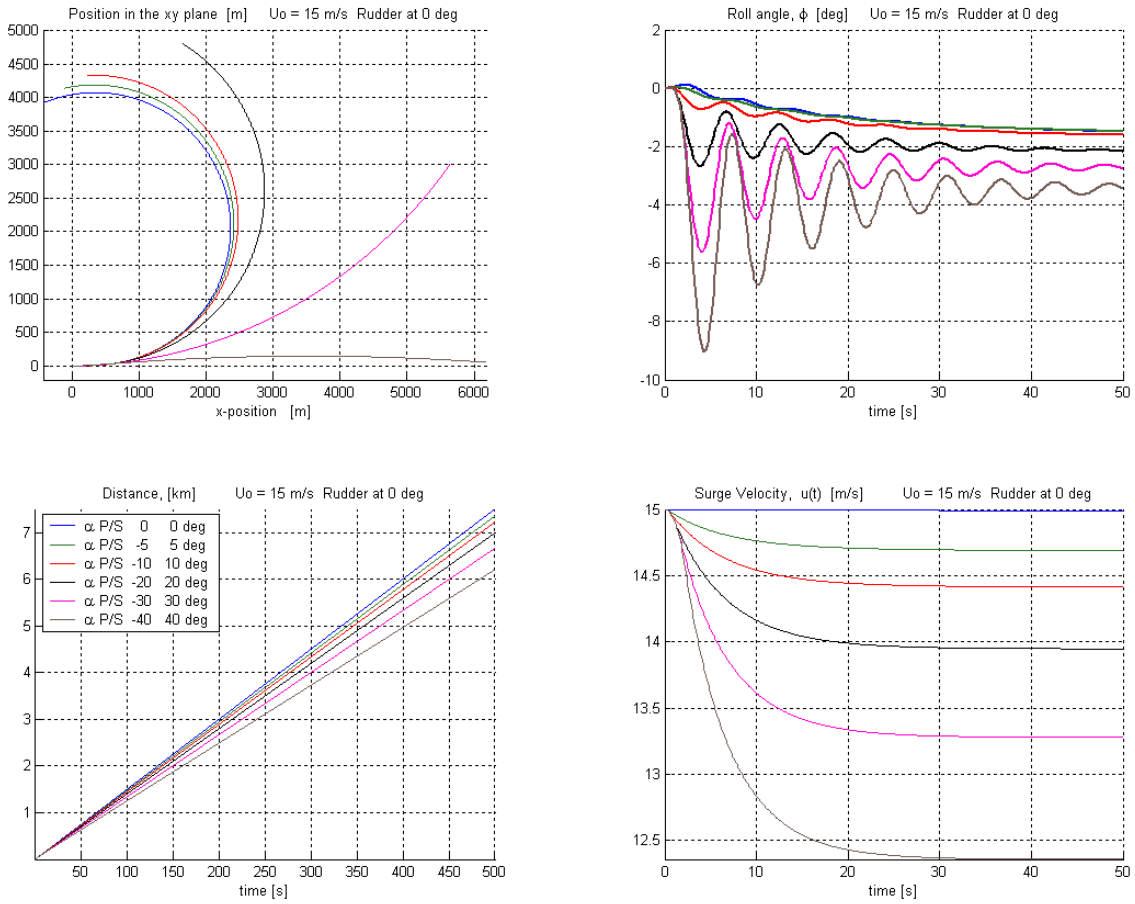

Figure 24. 29 Knots, No Rudder – Fins: Angles of Attack Sum to 0, Port <0 $\beta_p = \beta_s = 34^\circ$.

3. Fin Angles Mixed

With $\alpha_P + \alpha_S = Constant$, the flexibility afforded by independent control of each fin's angle of attack becomes apparent. Judicious fin angle selection can induce rolls that vary not only in magnitude, but in sense with respect to heading change as well (*i.e.*, inward or outward heel at various angles can be induced).

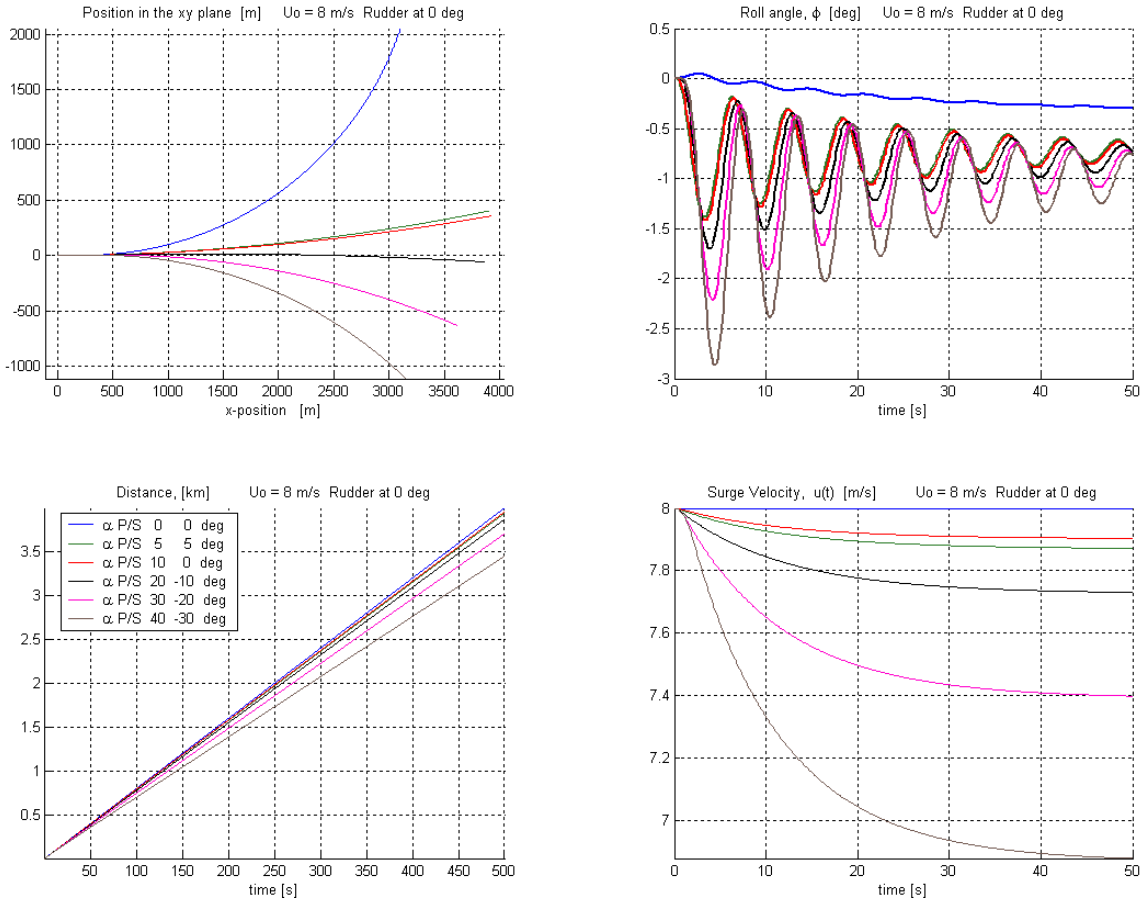

Figure 25. 15.5 Knots, No Rudder – Fins: Angles of Attack Sum to 10, Port ≥ 0 $\beta_p = \beta_s = 34^\circ$.

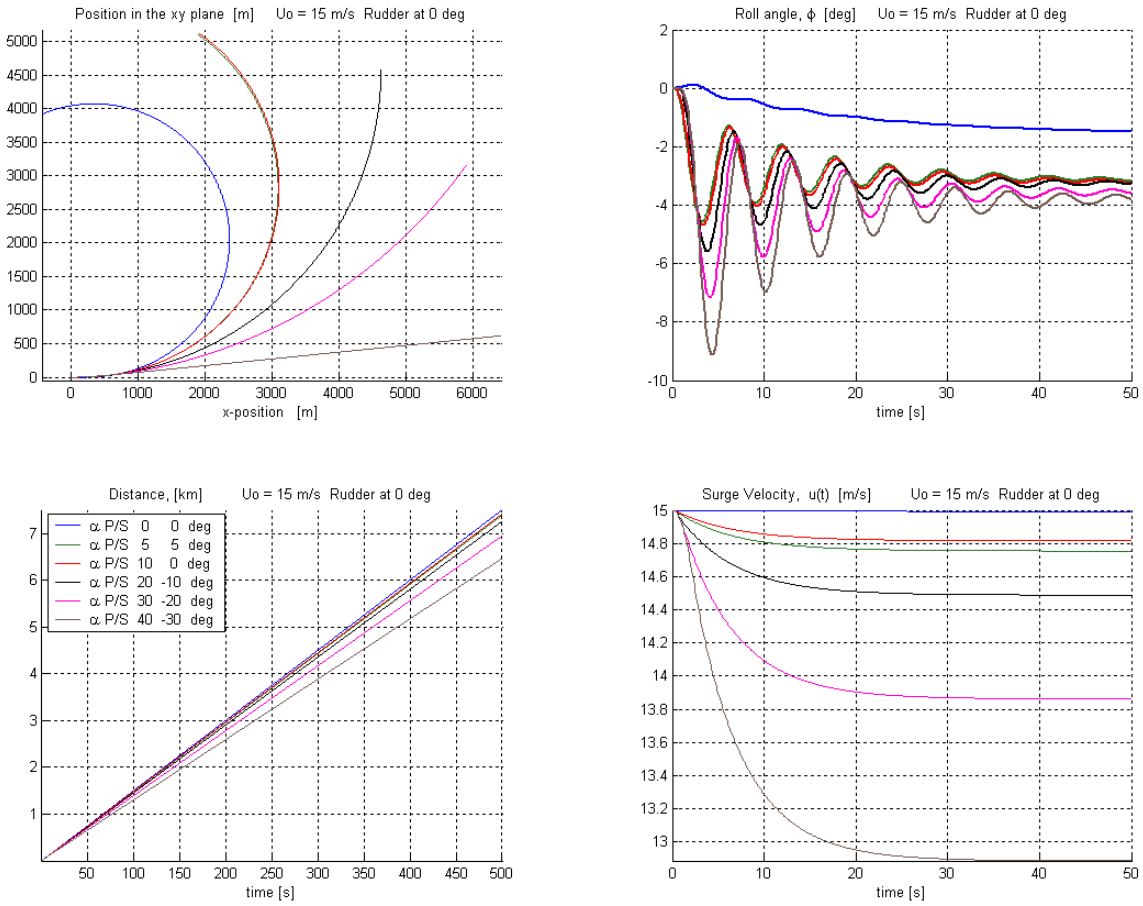

Figure 26. 29 Knots, No Rudder – Fins: Angles of Attack Sum to 10, Port ≥ 0 $\beta_p = \beta_s = 34^\circ$.

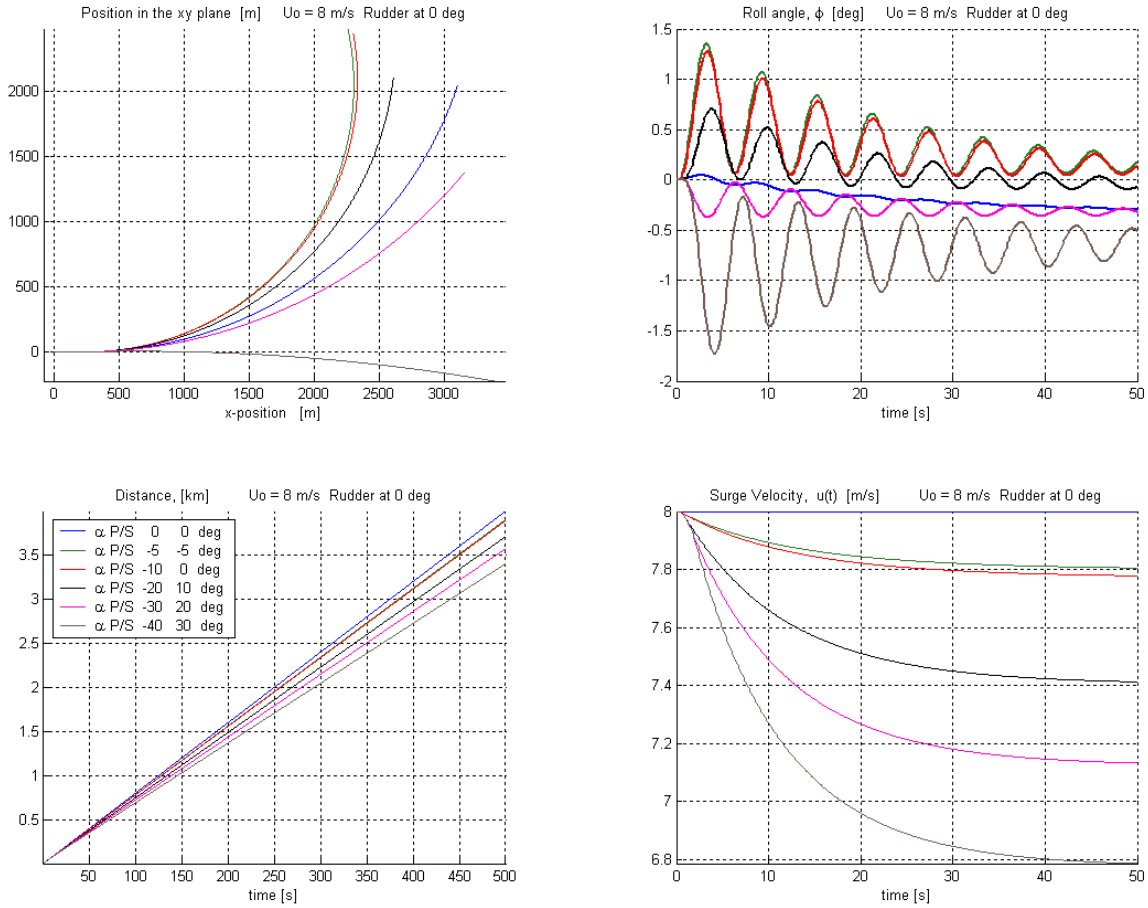

Figure 27. 15.5 Knots, No Rudder – Fins: Angles of Attack Sum to 10, Port ≤ 0 $\beta_p = \beta_s = 34^\circ$.

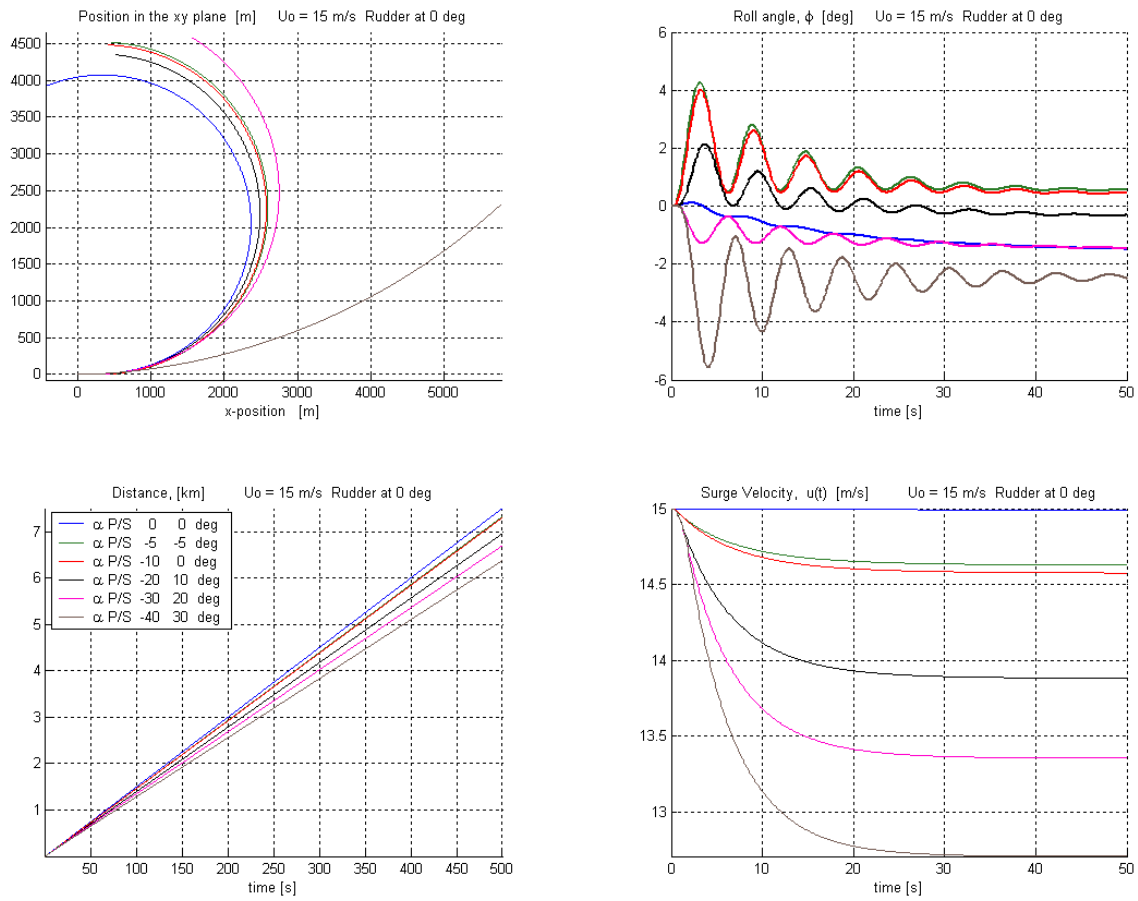

Figure 28. 29 Knots, No Rudder – Fins: Angles of Attack Sum to 10, Port ≤ 0 $\beta_p = \beta_s = 34^\circ$.

C. EFFECTS OF FIN SPANWISE ANGLE β ALONE

A battery of tests over a simulated time period of 500 seconds was conducted using various combinations of fin spanwise angle and angle of attack input. For these tests, the rudder was held steady amidships and initial surge velocity was 15 m/s (about 29 knots).

1. Fin Angle of Attack Nearly Zero

The model is constructed in a way that all fin forces and moments are zero at zero fin angle of attack. The effects of a real fin at about zero angle of attack were simulated using $\alpha_P = \alpha_S = .001^\circ$. With $\beta_P = \beta_S$, as β increases, the ship's natural tendency to turn to starboard is diminished, surge velocity losses and steady state heel angle decrease. Neither surge velocity nor heel angle reaches steady state after 50 seconds.

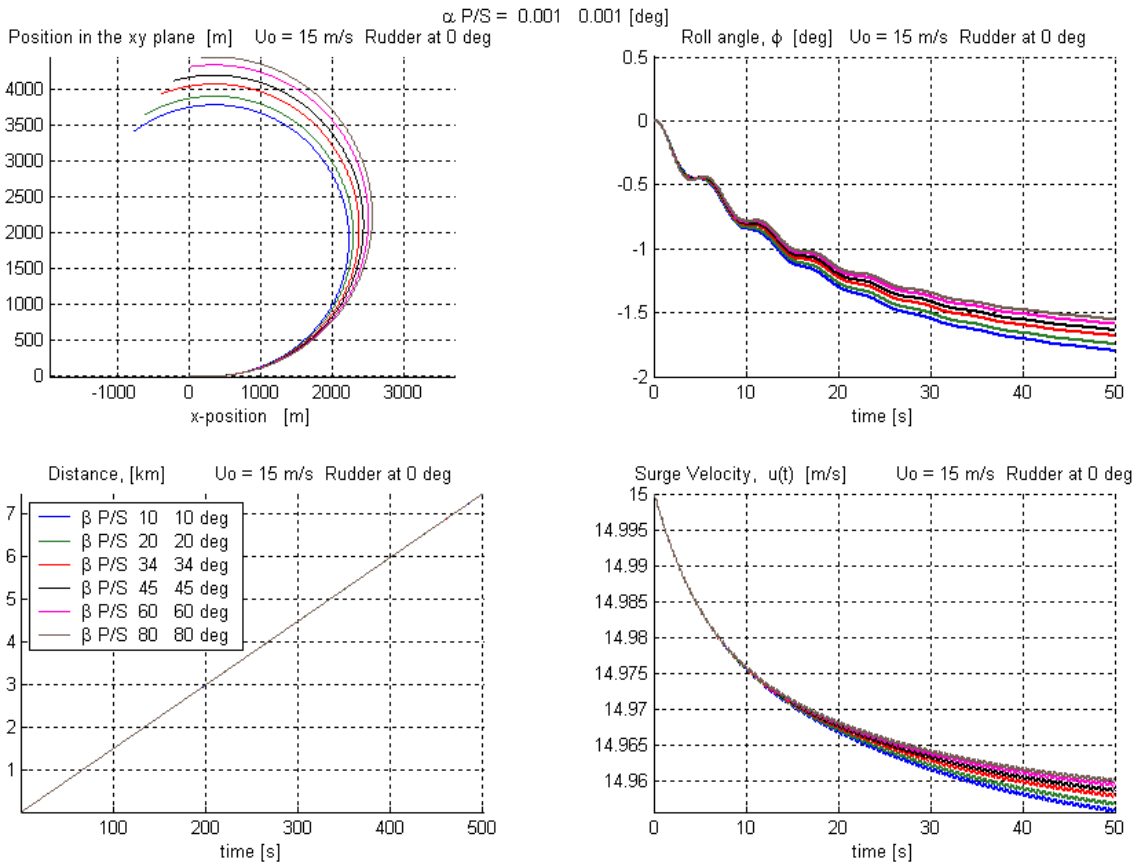

Figure 29. 29 Knots, No Rudder, Fins: $\alpha_P = \alpha_S = .001^\circ \quad \beta_P = \beta_S$.

With $\beta_P = \left|90^\circ - \beta_S\right|$, increasing or decreasing β has virtually no effect on any of the measured parameters.

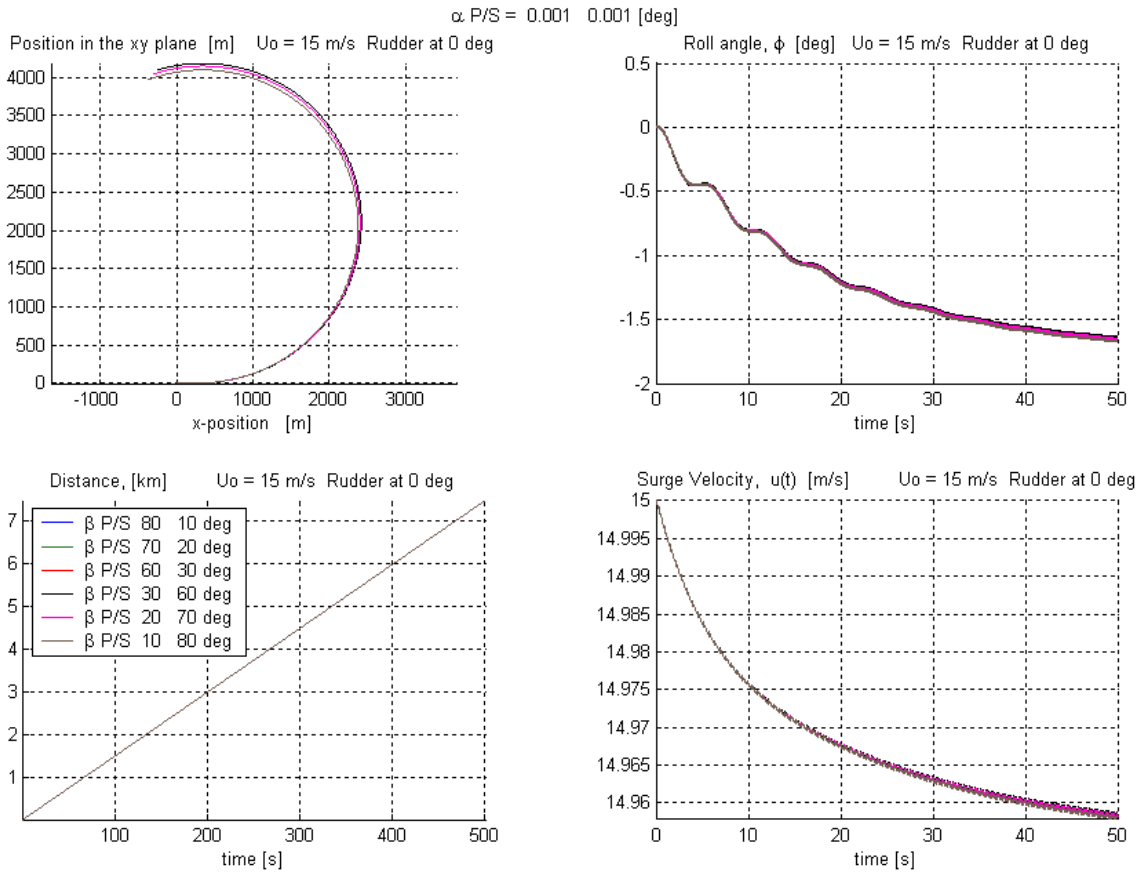

Figure 30. 29 Knots, No Rudder, Fins: $\alpha_P = \alpha_S = .001^\circ \quad \beta_P = \left|90^\circ - \beta_S\right|$.

2. Fin Angle of Attack Paired

With $\alpha_P = \alpha_S = 5^\circ$ and $\beta_P = \beta_S$, increasing β magnifies considerably the fins' neutralizing effect on the ship's natural tendency to turn to starboard. For very large values of β, the starboard turn is overcome and the ship turns to port. The loss in surge velocity and the steady state outward heel angle decrease. For values of $\beta \geq 34^\circ$ surge velocity and heel angle reach steady state within the first 50 seconds.

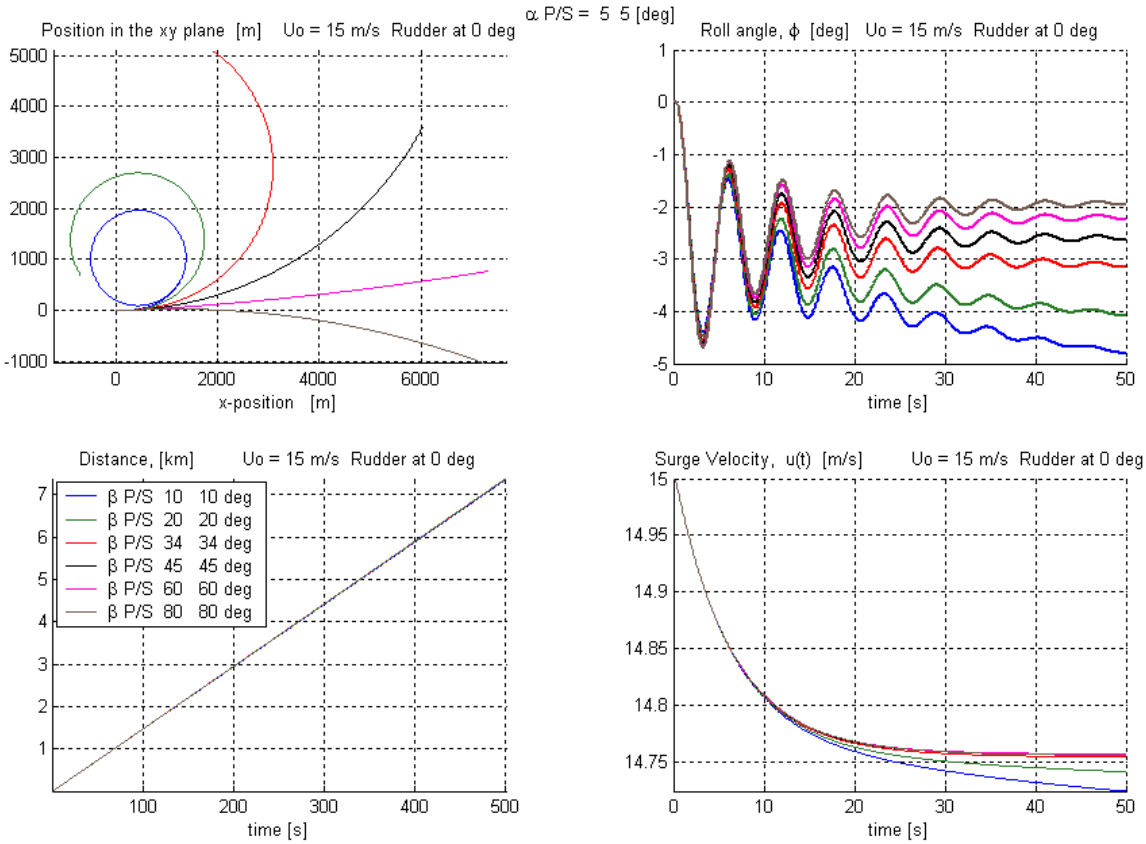

Figure 31. 29 Knots, No Rudder, Fins: $\alpha_P = \alpha_S = 5^\circ \quad \beta_P = \beta_S$.

With $\alpha_P = \alpha_S = -5^\circ$ and $\beta_P = \beta_S$, increasing β magnifies the ship's natural tendency to turn to starboard. The loss in surge velocity increases and the steady state outward heel angle decreases or is replaced by an inward heel angle. Both approach steady state within the first 50 seconds.

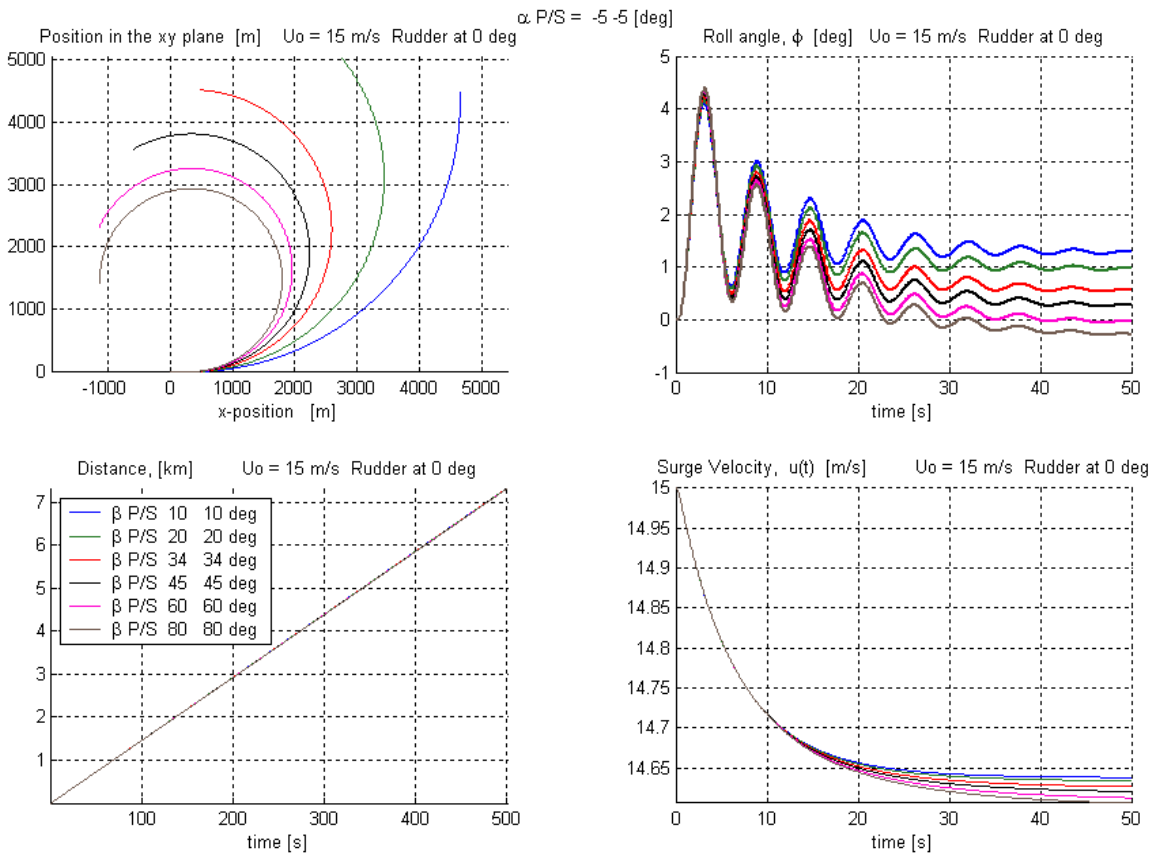

Figure 32. 29 Knots, No Rudder, Fins: $\alpha_P = \alpha_S = -5^\circ \quad \beta_P = \beta_S$.

The results with a fin angle of attack $\alpha_P = \alpha_S = 30^\circ$ are very similar to those with smaller angle of attack. At very small values of β the fins can overcome the ship's natural tendency to turn to starboard.

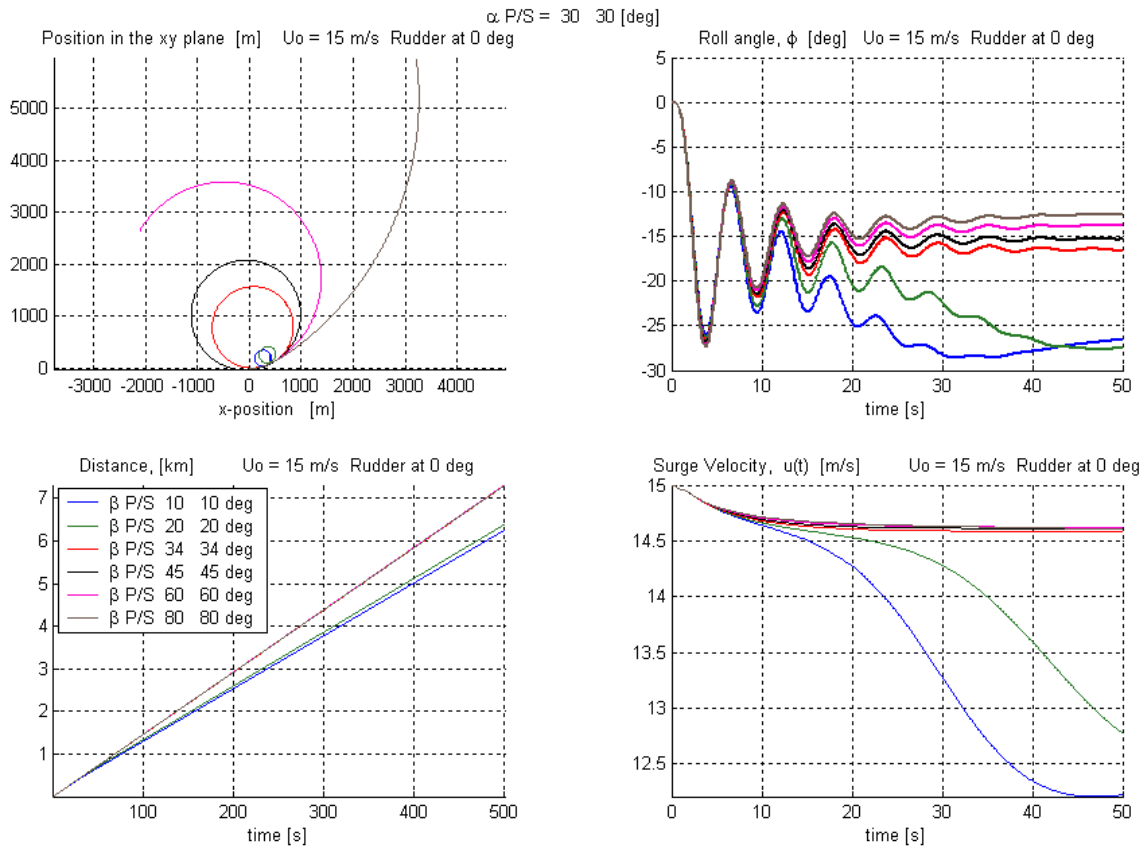

Figure 33. 29 Knots, No Rudder, Fins: $\alpha_P = \alpha_S = 30^\circ \quad \beta_P = \beta_S$.

At a fin angle of attack $\alpha_P = \alpha_S = -30^\circ$ and very small values of β , fin generated forces can overcome the ship's natural tendency to turn to starboard.

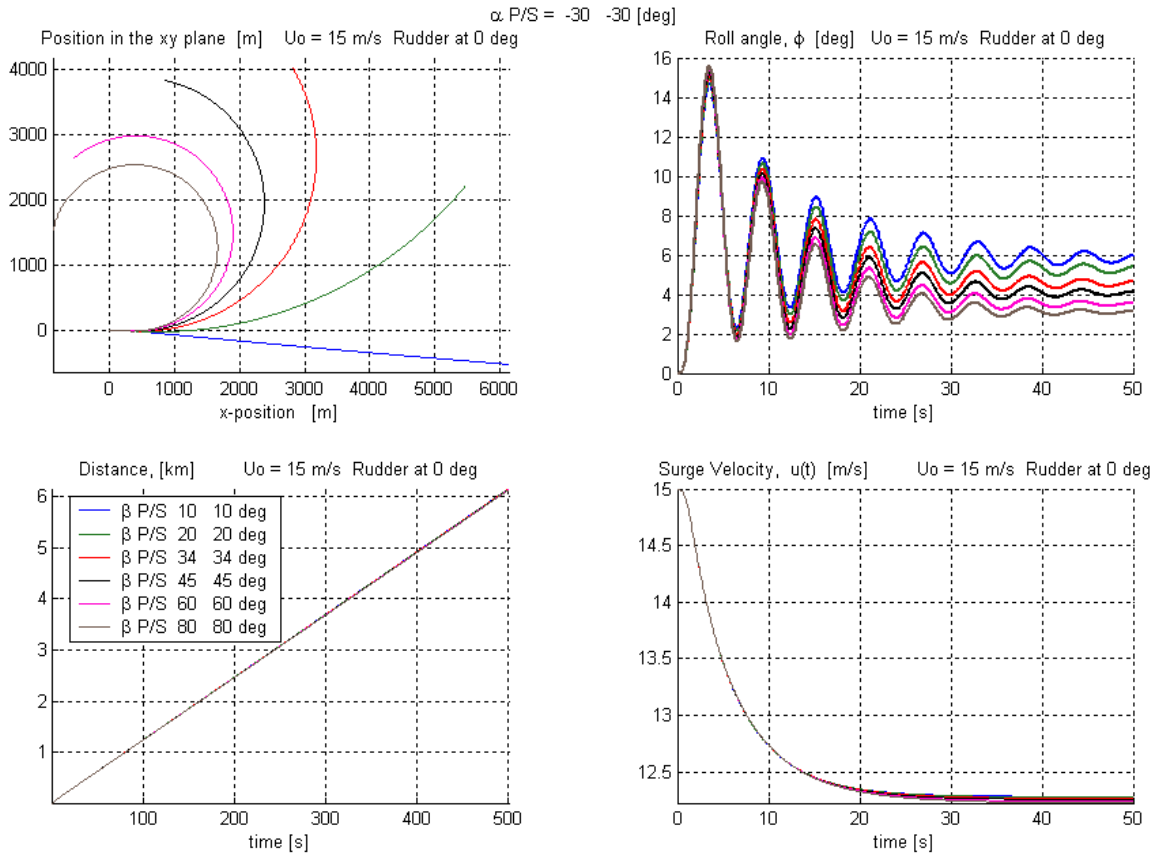

Figure 34. 29 Knots, No Rudder, Fins: $\alpha_P = \alpha_S = -30^\circ \quad \beta_P = \beta_S$.

As was the case with fin angle of attack nearly zero, with $\beta_P = \left|90^\circ - \beta_S\right|$, increasing or decreasing β has very little effect on any of the measured parameters.

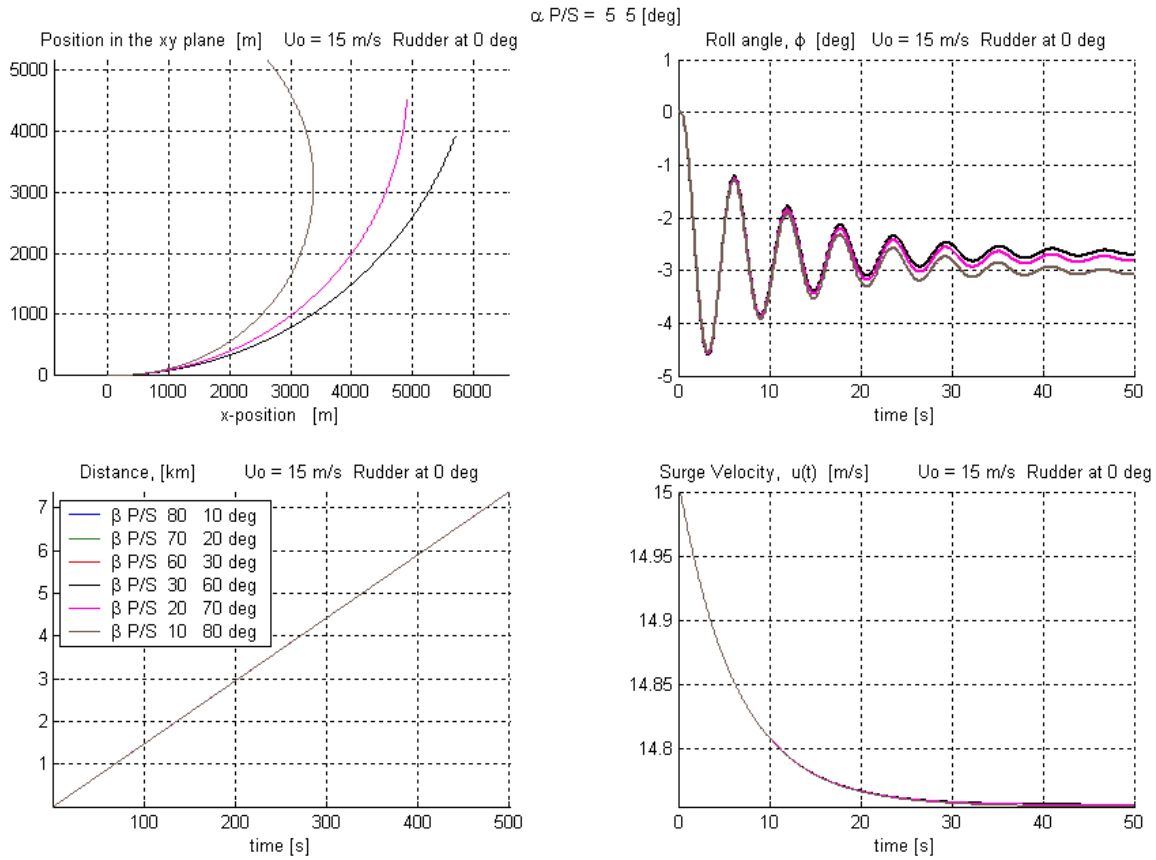

Figure 35. 29 Knots, No Rudder, Fins: $\alpha_P = \alpha_S = 5^\circ \quad \beta_P = \left|90^\circ - \beta_S\right|$.

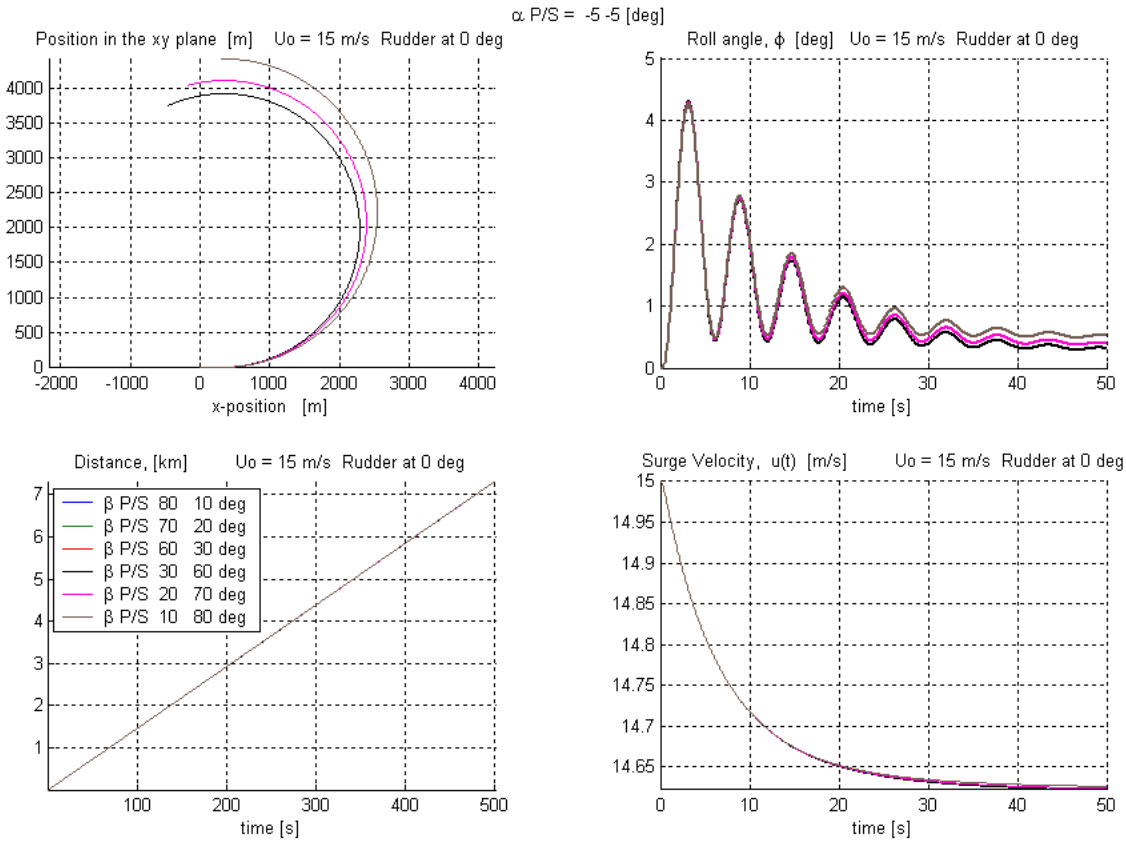

Figure 36. 29 Knots, No Rudder, Fins: $\alpha_P = \alpha_S = -5^\circ \quad \beta_P = \left|90^\circ - \beta_S\right|$.

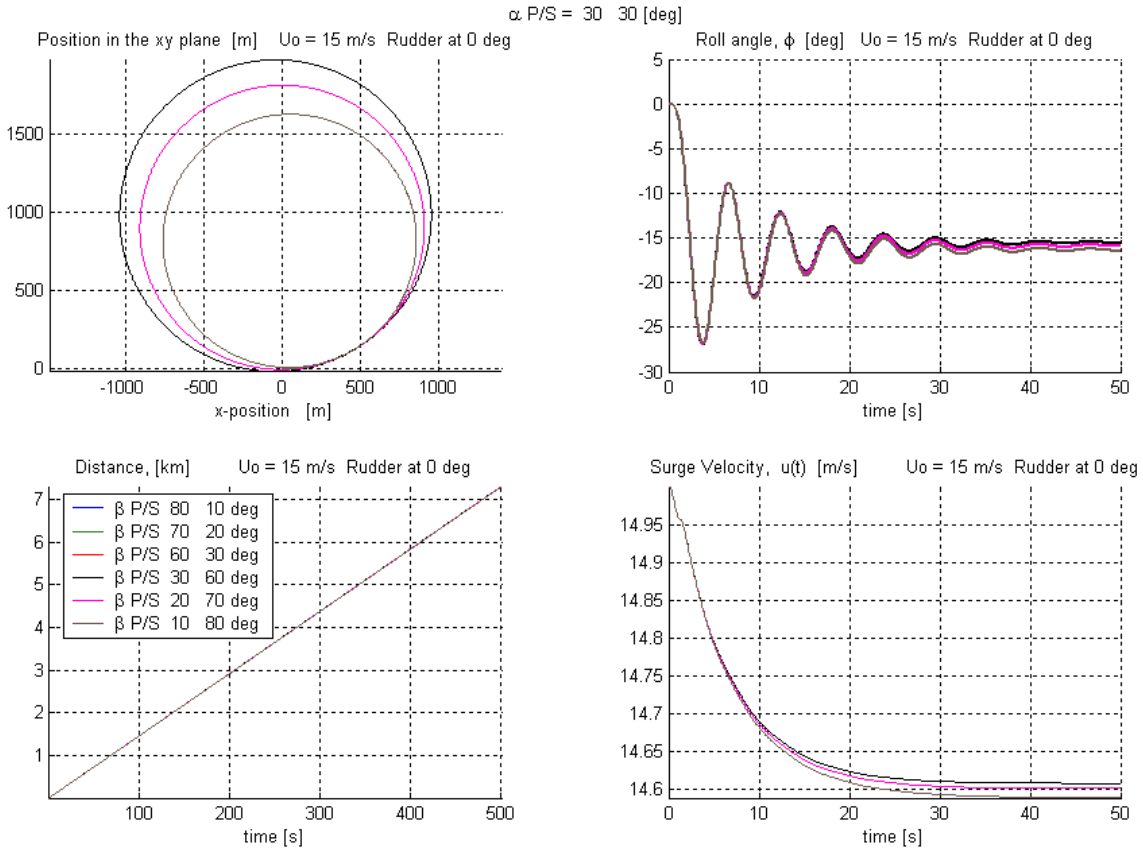

Figure 37. 29 Knots, No Rudder, Fins: $\alpha_P = \alpha_S = 30^\circ \quad \beta_P = \left|90^\circ - \beta_S\right|$.

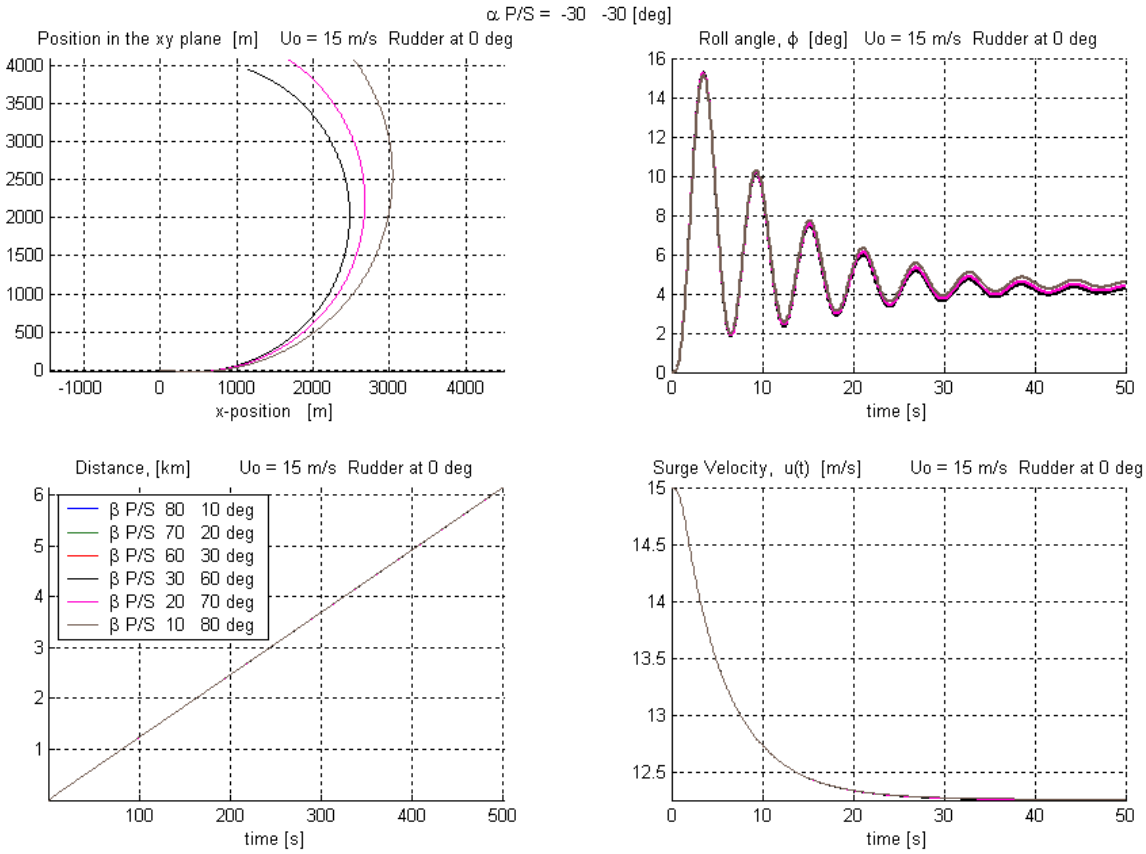

Figure 38. 29 Knots, No Rudder, Fins: $\alpha_P = \alpha_S = -30^\circ \quad \beta_P = \left|90^\circ - \beta_S\right|$.

3. Net Fin Angle of Attack Zero

With $\alpha_P = -\alpha_S = \pm 5^\circ$ and $\beta_P = \beta_S$, increasing β magnifies slightly the fins' neutralizing effect on the ship's natural tendency to turn to starboard. The effects on surge velocity and steady state outward heel angle are very small. Both approach steady state within the first 50 seconds.

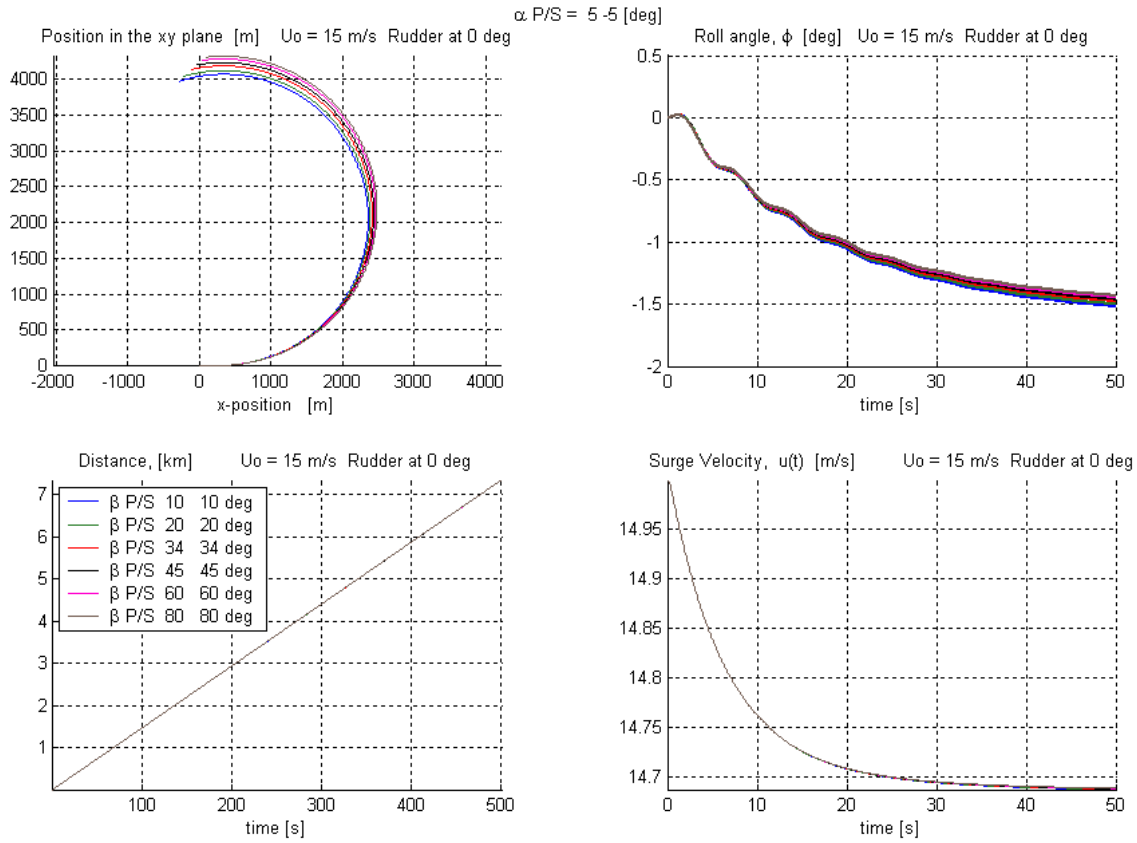

Figure 39. 29 Knots, No Rudder, Fins: $\alpha_P = -\alpha_S = 5^\circ \quad \beta_P = \beta_S$.

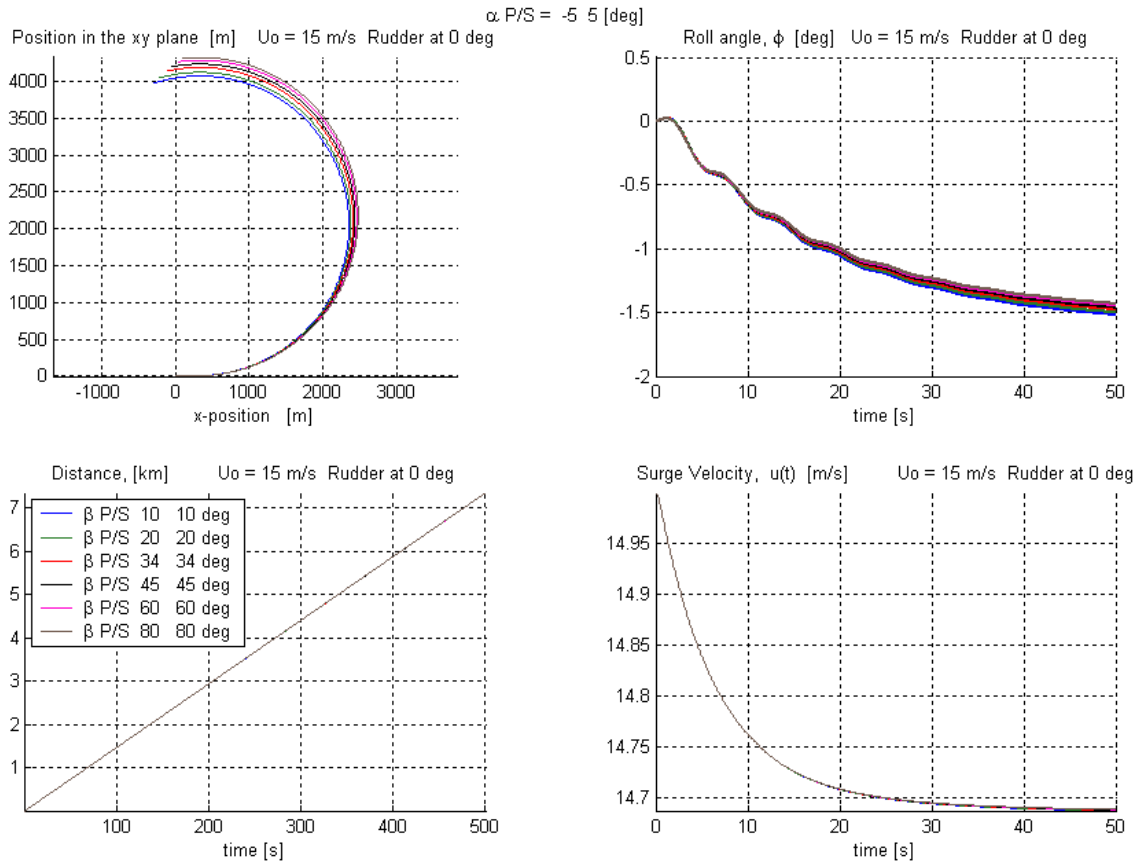

Figure 40. 29 Knots, No Rudder, Fins: $\alpha_P = -\alpha_S = -5^\circ \quad \beta_P = \beta_S$.

With $\alpha_P = -\alpha_S = \pm 30^\circ$ and $\beta_P = \beta_S$, increasing β significantly magnifies the fins' neutralizing effect on the ship's natural tendency to turn to starboard. The effects on surge velocity are very small, but the steady state outward heel angle decreases. Both approach steady state within the first 50 seconds.

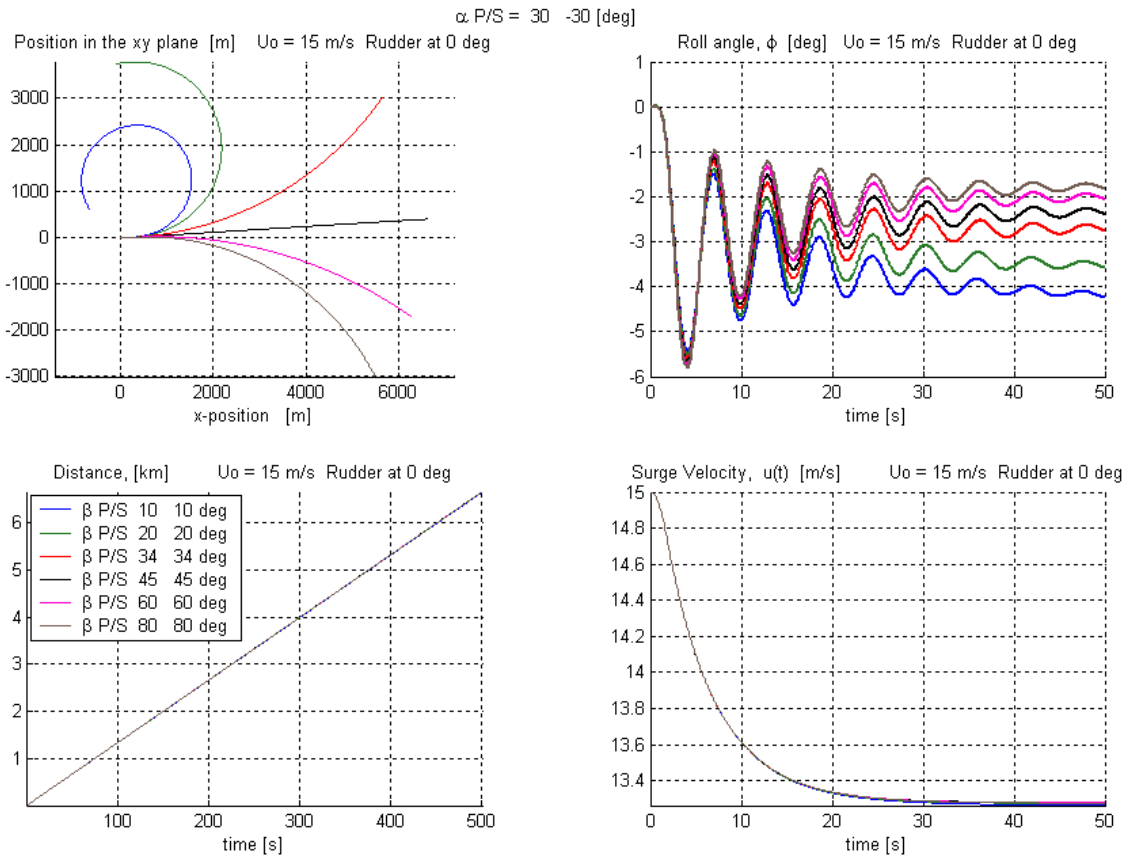

Figure 41. 29 Knots, No Rudder, Fins: $\alpha_P = -\alpha_S = 30^\circ \quad \beta_P = \beta_S$.

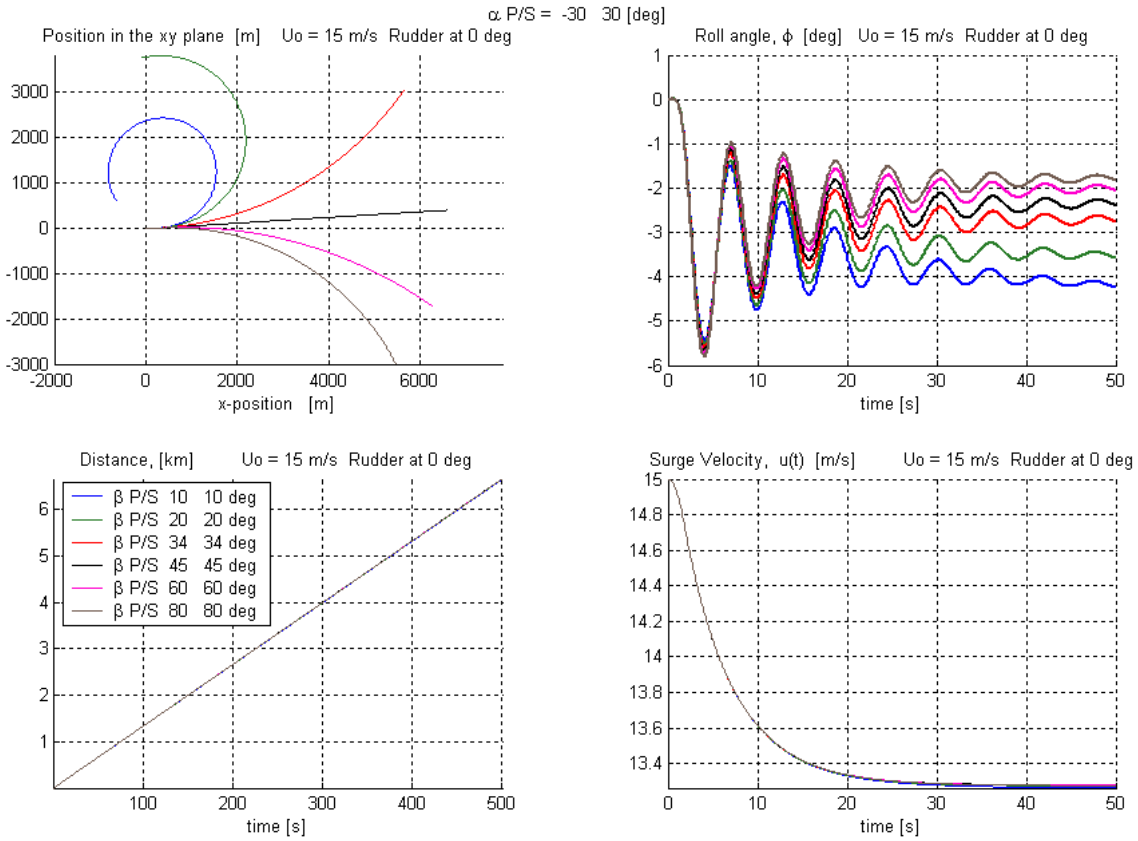

Figure 42. 29 Knots, No Rudder, Fins: $\alpha_P = -\alpha_S = -30^\circ \quad \beta_P = \beta_S$.

In sharp contrast to the cases of fin angle of attack nearly zero and fin angles paired, when fin angles sum to zero, varying the value of β, with $\beta_P = \left|90^\circ - \beta_S\right|$, causes significant effects on both heel angle and turning radius. For $\alpha_P > 0$, the steady state heel angle decreases with increasing β. For large values of both α_P and β, a steady state inward heel angle is established. Additionally, increasing β reduces and, for large values of α_P, ultimately overcomes the ship's natural tendency to turn to starboard. The turning radius increases to infinity, becoming smaller when the ship turns in the opposite direction. Finally, the ship's transient roll behavior is also affected. For small values of α_P, increasing β decreases or overcomes the initial inward roll. For large values of α_P, increasing β increases the initial outward roll peak.

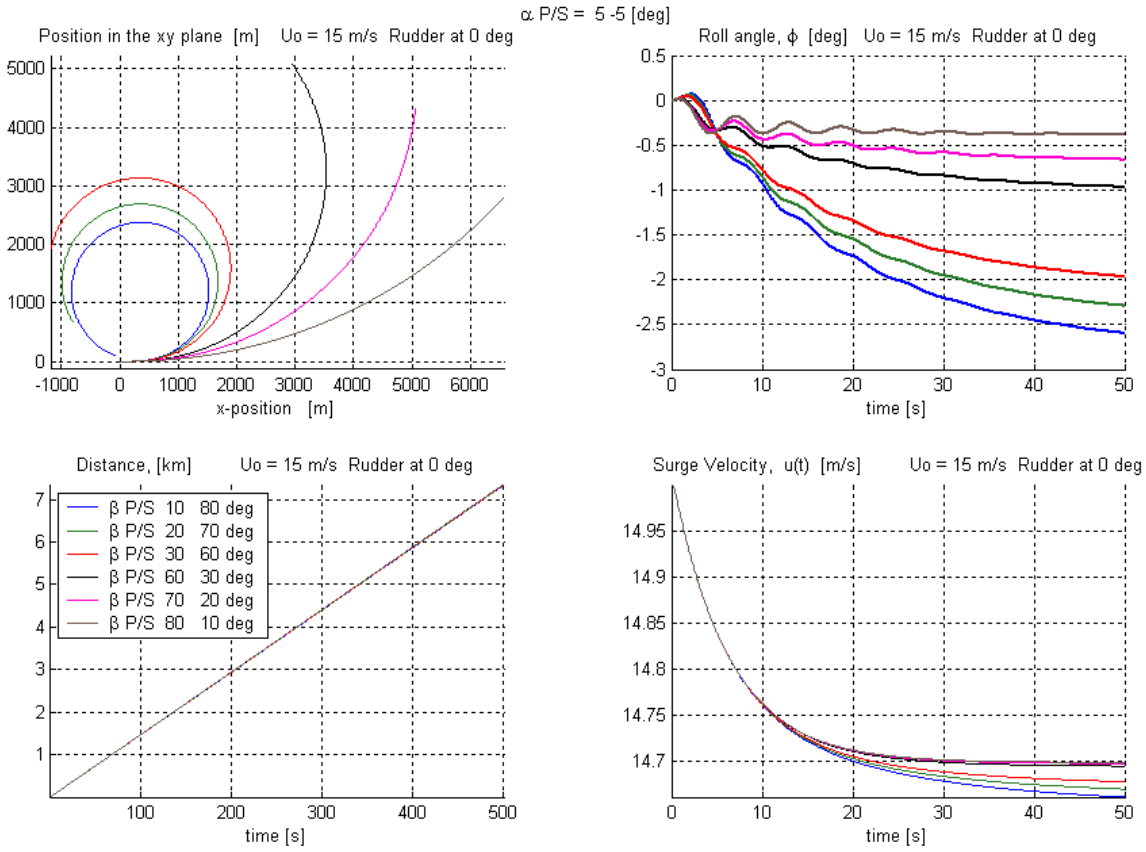

Figure 43. 29 Knots, No Rudder, Fins: $\alpha_P = -\alpha_S = 5^\circ \quad \beta_P = \left|90^\circ - \beta_S\right|$.

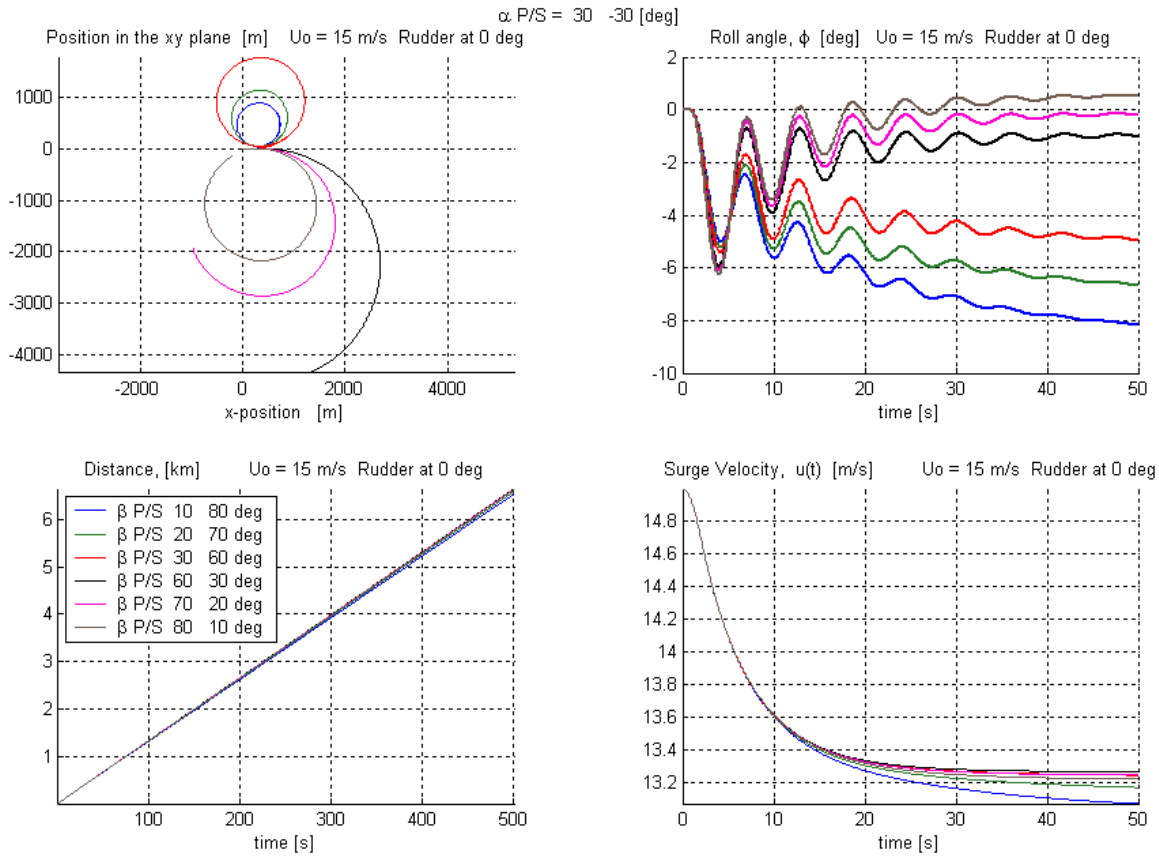

Figure 44. 29 Knots, No Rudder, Fins: $\alpha_P = -\alpha_S = 30^\circ \quad \beta_P = \left|90^\circ - \beta_S\right|$.

For $\alpha_P < 0$, the mirror image of the above-described effects are observed.

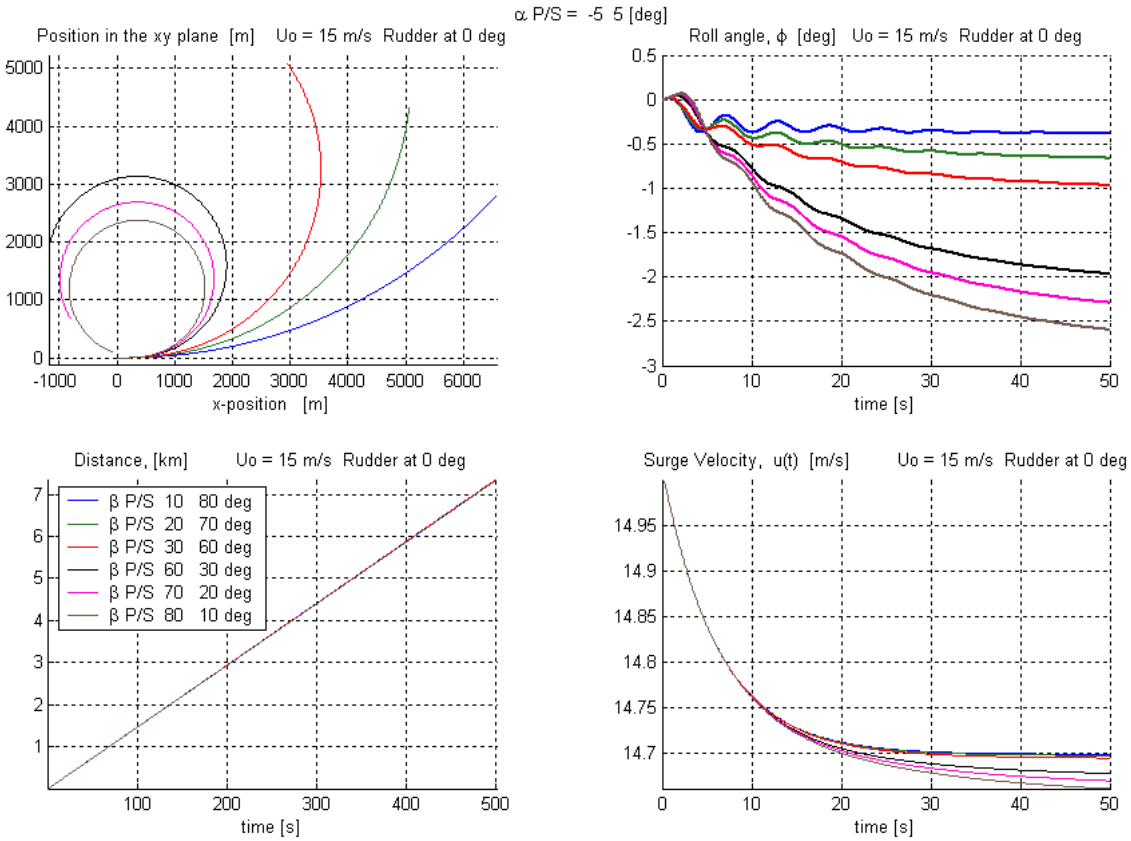

Figure 45. 29 Knots, No Rudder, Fins: $\alpha_P = -\alpha_S = -5^\circ \quad \beta_P = \left|90^\circ - \beta_S\right|$.

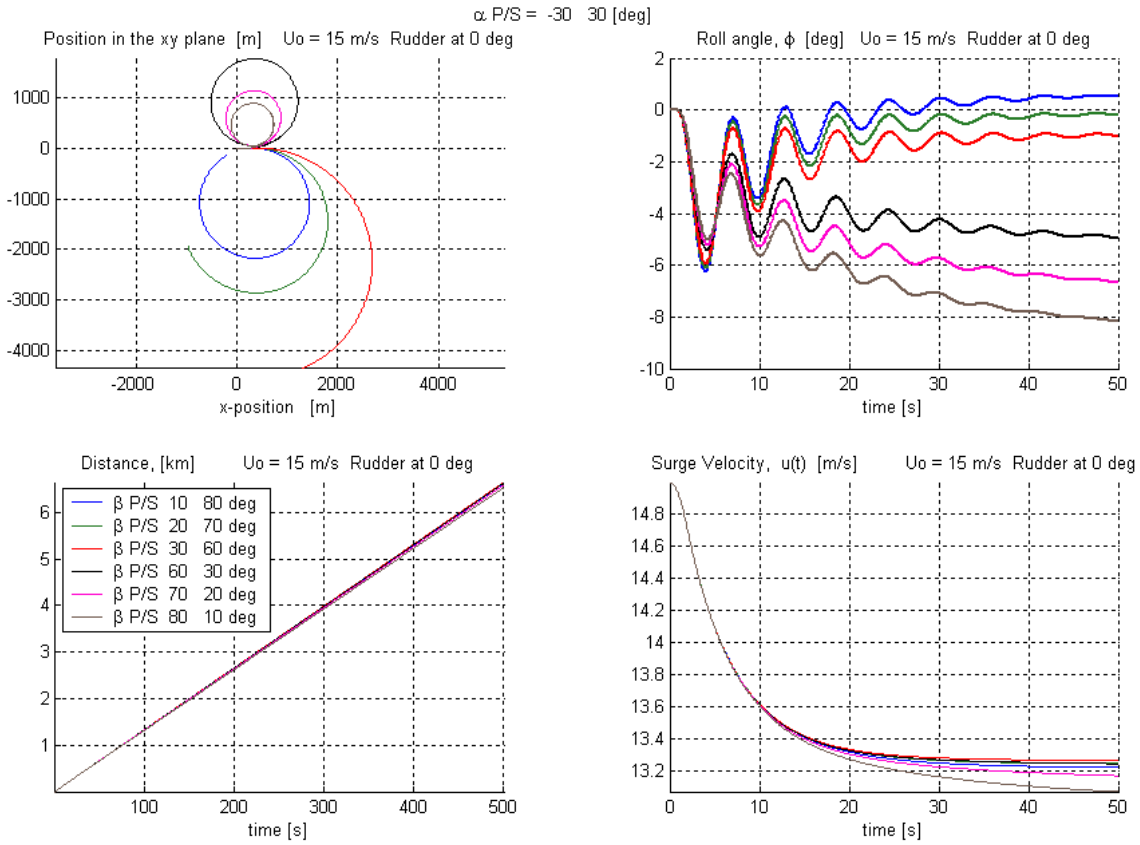

Figure 46. 29 Knots, No Rudder, Fins: $\alpha_P = \alpha_S = -30^\circ \quad \beta_P = \left|90^\circ - \beta_S\right|$.

4. Fin Angles of Attack Mixed

For this set of tests, $\alpha_P + \alpha_S = Constant$. With $\alpha_P = 30^\circ, \alpha_s = -20^\circ$ or $\alpha_P = -30^\circ, \alpha_s = 20^\circ$ and $\beta_P = \beta_S$, increasing β decreases or overcomes the ship's natural tendency to turn to starboard, and decreases the steady state heel angle. The loss in surge velocity decreases slightly or is unchanged. In the former case, the effects are stronger than the latter case.

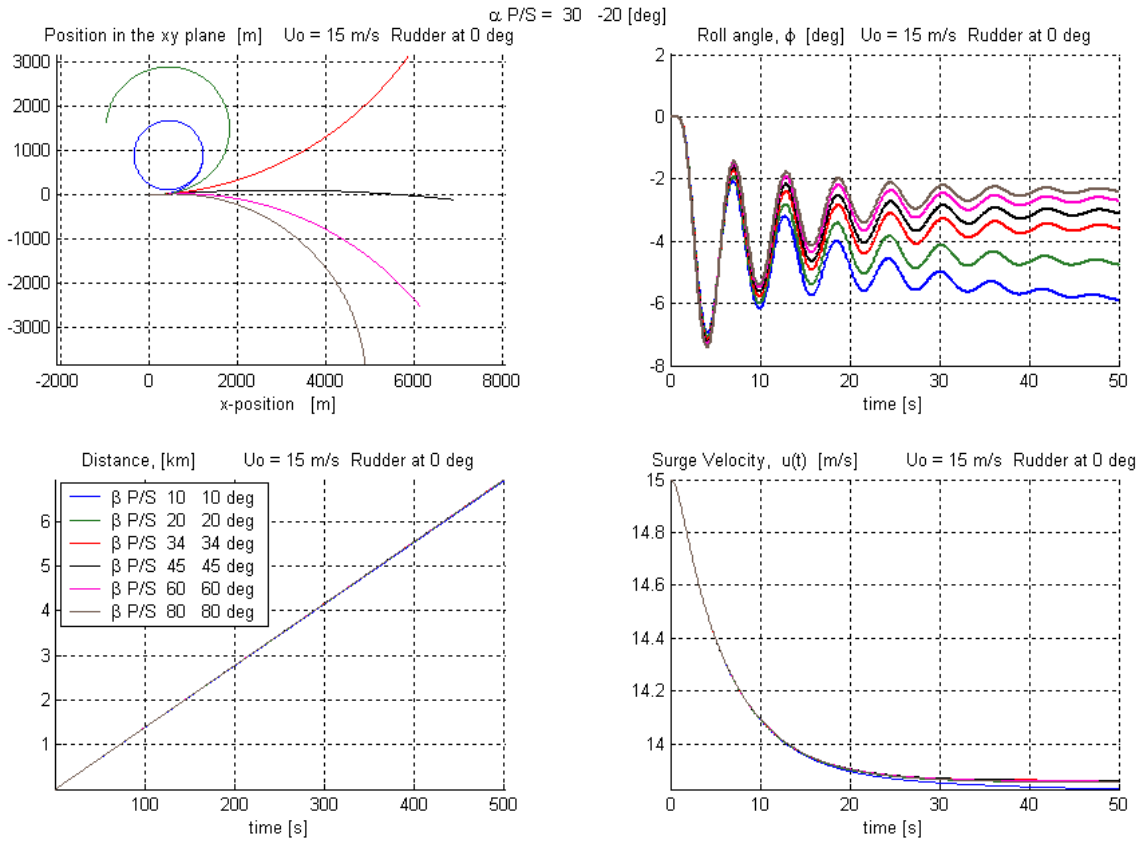

Figure 47. 29 Knots, No Rudder, Fins: $\alpha_P = 30^\circ$ $\alpha_S = -20^\circ$ $\beta_P = \beta_S$.

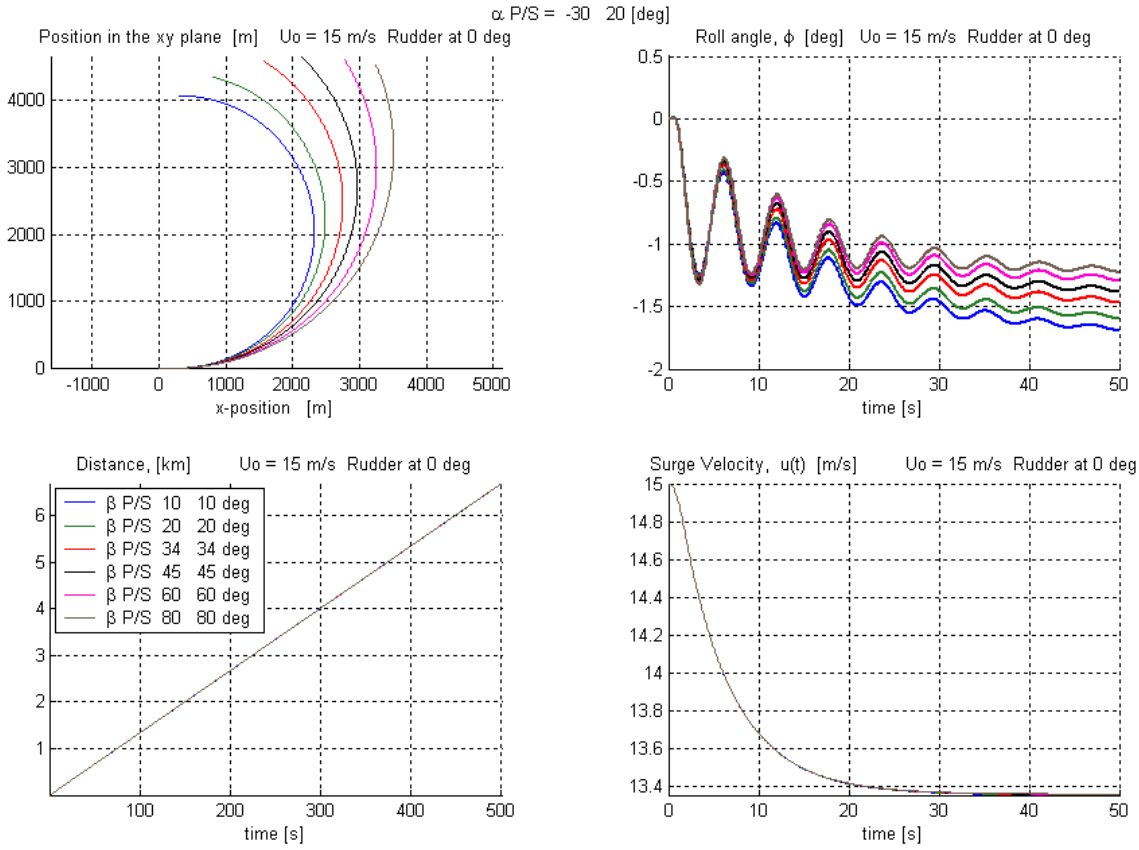

Figure 48. 29 Knots, No Rudder, Fins: $\alpha_P = -30^\circ \; \alpha_S = 20^\circ \quad \beta_P = \beta_S$.

With $\alpha_P = 30^\circ, \alpha_s = -20^\circ$ and $\beta_P = \left|90^\circ - \beta_S\right|$, increasing β decreases or overcomes the ship's natural tendency to turn to starboard, and decreases the steady state heel angle. The loss in surge velocity decreases slightly or is unchanged. All of these effects are in the same direction as, but stronger than in the case of $\beta_P = \beta_S$.

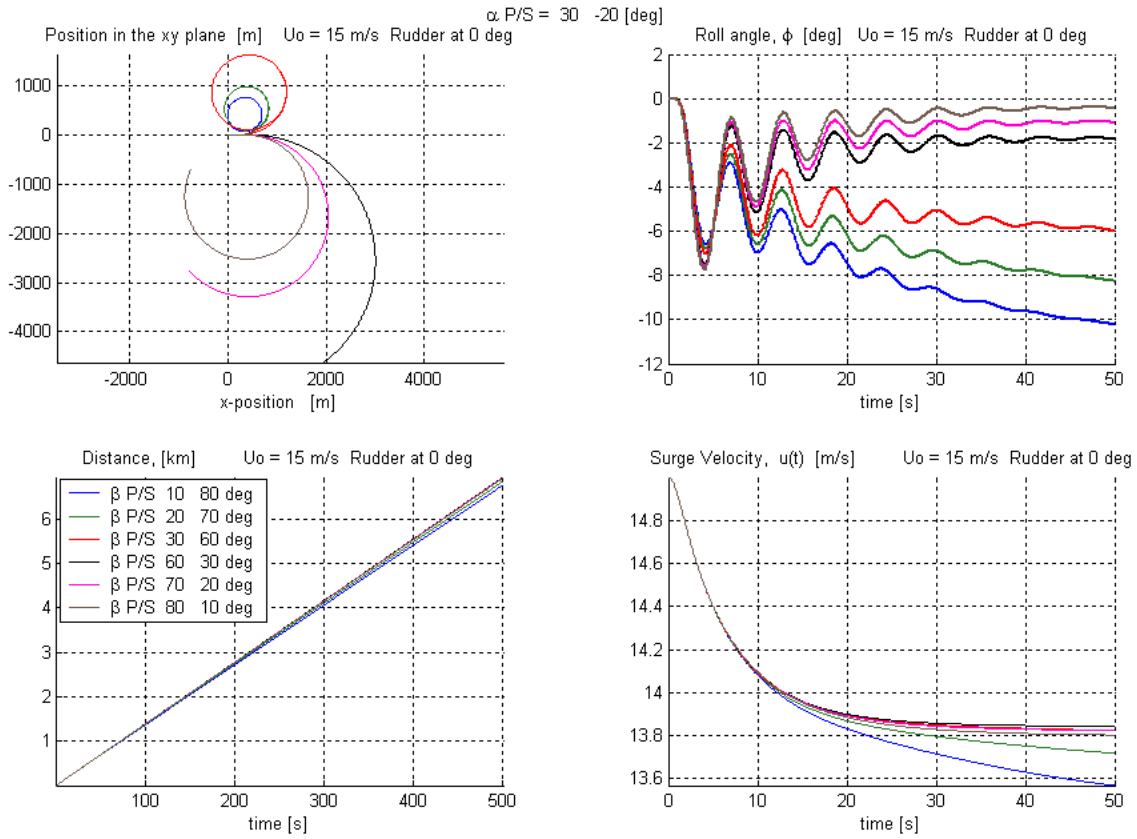

Figure 49. 29 Knots, No Rudder, Fins: $\alpha_P = 30^\circ \; \alpha_S = -20^\circ \quad \beta_P = \left|90^\circ - \beta_S\right|$.

With $\beta_P = \left|90^\circ - \beta_S\right|$ and fin angles of attack to $\alpha_P = -30^\circ, \alpha_s = 20^\circ$, the results resemble the case of $\beta_P = \left|90^\circ - \beta_S\right| \quad \alpha_P = -5^\circ, \alpha_s = 5^\circ$.

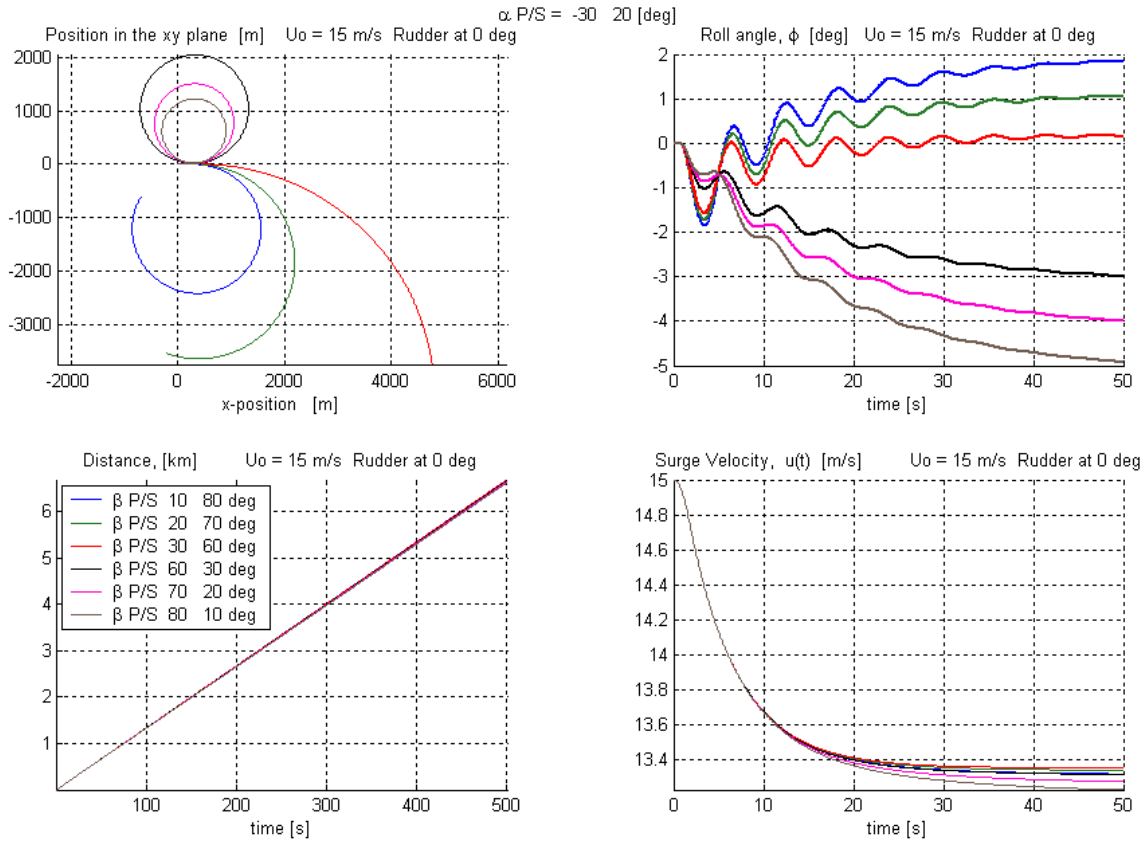

Figure 50. 29 Knots, No Rudder, Fins: $\alpha_P = -30^\circ$ $\alpha_S = 20^\circ$ $\beta_P = \left|90^\circ - \beta_S\right|$.

D. FINS AND RUDDERS COMBINED, CONSTANT INPUT

A battery of tests over a simulated time period of 150 seconds was conducted using various combinations of fin angle input, rudder input and initial surge velocity. Representative samples from those tests, emphasizing the ship's performance with large commanded rudder angles at moderate to high speed, are presented and analyzed.

1. Fin Angles Paired for Maximum Roll Moment

With $\delta_{Commanded} = 30^\circ$, $\beta_P = \beta_S = 34^\circ$ and $\alpha_P = \alpha_S$, both positive, and an initial surge velocity of about 15 knots, the vessel's turning radius and initial inward heel angle increase with increasing values of α, but the steady outward heel angle is reduced, eliminated, or replaced with a steady inward heel angle of equal or greater magnitude. Steady state heel is reached before 50 seconds have elapsed.

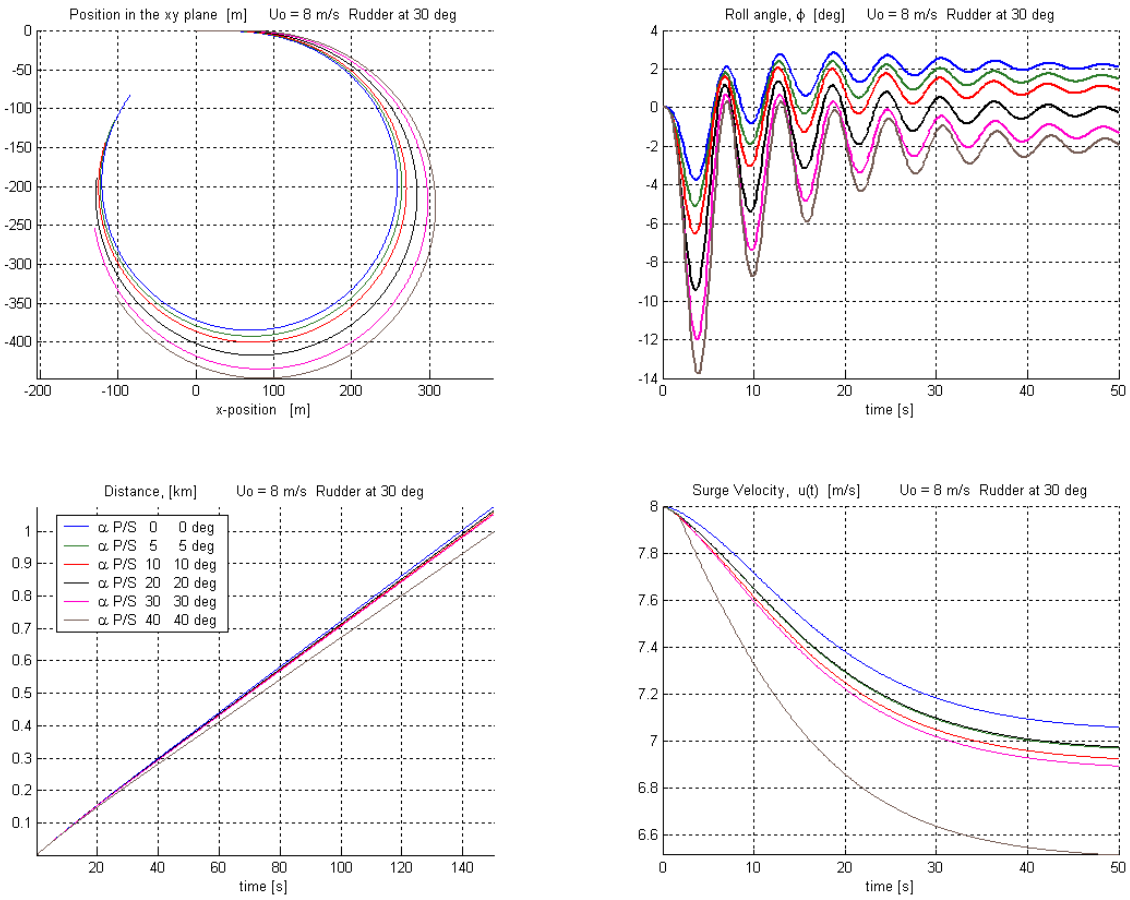

Figure 51. 15.5 Knots, Rudder 30° – Fins: Angles of Attack Paired >0 $\beta_P = \beta_S = 34^\circ$.

Changing the rudder input to $\delta_{Commanded} = -30^\circ$, but leaving all other conditions the same causes dramatically different results. Increasing α now decreases the ship's turning radius and increases the steady state outward heel angle. The initial inward heel is either diminished, negated, or replaced with a peak outward heel that exceeds the steady state value.

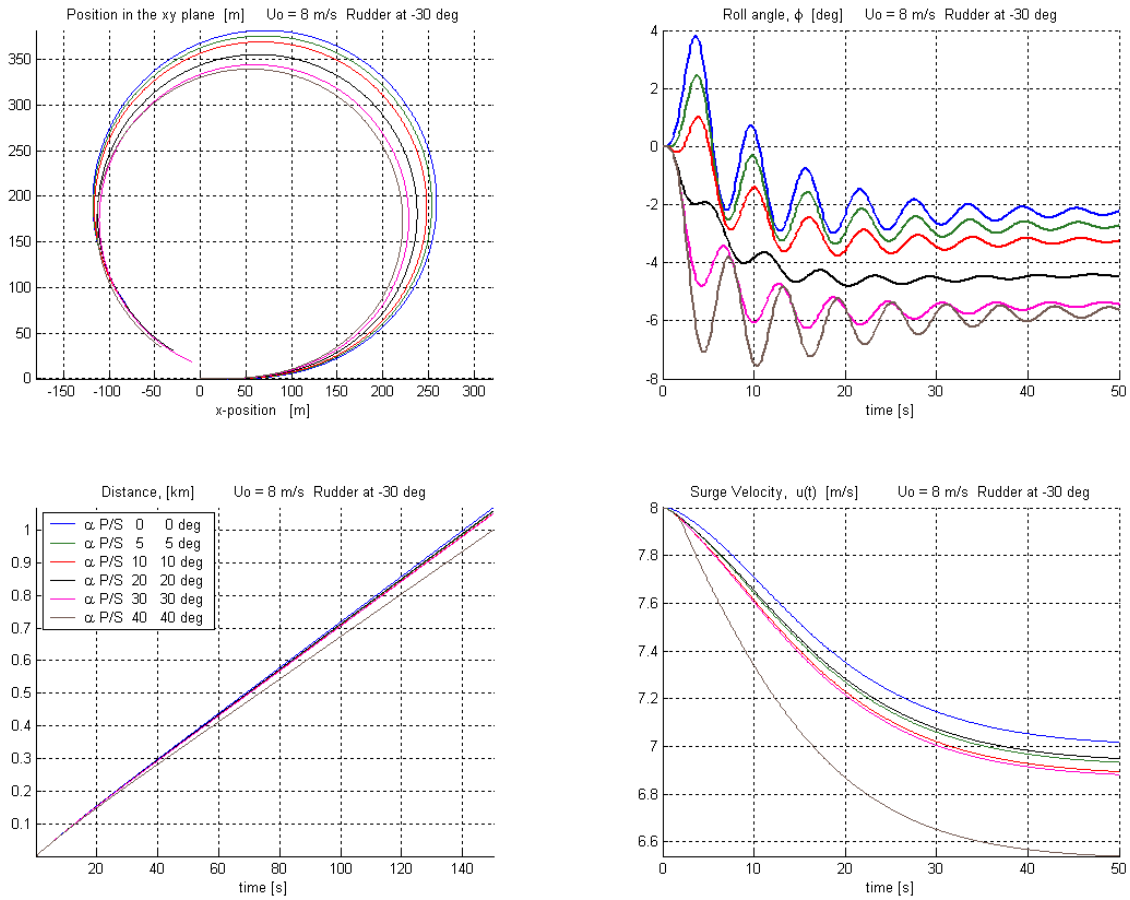

Figure 52. 15.5 Knots, Rudder -30° – Fins: Angles of Attack Paired >0 $\beta_P = \beta_S = 34^\circ$.

As expected, changing the sign of α_P *and* α_S to both negative causes the response to act as the mirror image of the cases with both angles positive. Thus, with $\delta_{Commanded} = 30^\circ$ *and* $\delta_{Commanded} = -30^\circ$, respectively:

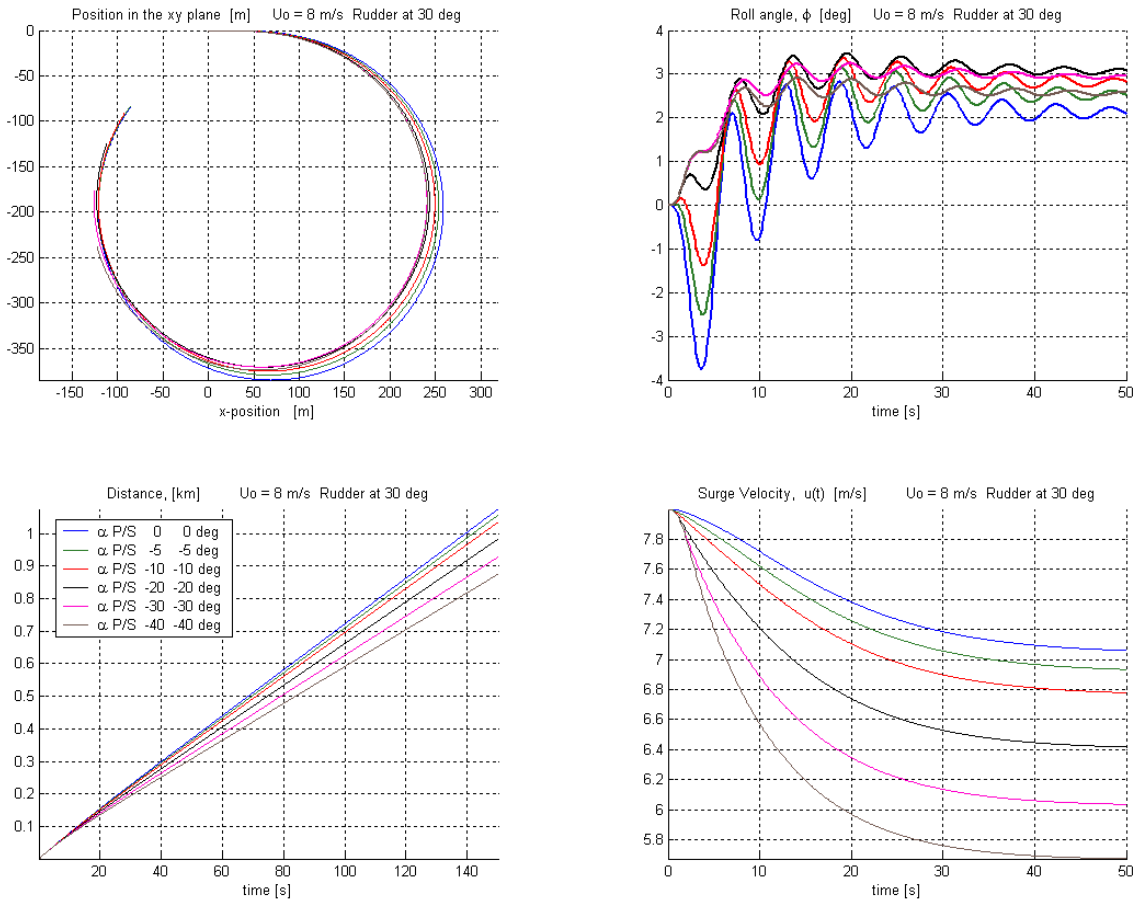

Figure 53. 15.5 Knots, Rudder 30° – Fins: Angles of Attack Paired <0 $\beta_P = \beta_S = 34^\circ$.

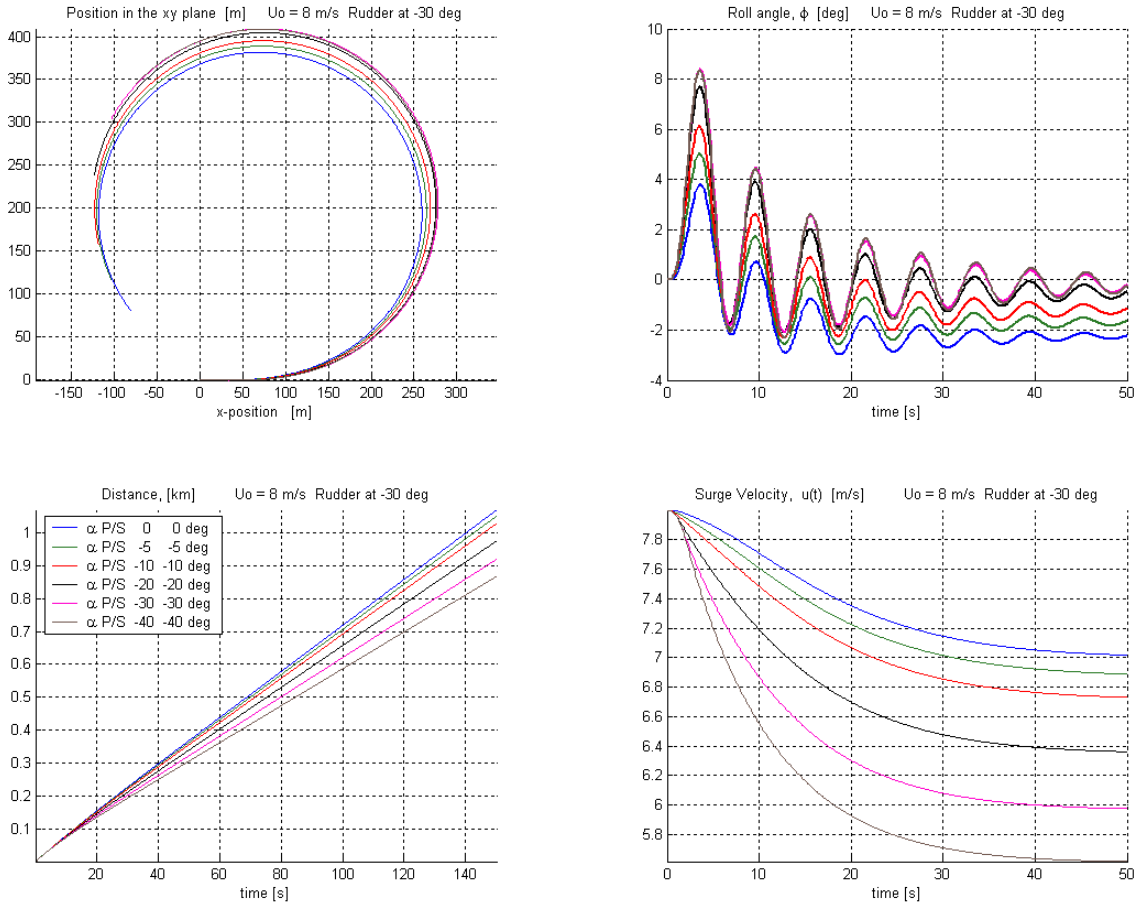

Figure 54. 15.5 Knots, Rudder -30° – Fins: Angles of Attack Paired <0 $\beta_P = \beta_S = 34^\circ$.

Increasing the vessel's initial surge velocity to 35 knots produces several interesting changes to the results. With $\delta_{Commanded} = 30^\circ$, $\beta_P = \beta_S = 34^\circ$ and $\alpha_P = \alpha_S$, both positive, or with $\delta_{Commanded} = -30^\circ$, $\beta_P = \beta_S = 34^\circ$ and $\alpha_P = \alpha_S$, both negative, it is no longer always the case that the reduction in surge velocity through the turn increases as the value of α increases. The increase in turning radius with increasing α becomes more pronounced. Steady state in both heel angle and surge velocity is reached much more quickly.

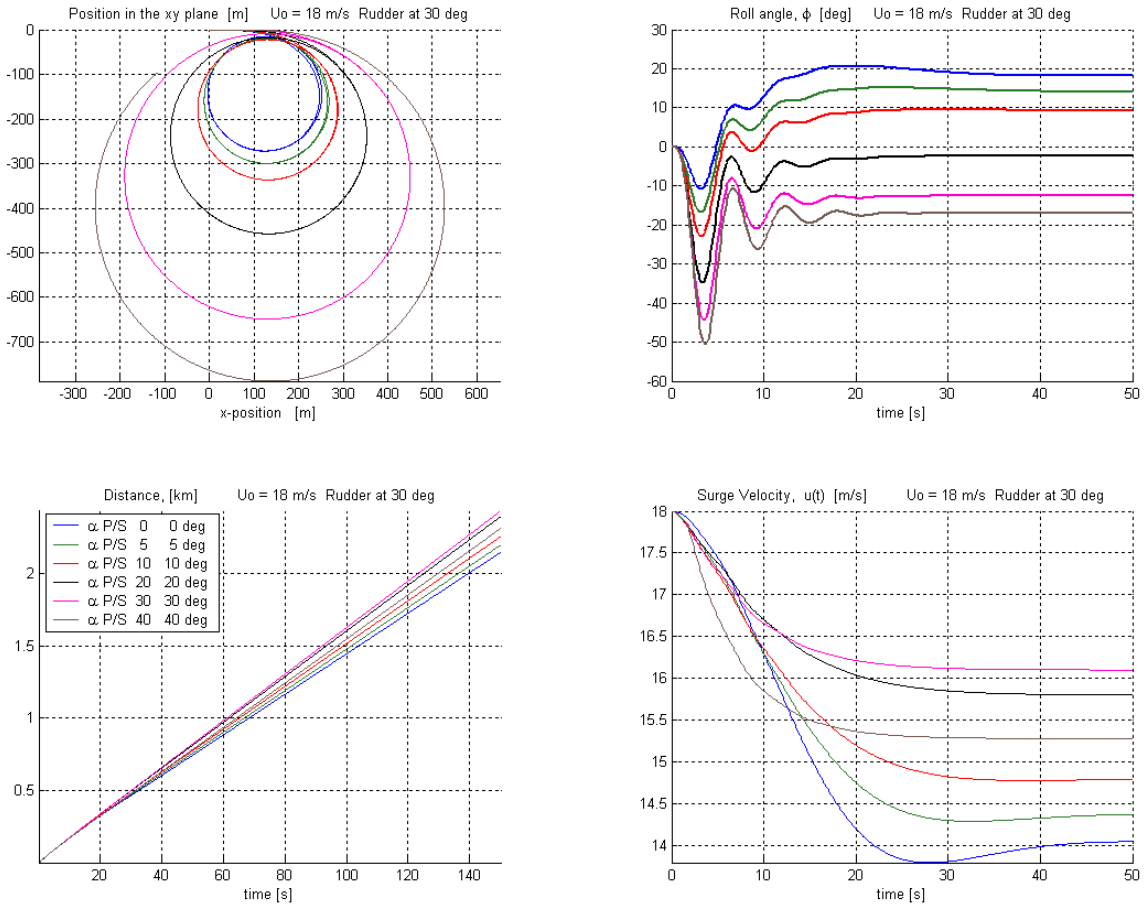

Figure 55. 35 Knots, Rudder 30° – Fins: Angles of Attack Paired >0 $\beta_P = \beta_S = 34^\circ$.

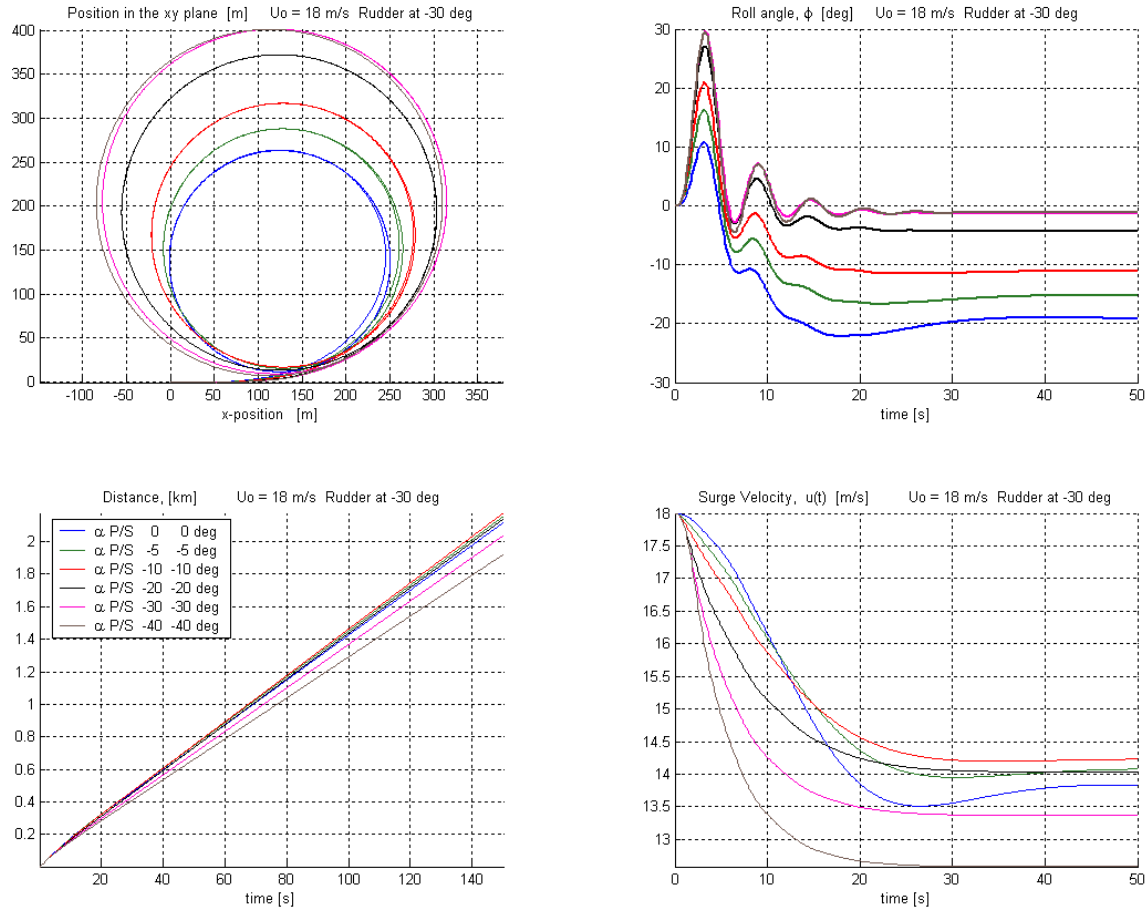

Figure 56. 35 Knots, Rudder -30° – Fins: Angles of Attack Paired <0 $\beta_P = \beta_S = 34^\circ$.

With $\delta_{Commanded} = -30^\circ$, $\beta_P = \beta_S = 34^\circ$ and $\alpha_P = \alpha_S$, both positive, or $\delta_{Commanded} = 30^\circ$, $\beta_P = \beta_S = 34^\circ$ and $\alpha_P = \alpha_S$, both negative, in addition to turning radius, the ship's advance and transfer are reduced with increasing values of α. Peak roll angle becomes very large, and cost in lost surge velocity grows significantly.

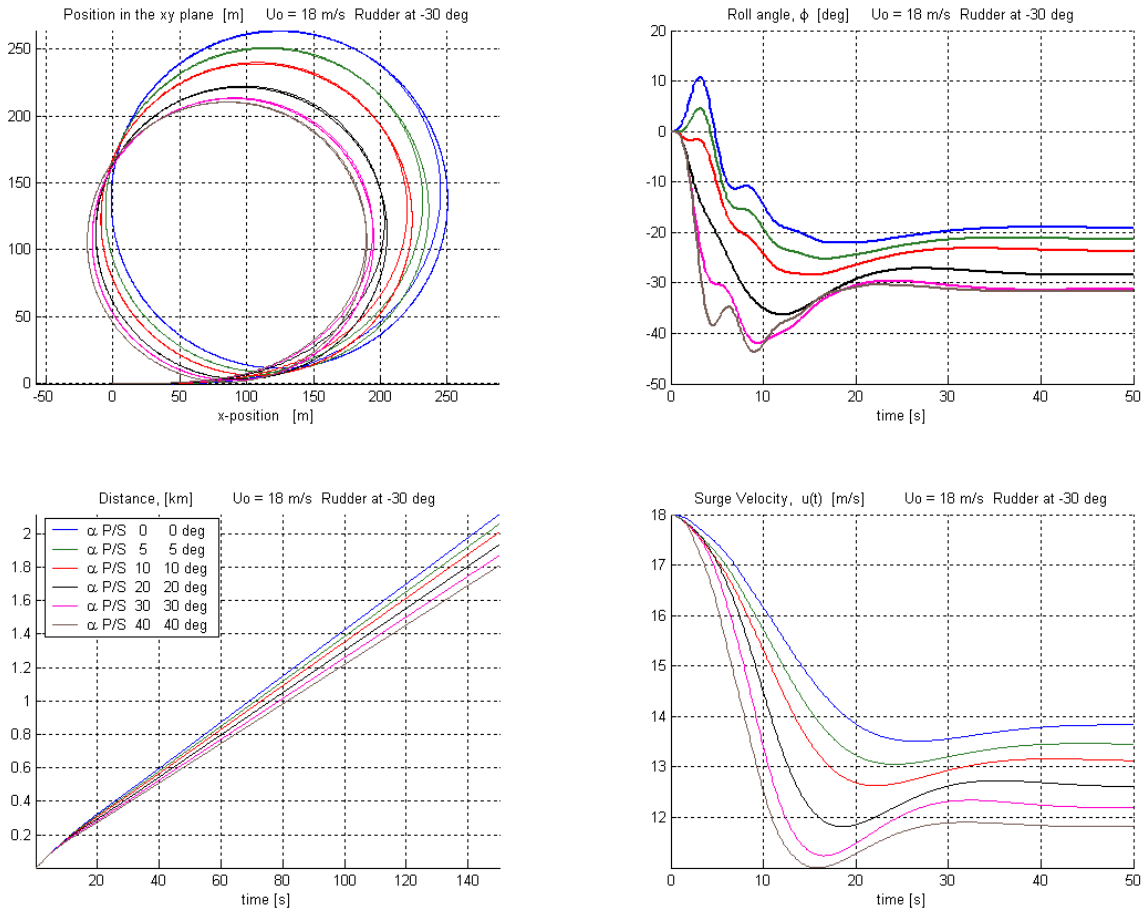

Figure 57. 35 Knots, Rudder -30° – Fins: Angles of Attack Paired >0 $\beta_P = \beta_S = 34^\circ$.

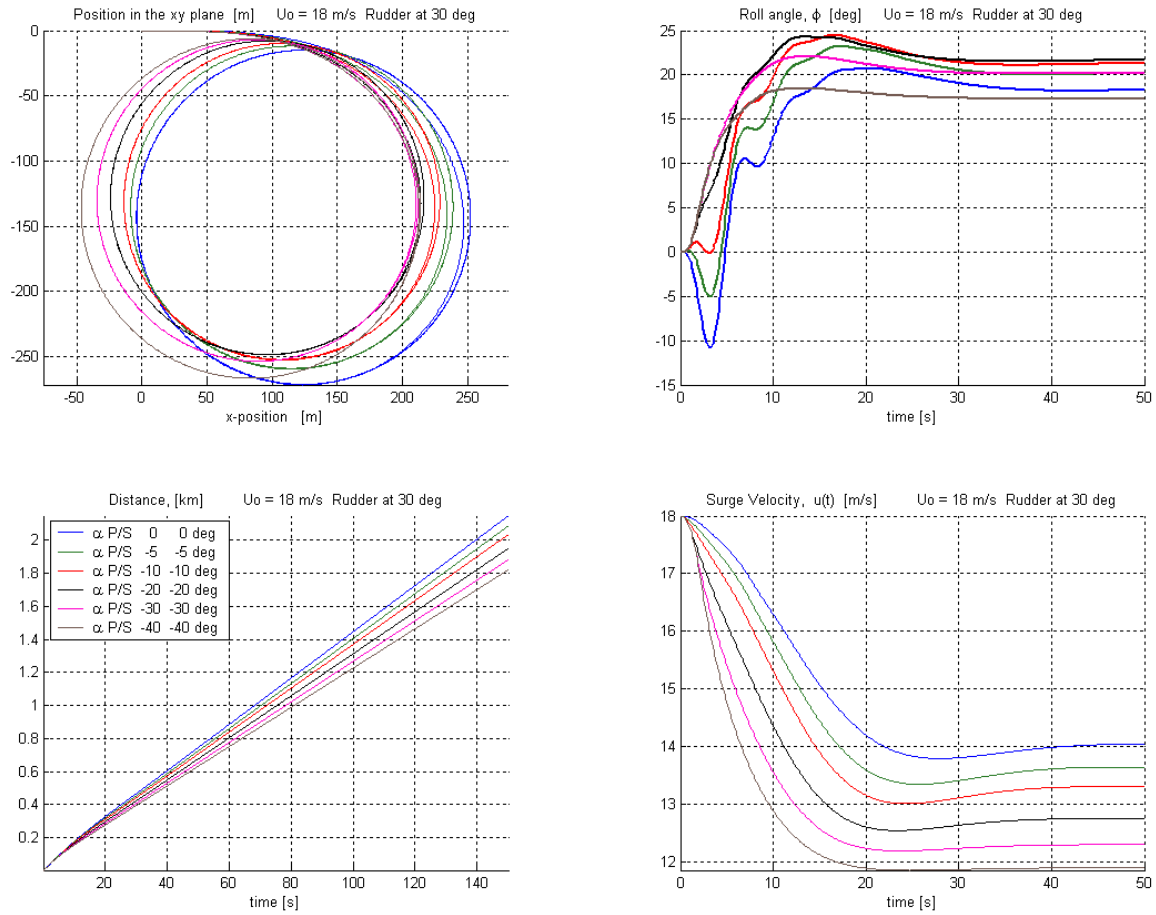

Figure 58. 35 Knots, Rudder 30° – Fins: Angles of Attack Paired <0 $\beta_P = \beta_S = 34^\circ$.

2. Net Fin Angle of Zero

With $\delta_{Commanded} = 30^\circ$, $\beta_P = \beta_S = 34^\circ$ and $\alpha_P = -\alpha_S$, ($\alpha_P > 0$ or $\alpha_P < 0$), and an initial surge velocity of about 15 knots, as α increases, peak inward roll angle increases, peak and steady state outward heel angles decrease, surge velocity decreases, and turning radius increases.

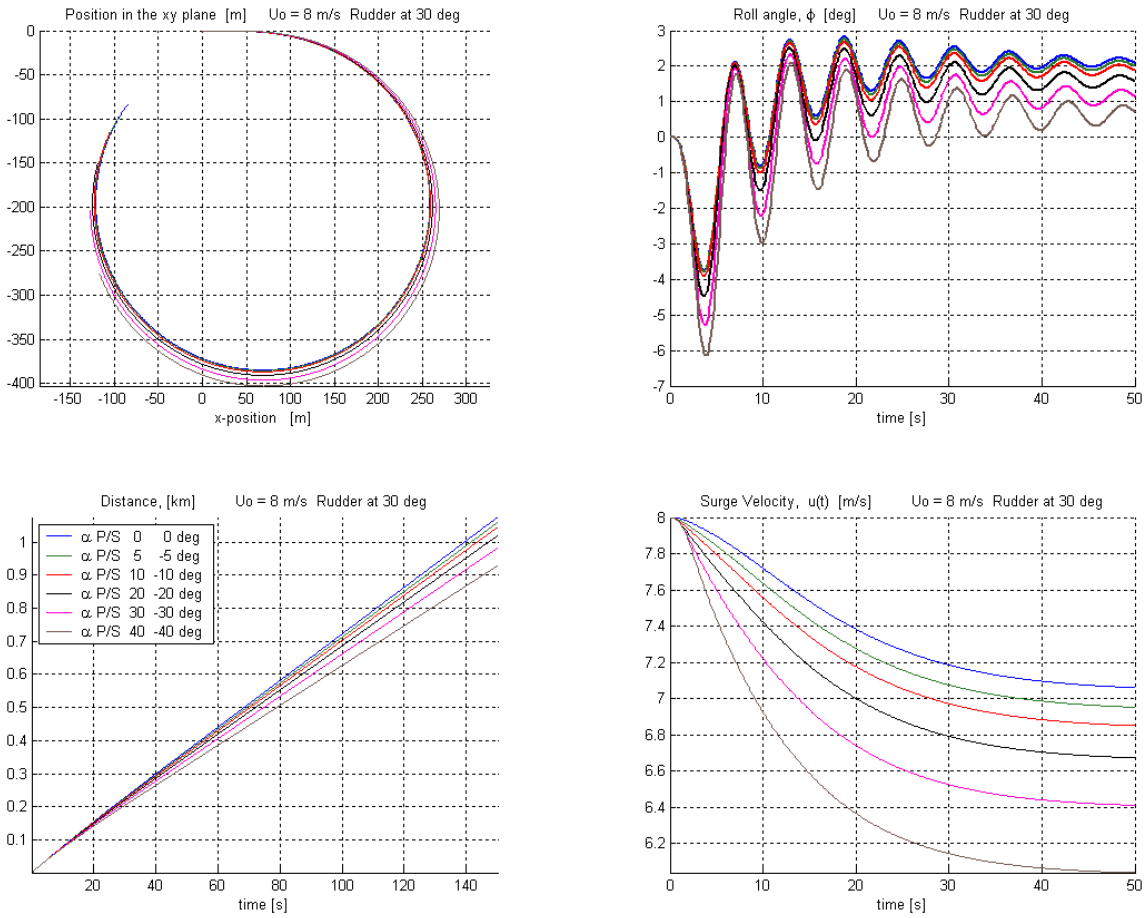

Figure 59. 15.5 Knots, Rudder 30° – Fins: $\alpha_P = -\alpha_S$; $\alpha_P > 0 \quad \beta_P = \beta_S = 34^\circ$.

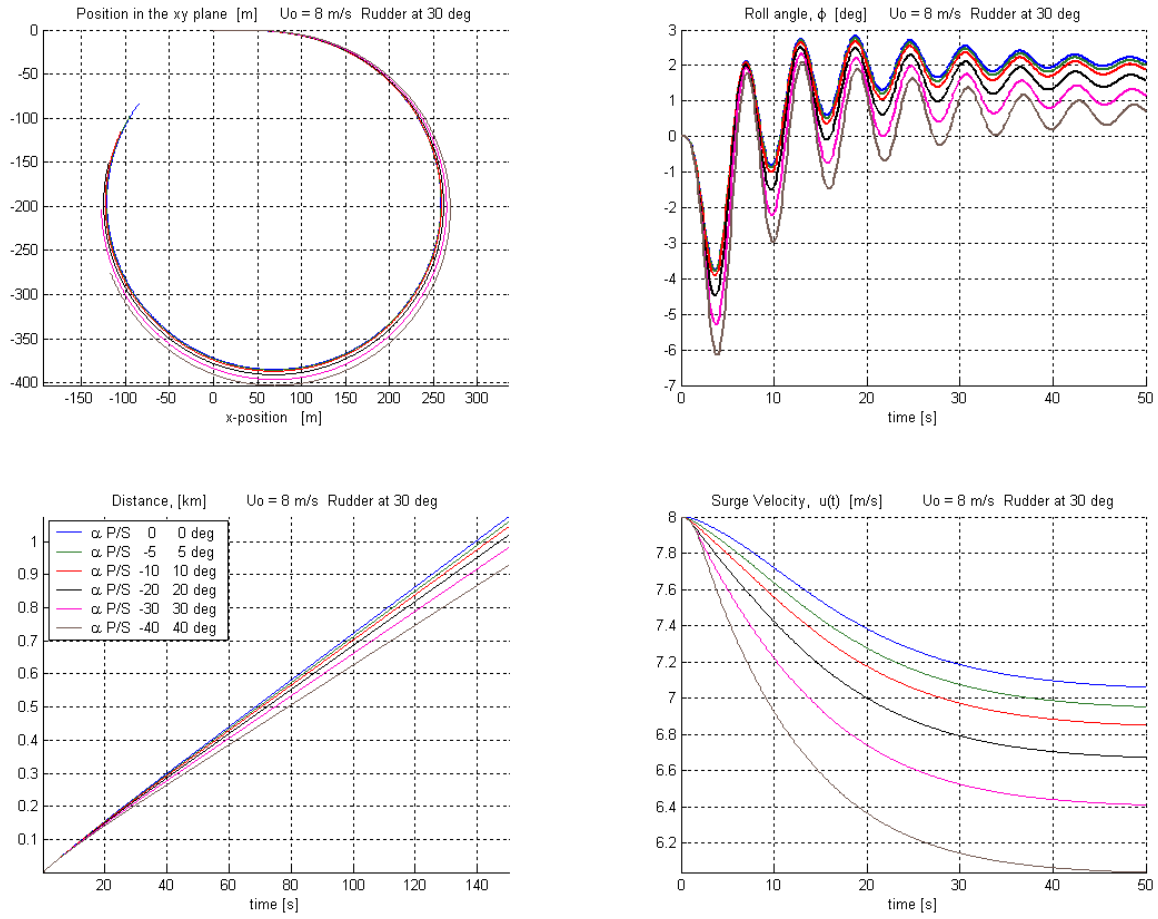

Figure 60. 15.5 Knots, Rudder 30° – Fins: $\alpha_P = -\alpha_S$; $\alpha_P < 0 \quad \beta_P = \beta_S = 34^\circ$.

Increasing the initial surge velocity to about 35 knots magnifies the roll, heel, and turning radius effects, as expected, but, the loss in surge velocity becomes significantly less severe for all but the largest values of α .

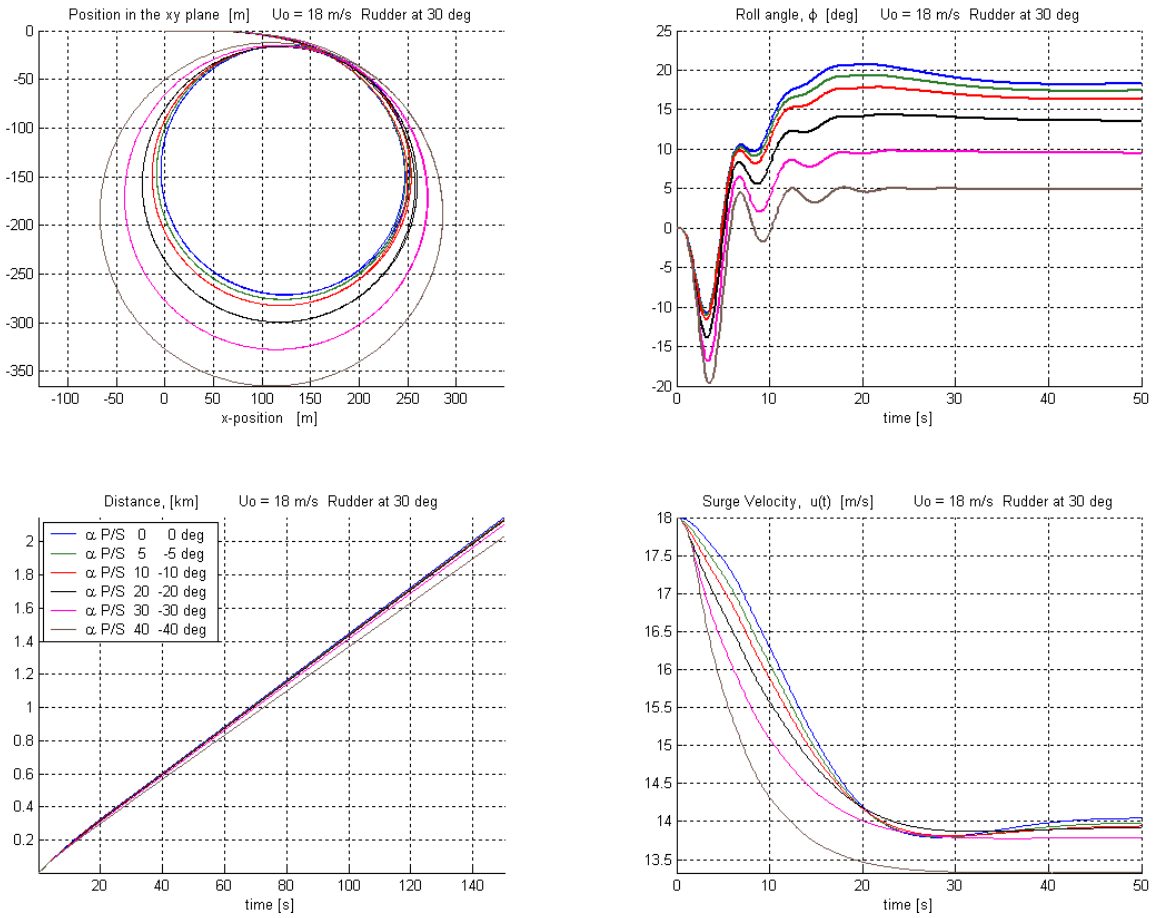

Figure 61. 35 Knots, Rudder 30° – Fins: $\alpha_P = -\alpha_S$; $\alpha_P > 0 \quad \beta_P = \beta_S = 34^\circ$.

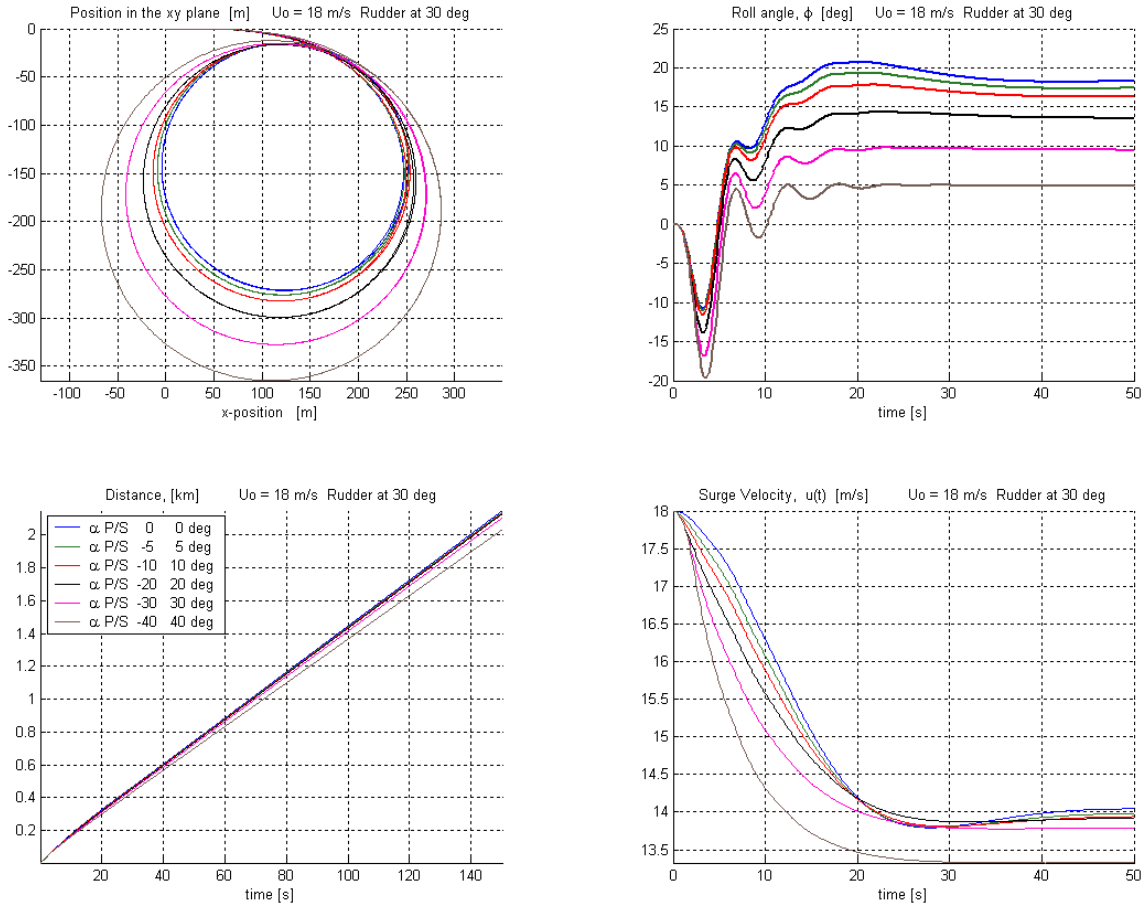

Figure 62. 35 Knots, Rudder 30° – Fins: $\alpha_P = -\alpha_S$; $\alpha_P < 0 \quad \beta_P = \beta_S = 34^\circ$.

Changing the rudder command to $\delta_{Commanded} = -30^\circ$, causes unexpected differences in the results. At moderate speed, as α increases, the inward roll angle and surge velocity decrease, while the peak and steady state outward heel angles increase. But the effect on turning radius is much smaller than with $\delta_{Commanded} = 30^\circ$.

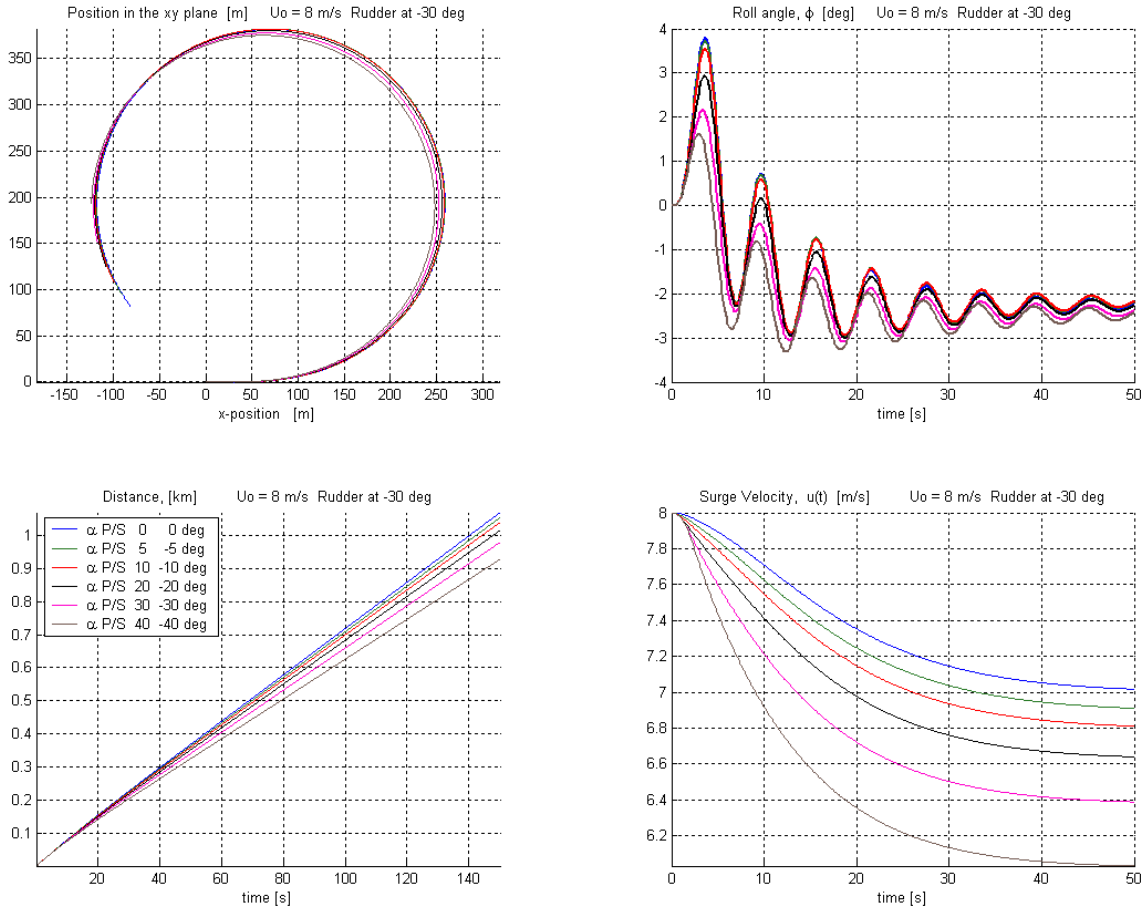

Figure 63. 15.5 Knots, Rudder -30° – Fins: $\alpha_P = -\alpha_S$; $\alpha_P > 0 \quad \beta_P = \beta_S = 34^\circ$.

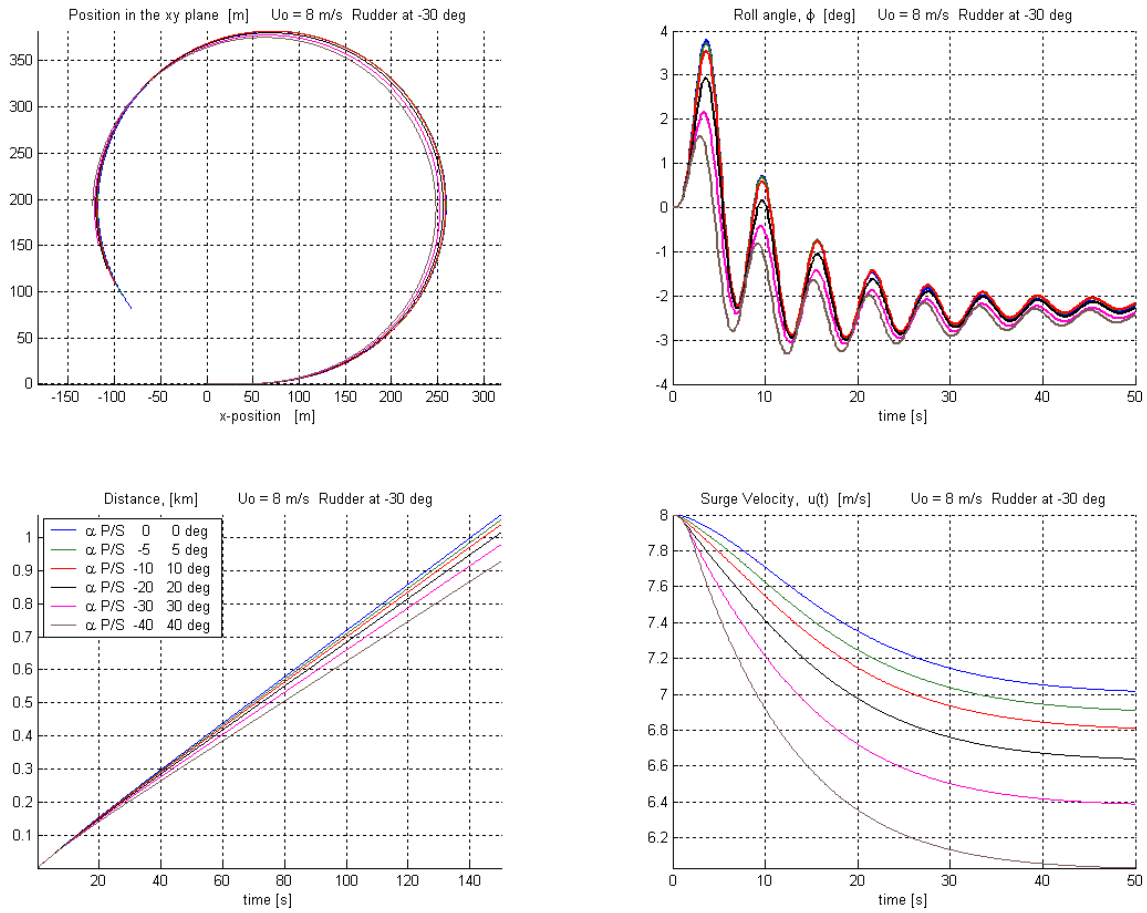

Figure 64. 15.5 Knots, Rudder -30° – Fins: $\alpha_P = -\alpha_S$; $\alpha_P < 0 \quad \beta_P = \beta_S = 34^\circ$.

With initial surge velocity of about 35 knots, as α increases, the inward roll angle and surge velocity decrease. Turning radius and transfer remain essentially constant, but advance decreases slightly. Peak and steady state outward heel angles converge to very nearly the same steady state value at about the same time.

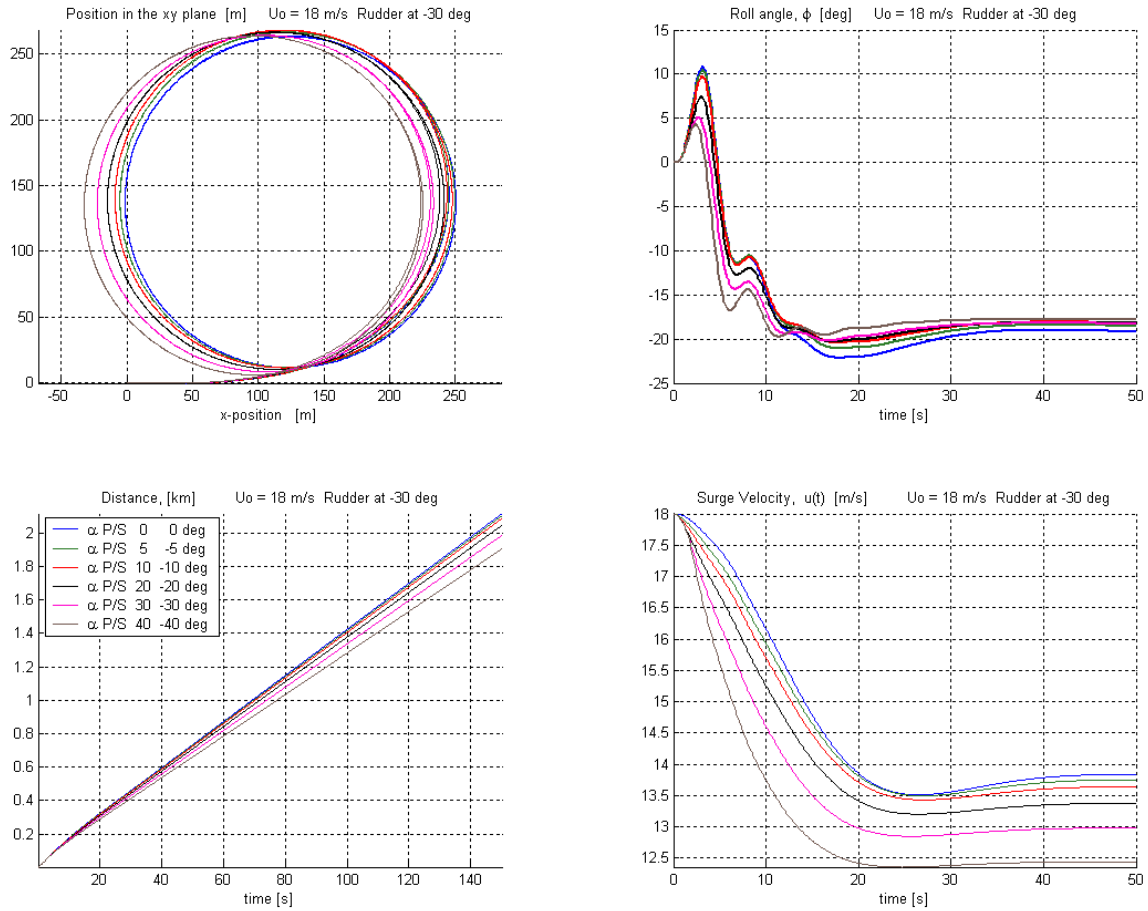

Figure 65. 35 Knots, Rudder -30° – Fins: $\alpha_P = -\alpha_S$; $\alpha_P > 0 \quad \beta_P = \beta_S = 34^\circ$.

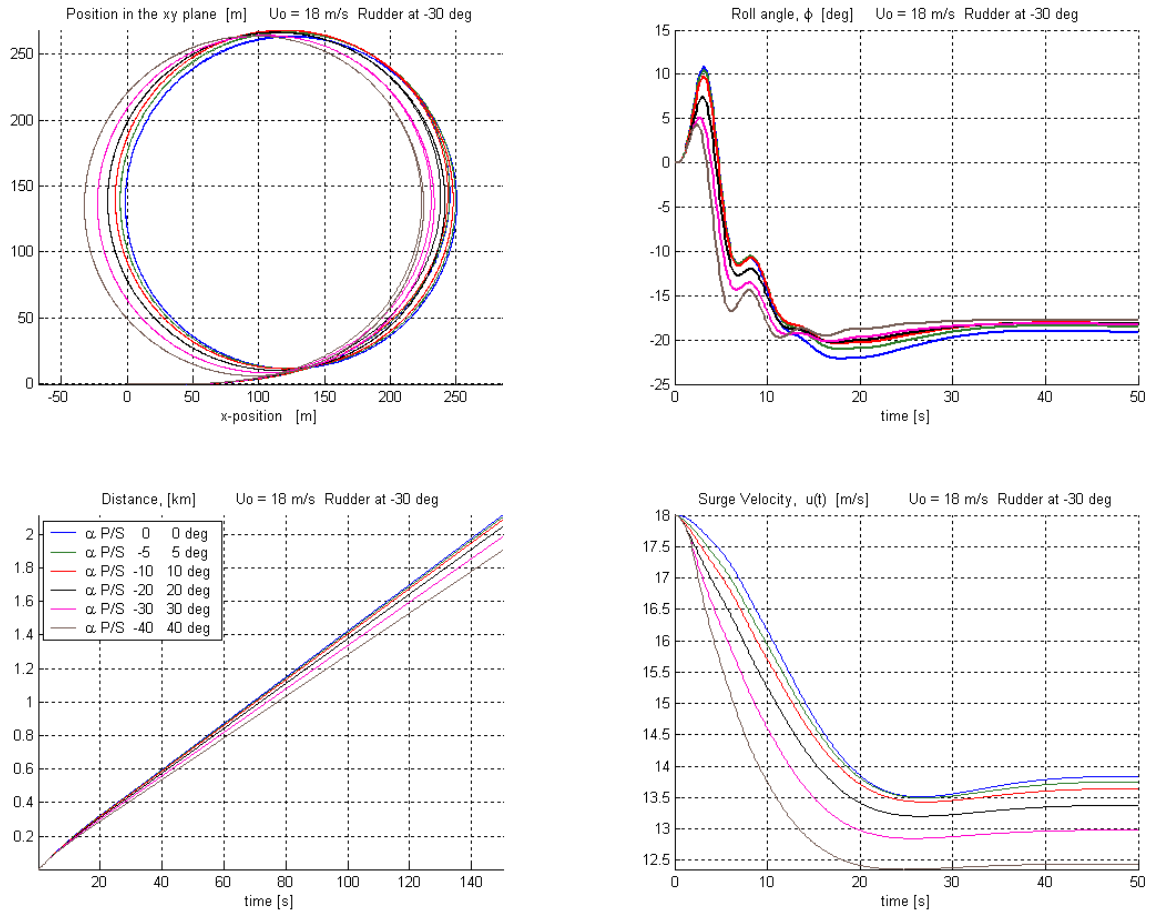

Figure 66. 35 Knots, Rudder -30° – Fins: $\alpha_P = -\alpha_S$; $\alpha_P < 0$ $\beta_P = \beta_S = 34^\circ$.

3. Fin Angles Mixed

All of the following tests were conducted with, $\beta_P = \beta_S = 34^\circ$, $\alpha_P + \alpha_S = Constant$.

a. Rudder Input Positive

With $\delta_{Commanded} = 30^\circ$, $\alpha_p > 0$, and an initial surge velocity of about 15 knots, as α_p increases, peak inward roll angle increases, steady state heel angle decreases, surge velocity decreases, and turning radius increases.

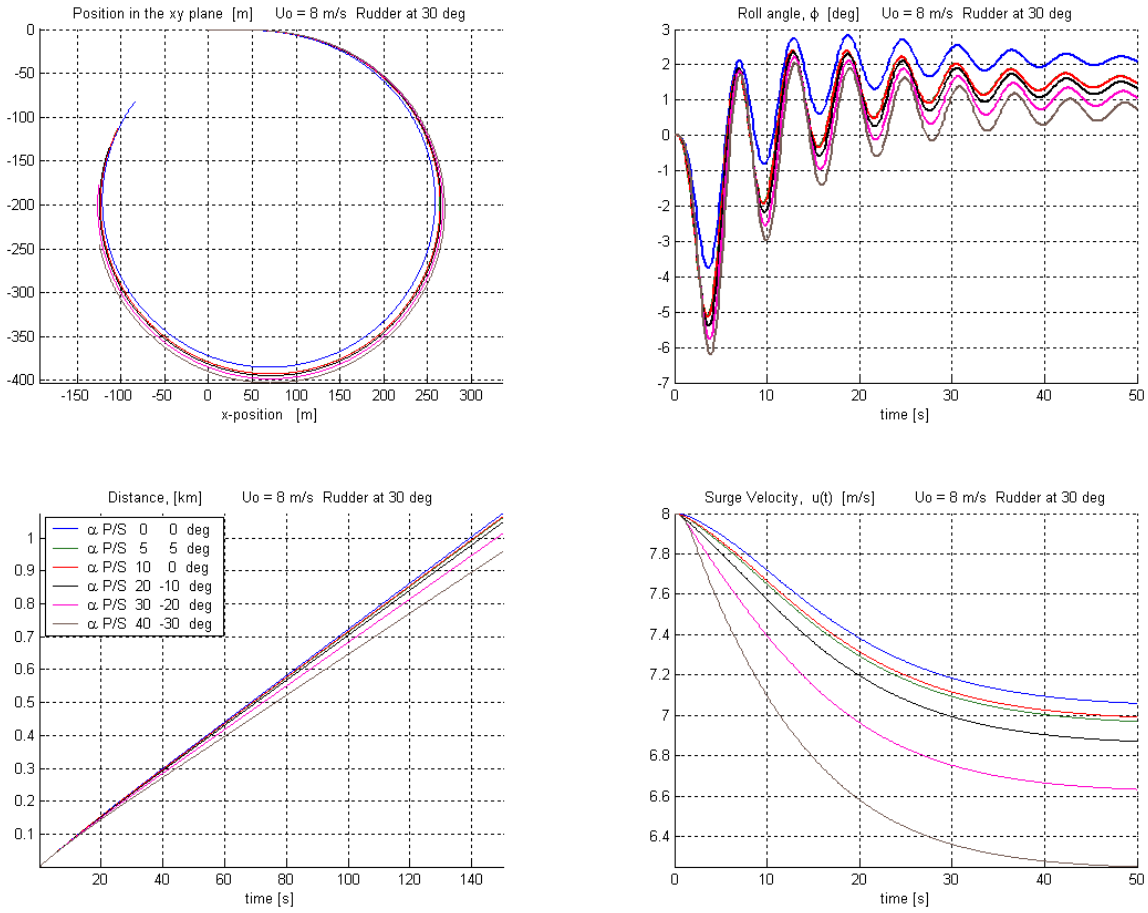

Figure 67. 15.5 Knots, Rudder 30° – Fins: $\alpha_P + \alpha_S = 10^\circ$; $\alpha_P > 0 \quad \beta_P = \beta_S = 34^\circ$.

With $\alpha_p < 0$, as α_p becomes increasingly negative, surge velocity decreases and turning radius increases. For small negative values of α_p, peak inward roll angle decreases and steady state heel angle increases, but for large negative values of α_p, the opposite is true.

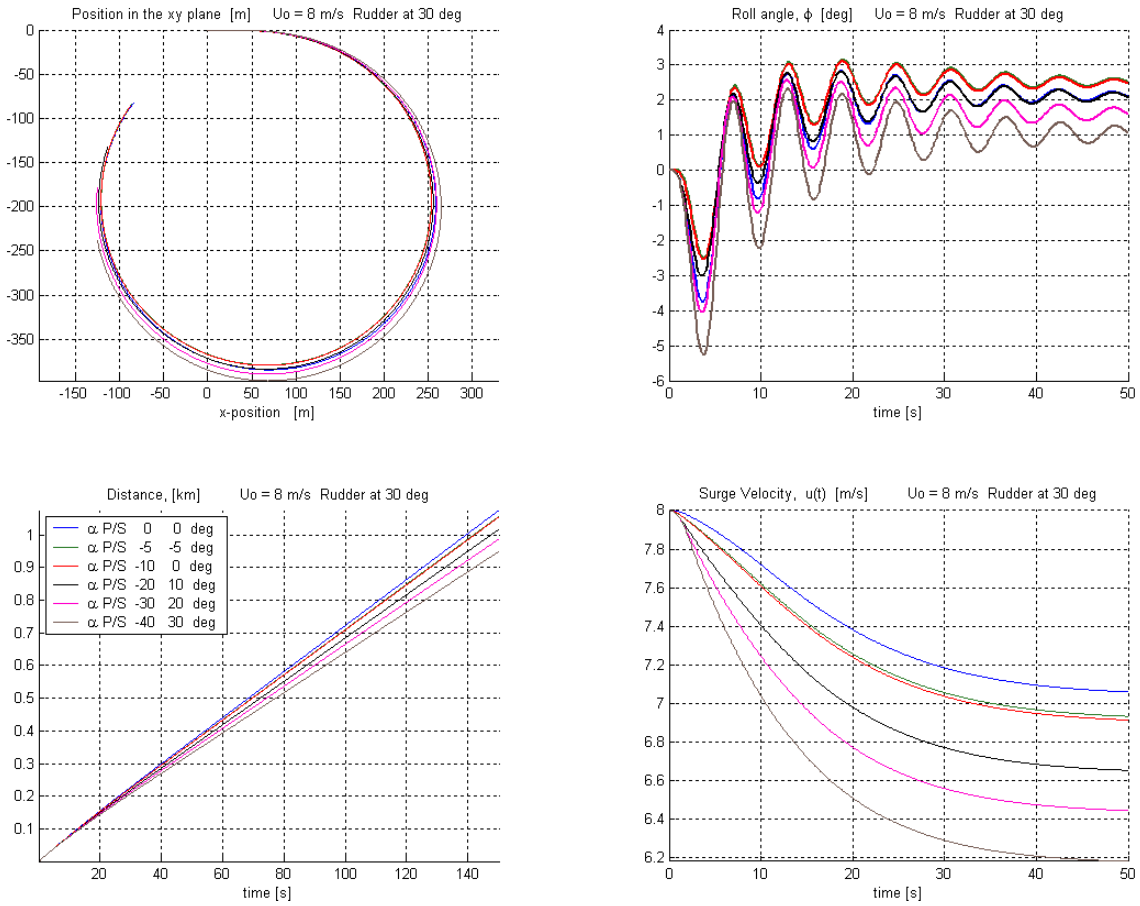

Figure 68. 15.5 Knots, Rudder 30° – Fins: $\alpha_P + \alpha_S = -10^\circ$; $\alpha_p < 0 \quad \beta_P = \beta_S = 34^\circ$.

Increasing the initial surge velocity to about 35 knots magnifies the effects on roll, heel, and turning radius seen at lower speed. It is no longer always the case that increasing values of $|\alpha_p|$ cause an increasing loss in surge velocity.

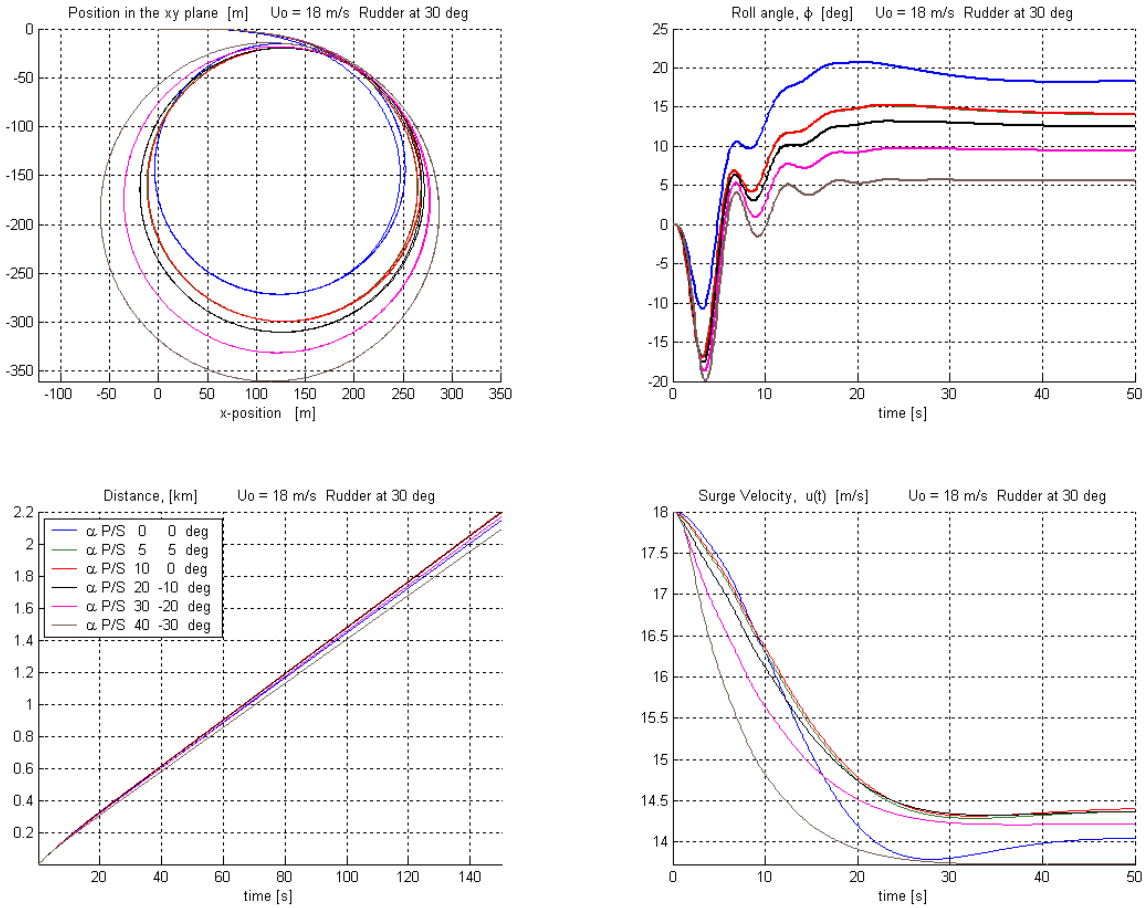

Figure 69. 35 Knots, Rudder 30° – Fins: $\alpha_P + \alpha_S = 10^\circ$; $\alpha_P > 0 \quad \beta_P = \beta_S = 34^\circ$.

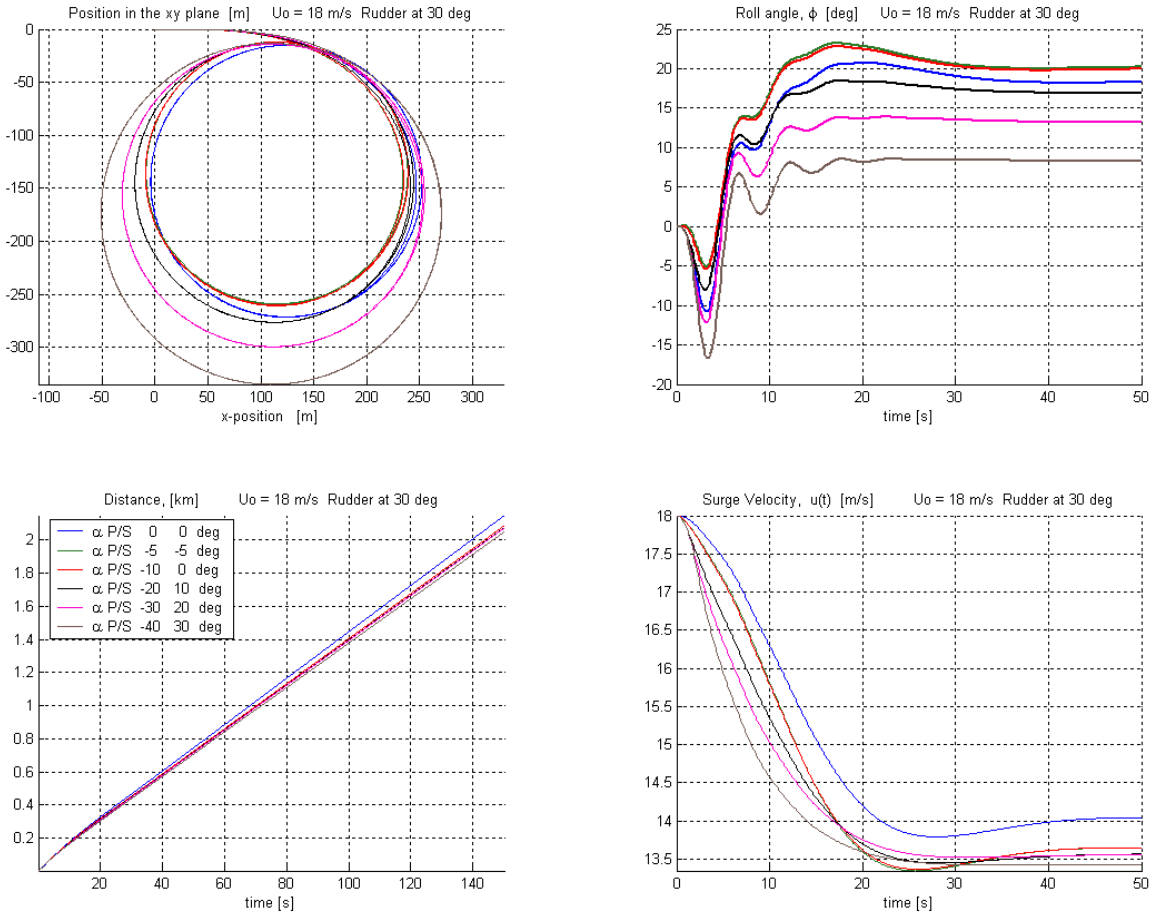

Figure 70. 35 Knots, Rudder 30° – Fins: $\alpha_P + \alpha_S = -10^\circ$; $\alpha_p < 0$ $\beta_P = \beta_S = 34^\circ$.

b. Rudder Input Negative

Changing the rudder input to $\delta_{Commanded} = -30^\circ$, causes both expected and unexpected differences in the results. At moderate speed, as $\alpha_p > 0$ increases, the inward roll angle and surge velocity decrease. But turning radius, advance, transfer, and steady state heel angle for all nonzero values of α_p are nearly identical.

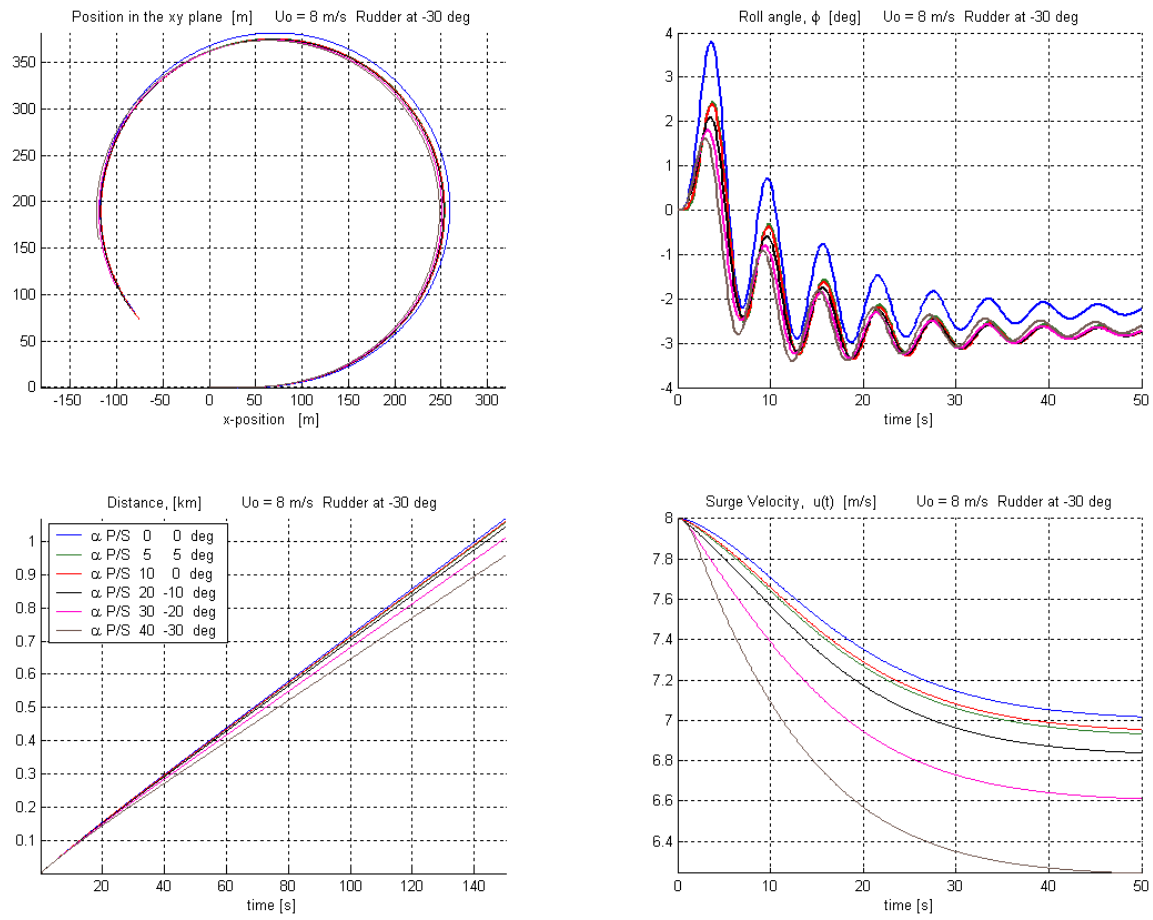

Figure 71. 15.5 Knots, Rudder -30° – Fins: $\alpha_P + \alpha_S = 10^\circ$; $\alpha_P > 0 \quad \beta_P = \beta_S = 34^\circ$.

At high speed, surge velocity and advance decrease with increasingly positive values of α_p, but peak inward roll, steady state heel, turning radius, and transfer remain close to a single value.

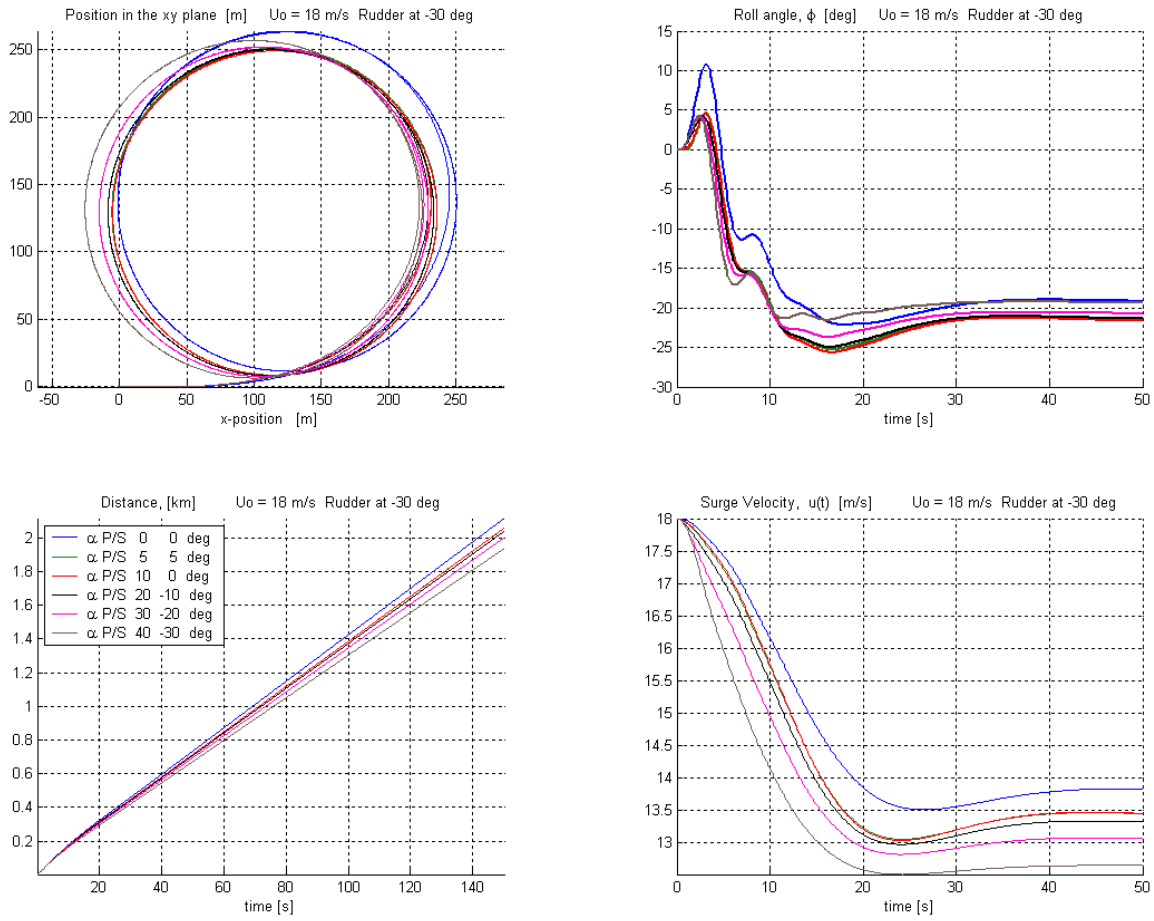

Figure 72. 35 Knots, Rudder -30° – Fins: $\alpha_P + \alpha_S = 10^\circ$; $\alpha_P > 0 \quad \beta_P = \beta_S = 34^\circ$.

With $\alpha_p < 0$, and moderate initial surge velocity, as α_p becomes increasingly negative, surge velocity decreases and turning radius, advance, and transfer remain about constant. For small negative values of α_p, peak inward roll angle increases and steady state heel angle decreases, but for large negative values of α_p, the opposite is true.

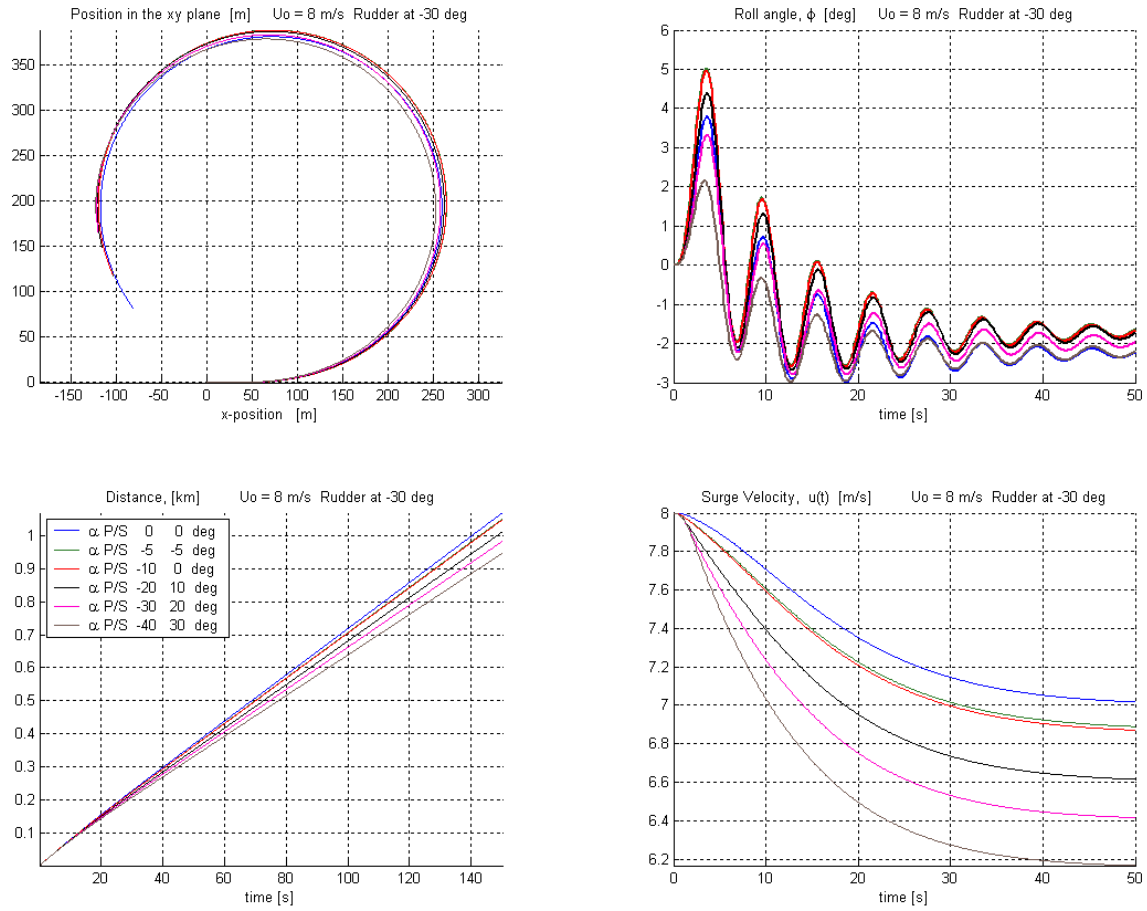

Figure 73. 15.5 Knots, Rudder -30° – Fins: $\alpha_P + \alpha_S = -10^\circ$; $\alpha_p < 0$ $\beta_P = \beta_S = 34^\circ$.

At high speed, nearly all parameters become dependent on the magnitude of α_p. For small negative values of α_p, advance, transfer, turning radius, and inward roll angle increase as α_p becomes increasingly negative. The loss in surge velocity is less with small negative values of α_p than with $\alpha_p = \alpha_s = 0$. But, for large negative values of α_p, as α_p becomes increasingly negative surge velocity losses and steady state heel angle increase, while inward roll angle, turning radius, advance, and transfer decrease. In all cases of non-zero α_p, peak outward heel angle remains smaller than when $\alpha_p = \alpha_s = 0$.

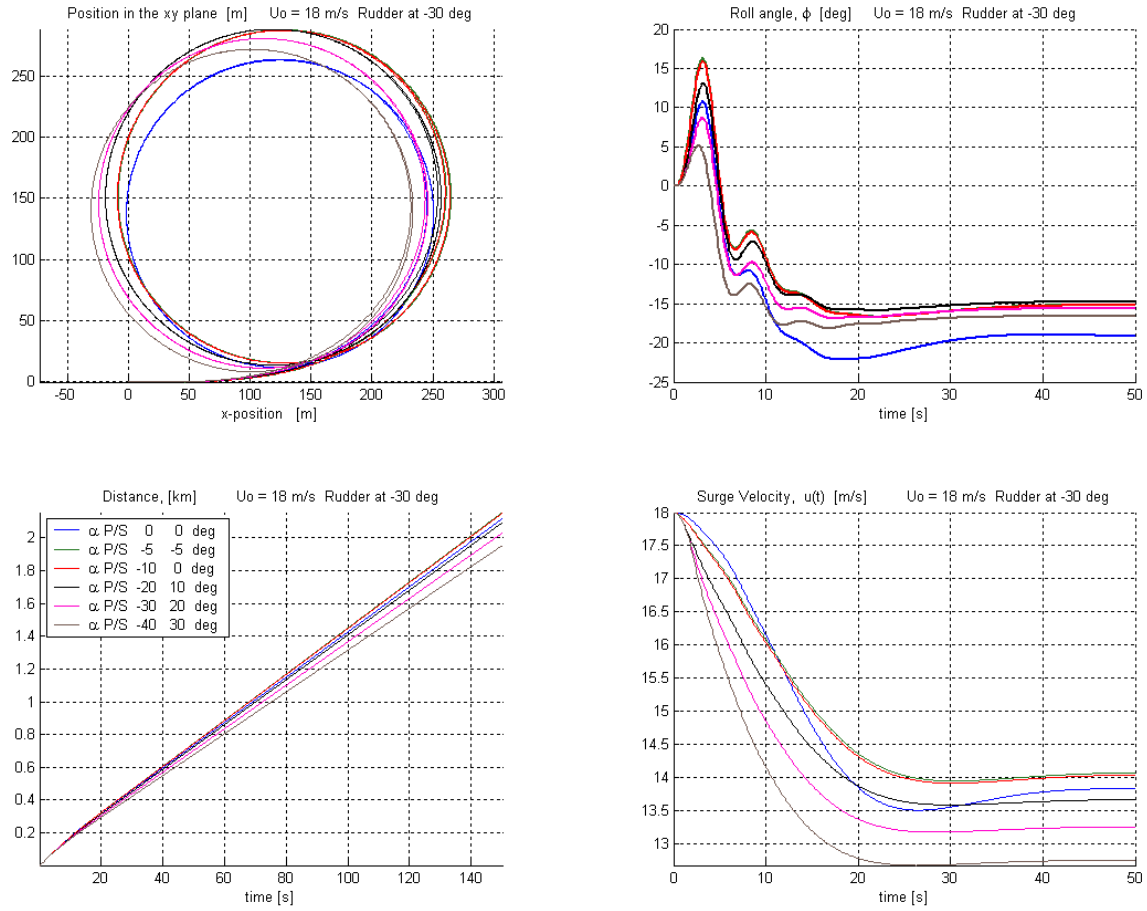

Figure 74. 35 Knots, Rudder -30° – Fins: $\alpha_P + \alpha_S = -10^\circ$; $\alpha_p < 0$ $\beta_P = \beta_S = 34^\circ$

E. STRATEGIC USE OF FINS AND RUDDERS

Careful review of the effects of constant fin and rudder input led to the development of strategies for employing fins in ways designed to improve specific characteristics of turns. Several example strategies are presented below.

1. Reducing Peak and Steady State Roll Angles in High Speed Turns

Figure 75 (repeated here) shows that, in the absence of any fin input, a sudden rudder command of $\pm 30^\circ$ made while the vessel is traveling in a straight line at about 35 knots will first generate an inward peak roll angle of $\left|10^\circ\right|$ followed by an outward sustained roll angle of roughly $\left|18^\circ\right|$.

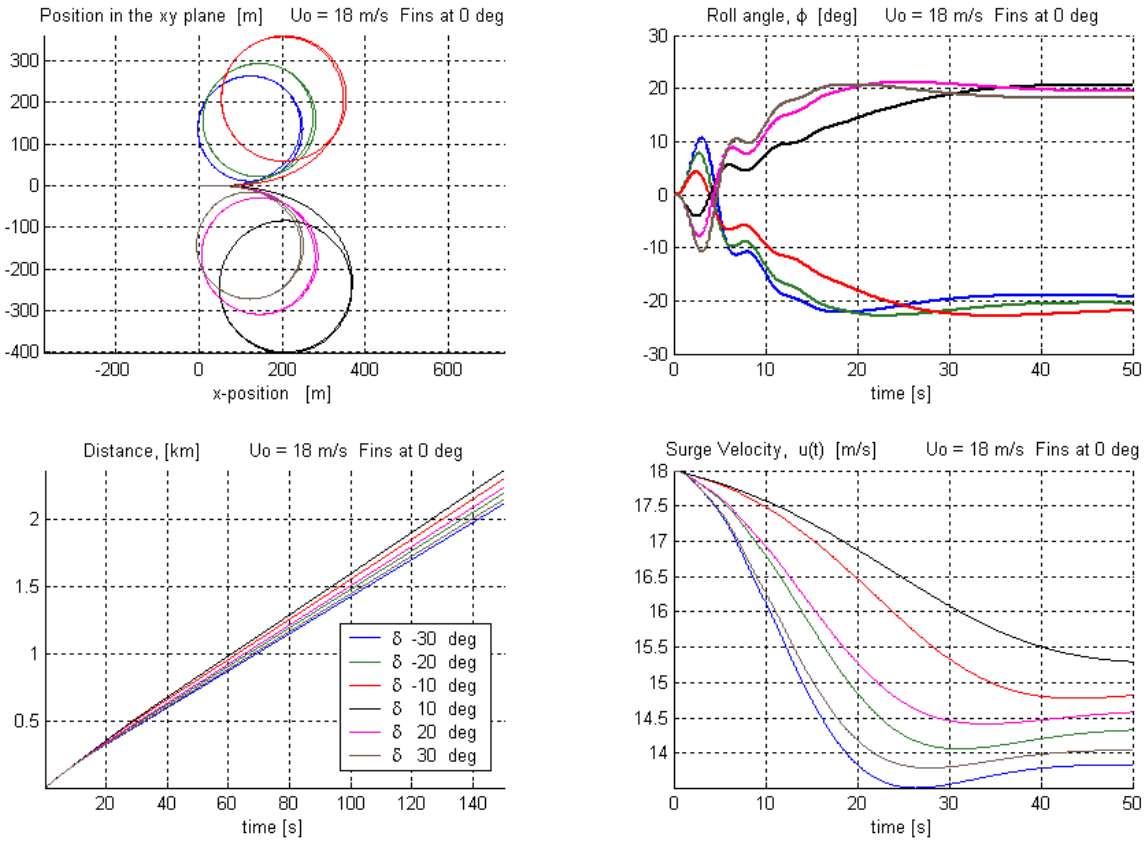

Figure 75. 35 Knots Rudder Only (Repeat of Figure 15).

Deploying the fins in a three-staged fashion (detailed in each Figure), eliminated the inward roll and reduced both the peak and steady outward roll angles to less than $\left|8^{\circ}\right|$. The cost for achieving these benefits is a greater loss in surge velocity and a fairly significant enlargement of the steady-turn radius.

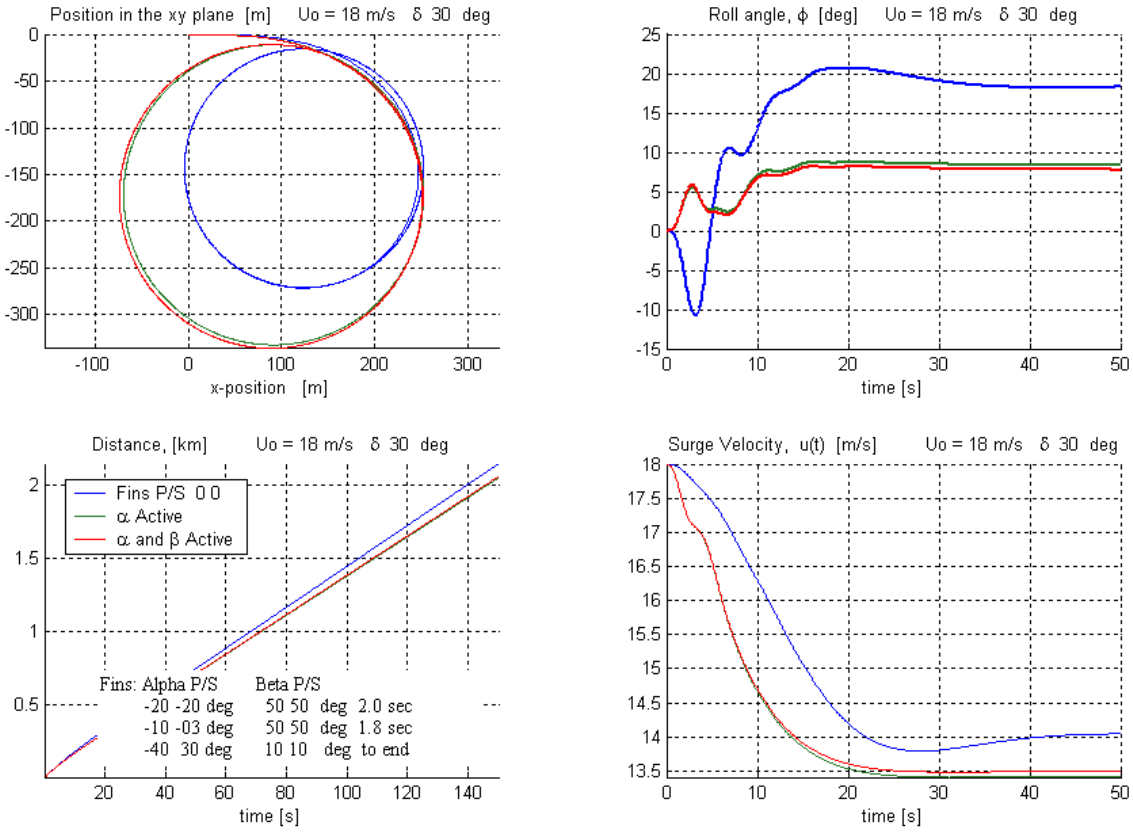

Figure 76. 35 Knots, Rudder 30° Roll Reduction Strategy.

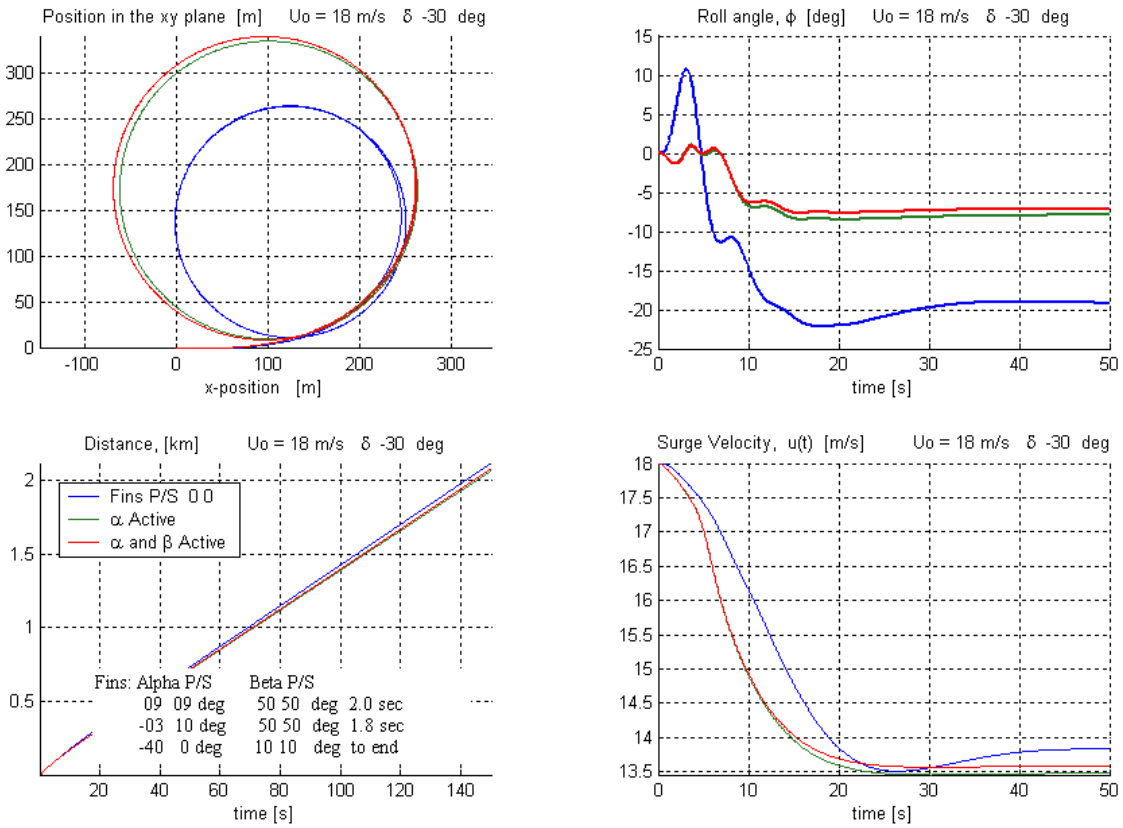

Figure 77. 35 Knots, Rudder -30° Roll Reduction Strategy.

2. Reducing Advance and Transfer without Increasing Roll Angle or Turning Radius in High Speed Turns

Figures 78 and 79 clearly establish that advance and transfer are inextricably linked to the initial two phases of a ship's turn. Both of these characteristics can be reduced without suffering an increase in peak or steady-state roll angle through staged fin deployment. The cost associated with this benefit is essentially limited to greater loss in surge velocity. The steady-turn radius is largely unaffected.

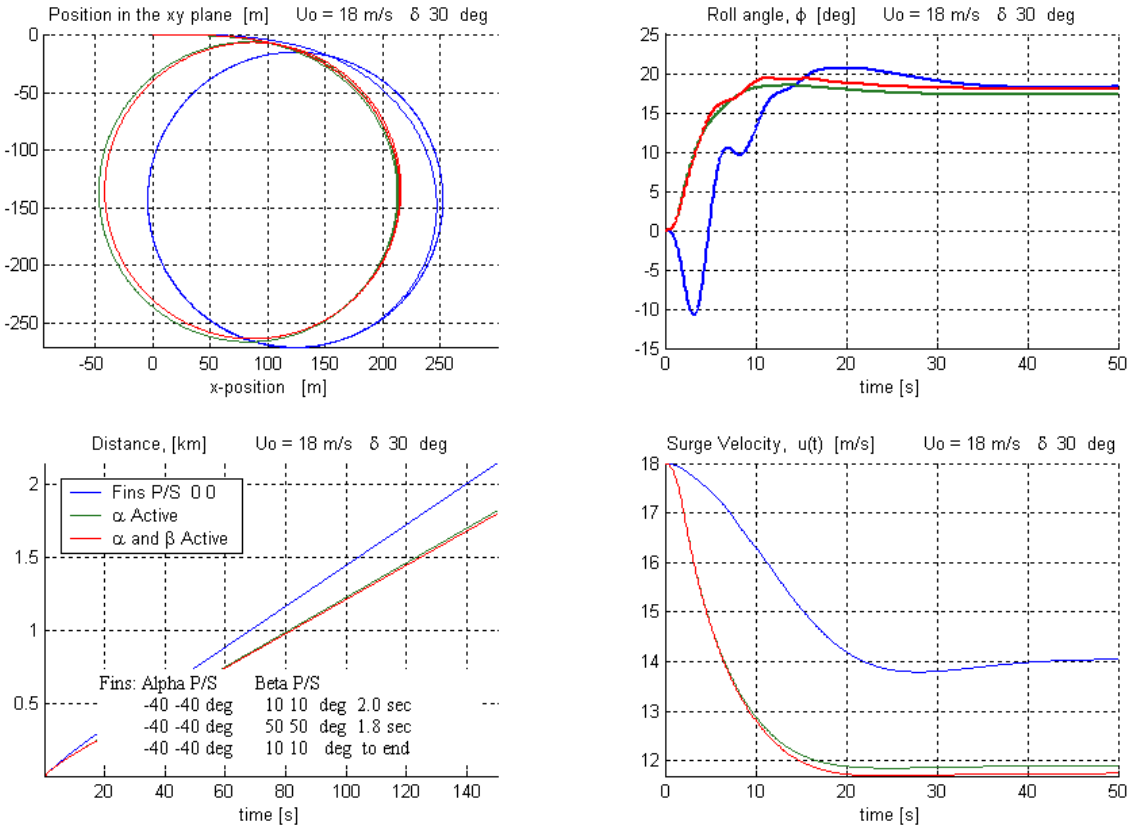

Figure 78. Rudder 30° Advance & Transfer Reduction Strategy – Roll Not Increased.

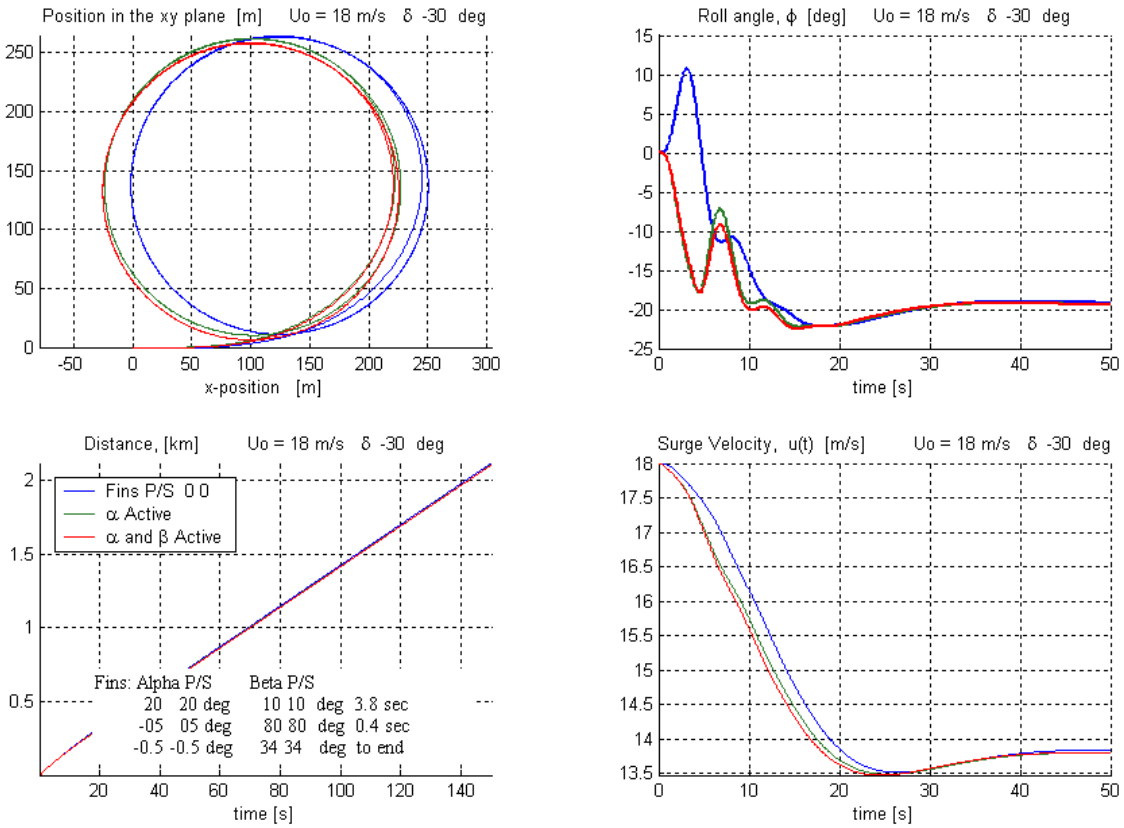

Figure 79. Rudder -30° Advance & Transfer Reduction Strategy – Roll Not Increased.

3. Reducing Advance and Transfer without Regard for Roll Angle in High Speed Turns

Both advance and transfer can be reduced further with only a slight modification in the deployment strategy of fins. For $\delta > 0$ this can be achieved with very little additional cost in surge velocity, but the ship will experience very large inward and outward peak roll angles. The steady-turn radius is again largely unaffected, but the steady turn can be made to cross the vessel's original path.

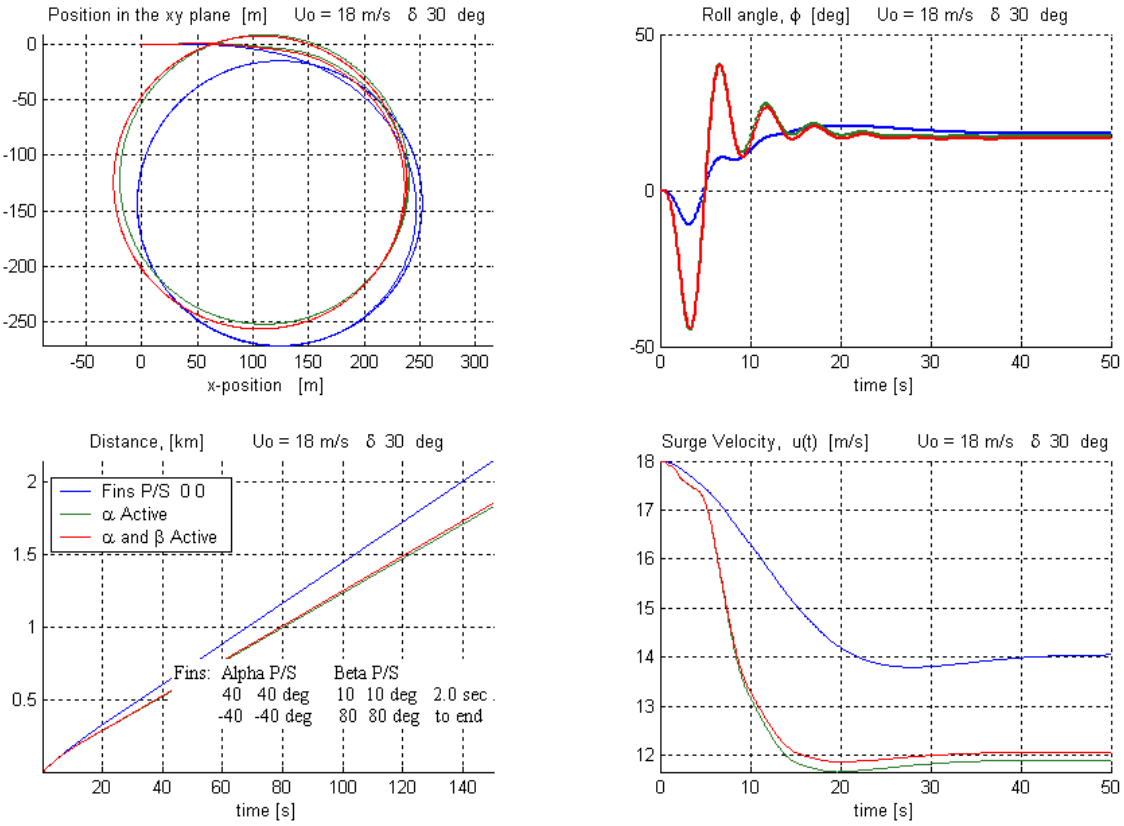

Figure 80. Rudder 30° Advance & Transfer Reduction Strategy – Roll Increased.

For $\delta < 0$ the cost in lost surge velocity as well as peak and steady state roll angles, grows significantly, but the steady-turn radius is markedly smaller.

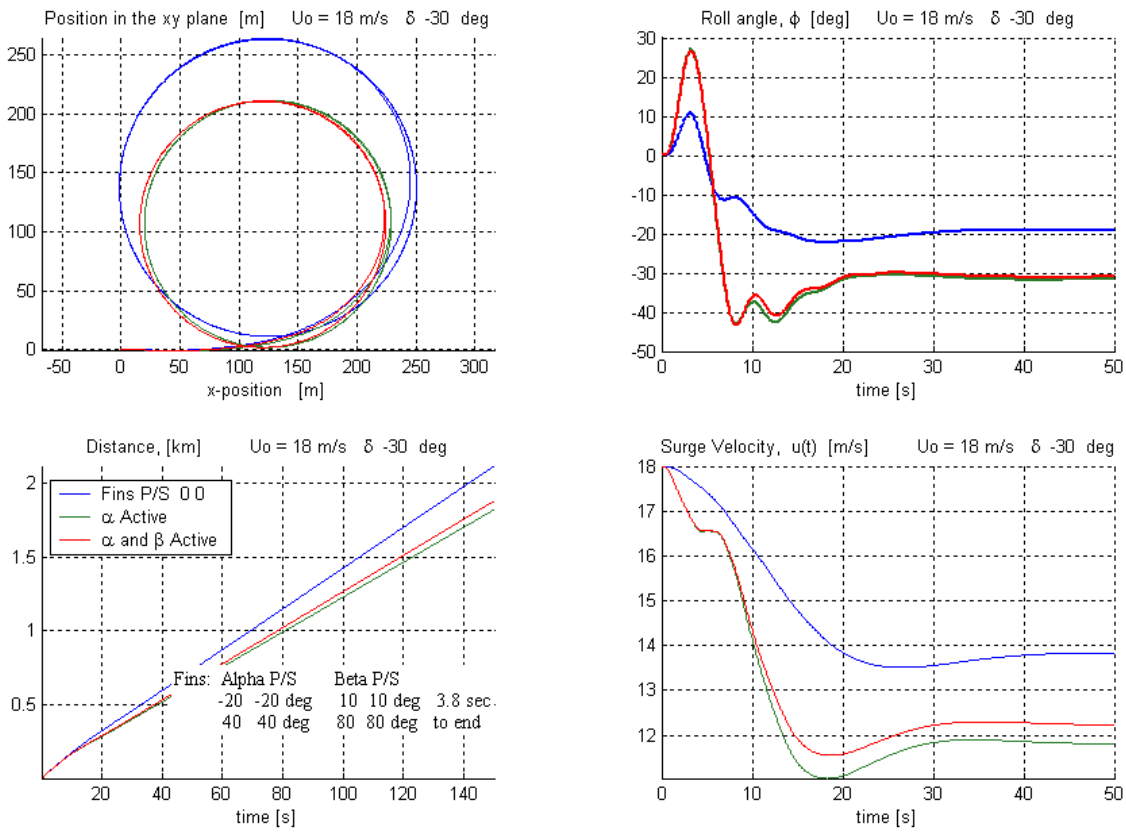

Figure 81. Rudder -30° Advance & Transfer Reduction Strategy – Roll Increased.

THIS PAGE INTENTIONALLY LEFT BLANK

V. REPEATED TURNS

A. RUDDER REVERSED AT $|\psi| = 30^{o}$

A battery of tests over a simulated time period of 100 seconds was conducted using various combinations of rudder angle and initial surge velocity. The commanded rudder angle was reversed as the ship's heading in the inertial reference frame, ψ, reached $\pm 30^{\circ}$. One goal of these tests was to locate critical combinations of speed and rudder angle commands that would excite the natural frequency of the ship, giving rise to large and/or frequent oscillations in roll. Some of the more interesting results of this series of tests are presented and analyzed below. In each figure, use of a 3-staged fin deployment strategy is compared with the case of $\alpha_P = \alpha_S = \beta_P = \beta_S = 0^{\circ}$.

1. Moderate Speed Repeated Rudder Reversals

At about 21 knots, repeated rudder reversals of 30 degrees can be used safely even without the use of fins. After a few rudder cycles, both the peak roll angle and the surge velocity establish an oscillating equilibrium. The fin deployment strategy reduces roll angles to nearly one half of those in the rudder-alone case, but increases the loss in surge velocity and, through decreasing the time taken to reach the reversal criteria, makes the path traveled considerably more linear.

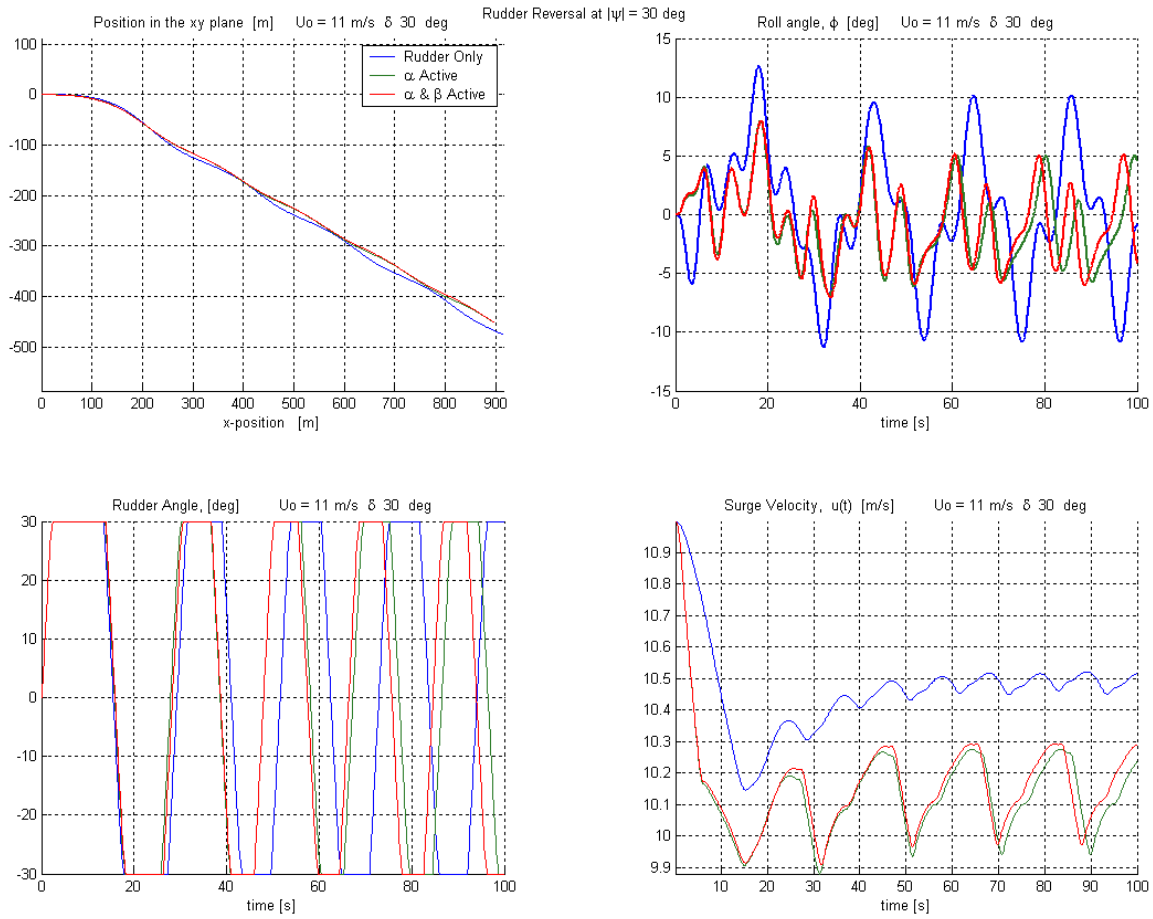

Figure 82. 21 Knots, 30° Rudder Command Reversed at $|\psi| = 30^{o}$.

	Delta > 0				Delta < 0			
Fins:	Alpha P/S		Beta P/S		Alpha P/S		Beta P/S	
-20	-20 deg	80	80 deg	05 seconds	1 0	20 deg	80	80 deg 05 seconds
10	03 deg	80	80 deg	15 seconds	-03	10 deg	80	80 deg 15 seconds
-40	40 deg	80	80 deg	to end	40	0 deg	80	80 deg to end

2. Instability in Roll Response Generated by Repeated Rudder Reversals at Moderate Speed

At an initial surge velocity of about 21 knots, instability in the roll angle response is found with repeated rudder reversals of 4 degrees. The instability begins to grow at about 100 seconds, so, for this test, the time was enlarged to 200 seconds. A 3-staged strategy for deploying the fins substantially reducing the magnitude of the oscillations is presented.

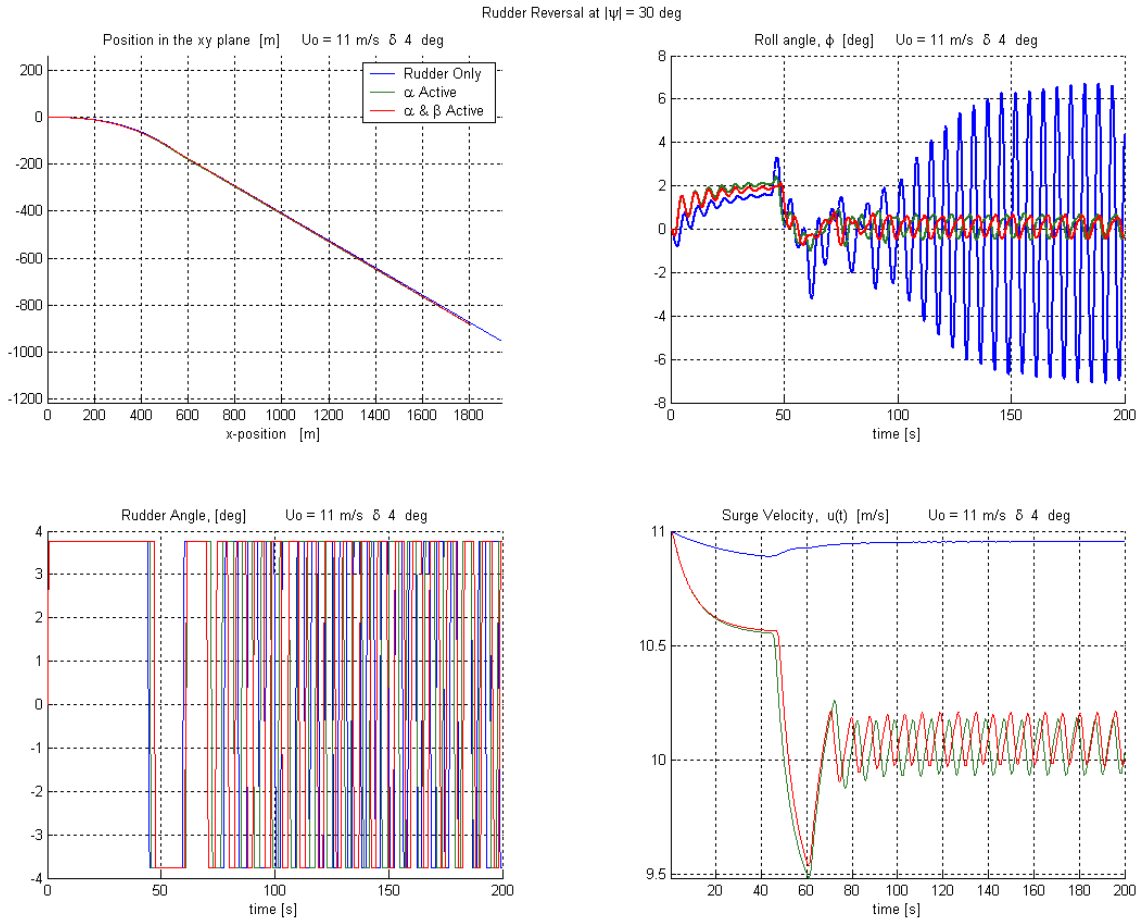

Figure 83. 21 Knots, 4° Rudder Command Reversed at $|\psi| = 30^{o}$ Produces Resonance.

	Delta > 0				Delta < 0			
Fins:	Alpha P/S	Beta P/S			Alpha P/S	Beta P/S		
	40 -20 deg	80 80 deg	0.3 seconds		-40 20 deg	80 80 deg	0.3 seconds	
	-10 03 deg	80 80 deg	49.7 seconds		-03 10 deg	80 80 deg	49.7 seconds	
	-40 40 deg	80 80 deg	to end		40 -0.1 deg	80 80 deg	to end	

3. High Speed Repeated Rudder Reversals

At an initial surge velocity of nearly 35 knots, reversing rudder commands of 30 degrees can produce peak roll angles exceeding 30 degrees. A 3-staged deployment of the fin stabilizers halving the peak roll angles is presented. As at moderate speed, the use of fins significantly alters the path traveled when the criteria triggering rudder reversal is the same as for the case using rudder alone.

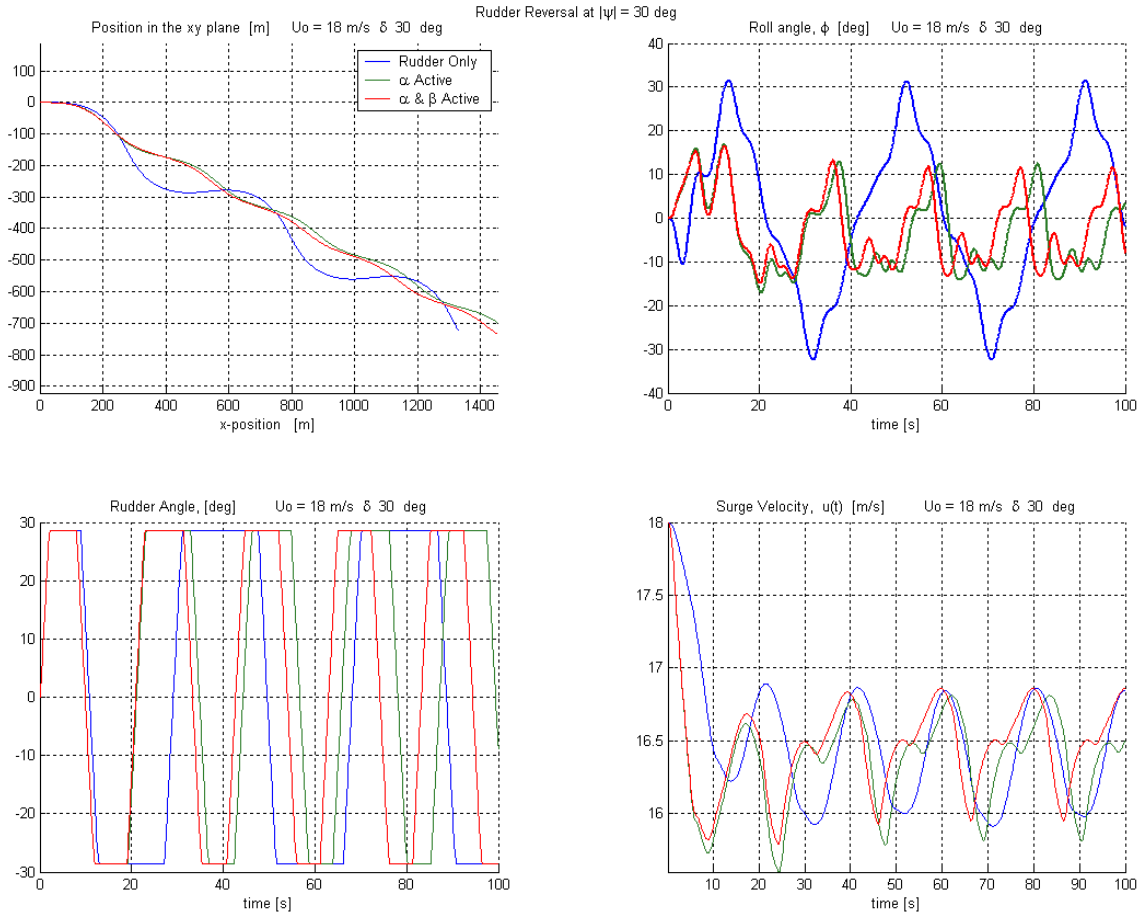

Figure 84. 35 Knots, 30° Rudder Command Reversed at $|\psi| = 30^{o}$.

Delta > 0				Delta < 0			
Fins:	Alpha P/S	Beta P/S		Alpha P/S	Beta P/S		
	-20 -20 deg	80 80 deg	5 seconds	10 20 deg	80 80 deg	5 seconds	
	10 03 deg	80 80 deg	20 seconds	-03 10 deg	80 80 deg	20 seconds	
	-40 40 deg	80 80 deg	to end	40 0 deg	80 80 deg	to end	

B. WILLIAMSON TURN

Elapsed time to complete a Williamson Turn can be shortened by using the fin stabilizers. While the use of fins causes the ship to lose more surge velocity during some parts of the maneuver, velocity along the reciprocal course is regained at least as quickly as the turn using rudder alone. The magnitudes of peak and sustained roll angles are essentially the same with or without the use of fins.

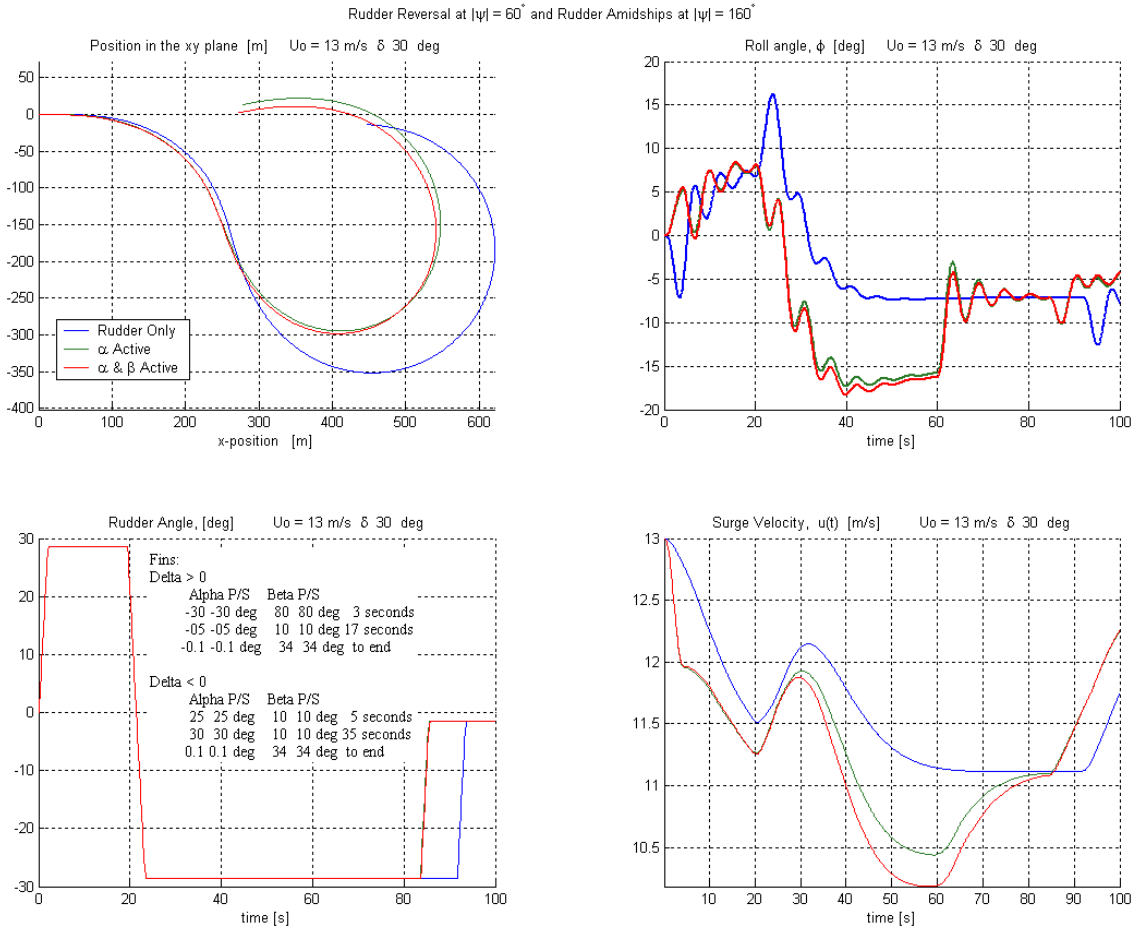

Figure 85. 25 Knots, 30° Rudder Reversed at $|\psi| = 60^{o}$, Then Amidships at $|\psi| = 160^{o}$.

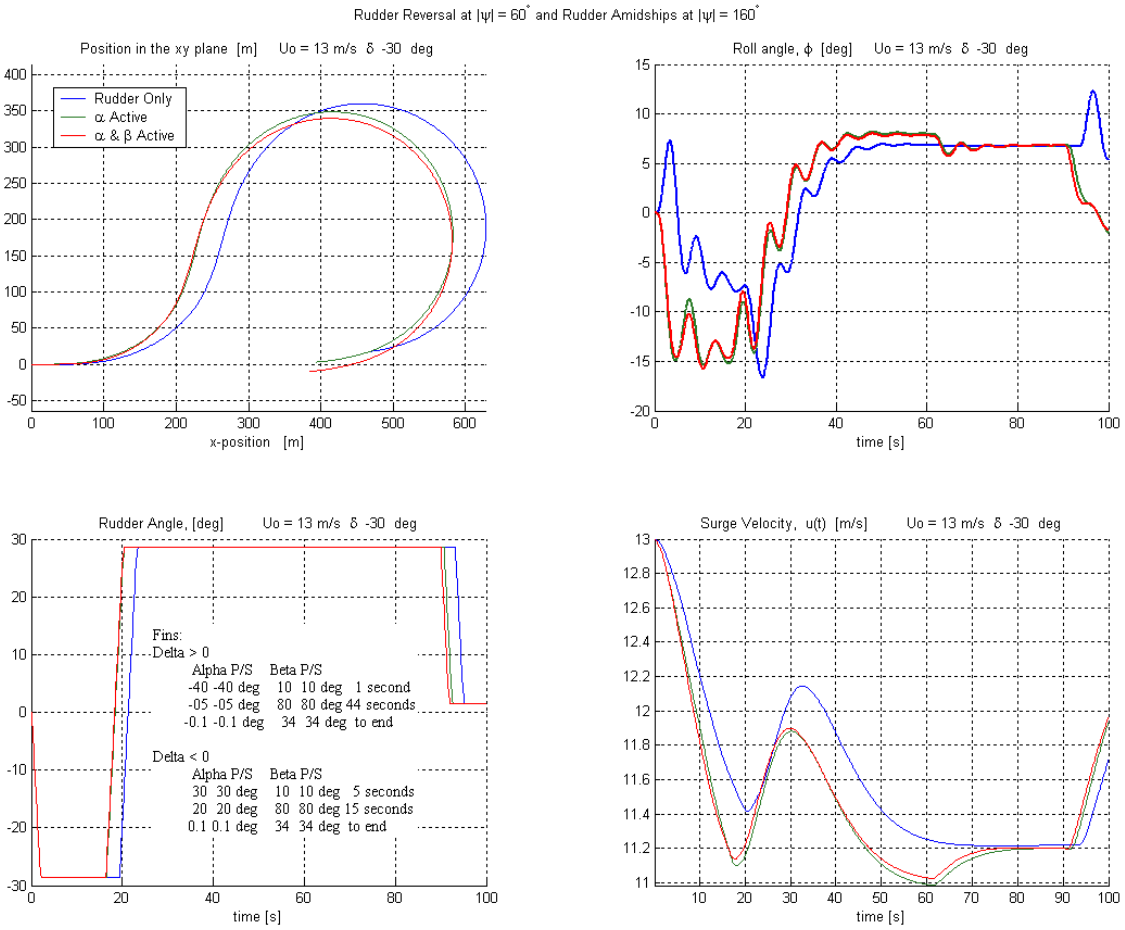

Figure 86. 25 Knots, -30° Rudder Reversed at $|\psi| = 60^{o}$, Then Amidships at $|\psi| = 160^{o}$.

VI. CONCLUSIONS AND RECOMMENDATIONS

A. CONCLUSIONS

A mathematical model was used to simulate, in four degrees of freedom, the motions of a ship maneuvering on a calm ocean surface using rudders and fin stabilizers. Four separate studies were conducted. The first study examined motions caused by various combinations of initial ship surge velocity and rudder deflection angles. The second study examined motions caused by various combinations of initial ship surge velocity and fin stabilizer deflections through the angle of attack between the fin and the free stream velocity of the surrounding fluid. The second study was sub-divided into three cases: (1) fin angles of attack equal; (2) one fin angle of attack equal to the additive inverse of the other; and (3) sum of the fin angles equal to a constant. The third study examined motions caused by various combinations of initial ship surge velocity and fin stabilizer deflections through both the angle of attack and the angle between a horizontal reference and the spanwise direction of the fin. The third study was further divided into sub-cases: (a) spanwise angles equal, and (b) port spanwise angle equal to the absolute value of 90°- starboard spanwise angle. A final study was conducted using various combinations of initial ship surge velocity and deflections of rudders and fin stabilizers through both fin angles. For all four studies, only constant commanded deflection angles were used. That is, each simulation commenced with a set of commanded deflections. Once the deflection angles were achieved, neither the rudders nor fins received any other commands.

These four studies quantified the effects of constant commanded rudder and fin angles. As predicted by theory, some combinations of rudder and fin deflection angles proved to be favorable to certain of the ship's turning characteristics. A strategy for taking advantage of the favorable influences afforded by the use of fin stabilizers during specific portions of turn maneuvers was then developed. A preliminary comparative study was made between a ship employing rudders alone, rudders combined with a strategic deployment of fin stabilizer angles of attack, and rudders combined with a strategic deployment of fin stabilizer deflections through both angles. The comparative

study was made for ships executing (i) basic turns at high speed, (ii) repeated rudder reversals at moderate and high speed, and (iii) Williamson turns. The comparative study supports the following conclusions:

- Strategic deployment of fin stabilizers during maneuvers can favorably influence several characteristics of basic turns. Peak roll and steady heel angles, advance, and transfer can all be reduced, but at a cost of greater loss in surge velocity.
- In some cases strategic deployment of fin stabilizers can decrease turning diameter, but in the majority of cases, turning diameter will either remain unchanged or increase.
- Strategic deployment of fin stabilizers can decrease the magnitude of roll angle oscillations and decrease the time necessary to reach specific heading changes during maneuvers requiring repeated rudder reversals.
- Strategic deployment of fin stabilizers can reduce the magnitude of roll angle oscillations produced in a situation involving an unstable roll response
- Strategic deployment of fin stabilizers can decrease the total time necessary to complete a Williamson turn.

B. RECOMMENDATIONS

This paper was intended merely as an exploration of the possibility that fin stabilizers can be used to improve certain characteristics of ship maneuvers. To accomplish this, an existing mathematical model was modified to incorporate the use of fin stabilizers that could be commanded in a strategic manner. The model did not take into account any change in the hull configuration, fin stabilizer size, machinery modifications, or other changes that may be required to ensure that the fins could safely be used in the manner simulated. The model also neglected a wide variety of known factors that may affect the results obtained. These factors include the effect of stall and other constraints on the forces and moments produced by rudders and fins, the angle-dependent nature of the Lift Coefficient for both rudders and fins, the true impact of engine thrust on a ship's turn characteristics, as well as environmental effects, such as wind, waves, currents, and wakes. Further study with a model that accounts correctly for these neglected factors, with a physical model that encounters scaled versions of them, or with a real ship in real conditions should be performed.

Further study is also necessary to convert the individual turn strategies developed in this paper into control logic and then a control law that can be applied to a variety of standard maneuvers. A real-time display of a ship's anticipated path, updated as the ship responds to actual helm commands could be incorporated into such a controller. A controller linked to selections made by an operator who has previewed the ship's turn characteristics before making helm commands could be developed. An optimization strategy that begins with the 3-stage strategies proposed herein updated with feedback taken at sampling intervals should also be explored.

THIS PAGE INTENTIONALLY LEFT BLANK

LIST OF REFERENCES

Abkowitz, M. A., Stability and Motion Control of Ocean Vehicles, M.I.T. Press, Cambridge, Massachusetts, 1969.

Bettcher, C. W., U.S. Patent No. 4,777,899, Washington, D.C., U.S. Patent and Trademark Office, October 1988, [http://patft.uspto.gov], Accessed 30 October 2003.

Blanke, M. and Christensen, A., "Rudder-Roll Damping Autopilot Robustness to Sway-Yaw-Roll Couplings," Proceedings of 10th Ship Control Systems Symposium, Ottawa, Canada, pp. 93-119, 1993.

Gatzoulis, J. and Keane, R. G., Upgrading Mission Capability and Performance Effectiveness of Naval Ships by the Use of Active Fin Stabilizers, 14th Annual Technical Symposium Association of Scientists and Engineers of the Naval Air and Sea Systems Command, Washington, D.C., 1977.

[http://kwon3d.com/theory/euler], Accessed 8 October 2003.

[http://web.nps.navy.mil/~me/tsse/NavArchWeb/1/module12/basics.htm], Accessed 05 October 2003.

[http://www.mathworks.com/access/helpdesk/help/toolbox/aeroblks/euleranglestodirectioncosinematrix.shtml], Accessed 08 October 2003.

Kallstrom, C. G., "Control of Yaw and Roll by a Rudder/Fin-Stabilization System," Sixth Ship Control Systems Symposium, Ottawa, Canada, Vol. 2, pp. 3-1 to 3-23, October 1981.

Lauvdal, T. and Fossen, T., "Matlab Simulation Program for Marine and Flight Vehicles," The University of Trondheim, The Norwegian Institute of Technology, Department of Cybernetics, NTH Report No. 94-43-W, Trondheim, Norway, 7 November 1994.

Lee, C. M., "Stability and Control of SWATH Ships by Stabilizing Fins," Proceedings of the Symposium on Control Theory and Navy Applications, Monterey, California, pp. 65-86, July 1975.

Lewis, E. V., ed., Principles of Naval Architecture, The Society of Naval Architects and Marine Engineers, Vol. III, Jersey City, New Jersey, 1989.

Logsdon, M., "Coupled Roll and Directional Stability Characteristics of Surface Ships," Graduate Thesis, Naval Postgraduate School, Monterey, California, June 1992.

Nomenclature for Treating the Motion of a Submerged Body Through a Fluid, *The Society of Naval Architects and Marine Engineers, Technical and Research Bulletin No. 1-5,* New York, NY, April 1950.

Oltmann, P., "Roll, an Often Neglected Element of Maneuvering," International Conference on Marine Simulation and Ship Maneuvrability, St. John's, Newfoundland, Canada, pp. 463-71, September-October 1993.

Papoulias, F., "Notes on Maneuvering Motions", Naval Postgraduate School, Monterey, California, 1995.

Perez, T. and Goodwin, G. C., "Constrained Control to Prevent Dynamic Stall of Ship Fin Stabilizers," Proceedings of 6th IFAC Conference on Maneuvering and Control of Marine Craft (MCMC 2003), Girona, Spain, September 2003.

Perez, T., "Ship Modeling for Stabilizer Control System Design," Technical Report EE03020.

Perez, T., and Blanke, M., *Mathematical Ship Modelling for Marine applications*, Technical University of Denmark, Section of Automation, ØRSTED-DTU, 2002.

Sgobbo, J. and Parsons, M., "Rudder/Fin Roll Stabilization of the USCG WMEC 901 Class Vessel," *Marine Technology*, Vol. 36, No. 3, pp. 157-170, July 1999.

"Six Degree of Freedom (6 D.O.F) Simulation," [http://www.erc.msstate.edu/~roy/Research/sixdof.htm], Accessed 03 October 2003.

Son, K. and Nomoto, K., "On the Coupled Motion of Steering and Rolling of a High Speed Container Ship," *Journal of the Society of Naval Architects of Japan*, Vol. 150, pp. 232-244, December 1981. (In Japanese)

Taylor, David W., Naval Ship Research and Development Center, "Vertical Plane and Roll Motion Stabilization for SWATH Ships," Bethesda, Maryland, September 1986.

Toxopeus, S. and Loeff, G., "Maneuvering Aspects of Fast Ships With Pods," Third International EuroConference on High-Performance Marine Vessels HIPER'02, Bergen, Norway, pp. 392-406, 14-17 September 2002.

U.S. Coast Guard Technical Publication TP 3907, Ship's Fin Stabilizing System 110' WPB Class Cutters, Ch. 8, p. 5 (2nd Issue, 1999).

VMA-CFD/Hydrodynamic Response Analysis Codes, [http://www.bodrum-bodrum.com/vorteks/arsenal/cfdcodes3.htm], Accessed 03 October 2003, (listing and describing several commercially available simulation programs).

Zubaly, R. B., Applied Naval Architecture, Cornell Maritime Press, Centreville, Maryland, 1996.

INITIAL DISTRIBUTION LIST

1. Defense Technical Information Center
   Ft. Belvoir, Virginia

2. Dudley Knox Library
   Naval Postgraduate School
   Monterey, California

3. U.S. Coast Guard Library
   Washington, DC
   Attn: Tom Haggerty, Librarian

4. Commandant, U.S. Coast Guard (G-SEN-1)
   Washington, DC

5. Martin G. Sarch
   Naval Postgraduate School
   Monterey, California